

Atmosphere

Volume 14 Number 3 1976

Canadian Meteorological Society
Société Météorologique du Canada

Atmosphere

Volume 14 Number 3 1976

Contents

145

Foreword
P.E. Merilees

147

Meteorological and Ozone Data for the Project STRATOPROBE
Balloon Flights of 8 and 22 July, 1974
S.E. Bain, C.L. Mateer and W.F.J. Evans

155

The Measurement of Minor Stratospheric Constituent Concentrations
by Far Infra-Red Emission Spectroscopy
T.A. Clark and D.J.W. Kendall

166

Measurement of Stratospheric Nitrogen Dioxide from
the AES Stratospheric Balloon Program
J.B. Kerr and C.T. McElroy

172

The Altitude Distribution of Nitric Acid at Churchill
W.F.J. Evans, C.I. Lin and C.L. Midwinter

180

Altitude Profile and Sunset Decay
Measurements of Stratospheric Nitric Oxide
B.A. Ridley, J.T. Bruin, H.I. Schiff and J.C. McConnell

189

Intercomparison of NO , NO_2 , and HNO_3 Measurements
with Photochemical Theory
*W.F.J. Evans, J.B. Kerr, D.I. Wardle
J.C. McConnell, B.A. Ridley and H.I. Schiff*

Continued on inside back cover

ISSN 0004-6973

Canadian Meteorological Society
Société Météorologique du Canada

Theoretical Simulation of Solar Ultraviolet Fluxes Measured
on the 8 July 1974 STRATOPROBE I Flights

M.W.P. Cann, R.W. Nicholls, W.F.J. Evans and D.J. McEwen

The Steady-State Structure of the Natural Stratosphere and Ozone
Distribution in a 2-D Model Incorporating Radiation and *O-H-N*
Photochemistry and the Effects of Stratospheric Pollutants

R. Krishna Rao Vupputuri

Notes and Correspondence

Book Reviews

Call for Papers — Eleventh Annual Congress

Appel de Textes — Onzième Congrès Annuel

Announcements

This special issue of *Atmosphere* presents the first fruits of a scientific program designed to measure the critical components of the system which leads to the ozone balance in the stratosphere. The program is called The AES Stratospheric Pollution Program or Project STRATOPROBE and it involves cooperation between the Atmospheric Environment Service, other government agencies and a number of Canadian universities and industries.

The Canadian Meteorological Society is particularly pleased with the leadership displayed in this matter by SOMAS (now the CMS Scientific Committee) through a recommendation made to the National Research Council and the Atmospheric Environment Service in October 1972. The text of the recommendation is as follows:

“The Subcommittee on Meteorology and Atmospheric Science (SOMAS)

noting the environmental concern, as expressed at the 1972 U.N. Stockholm Conference, for example, over significant increases in the pollution of the stratosphere, primarily by aircraft (potentially very great by supersonic aircraft),

recognizing that residence times for contaminants in the stratosphere greatly exceed those in the troposphere (due in part to the absence of rain-out and wash-out mechanisms),

being aware of the current controversies concerning the magnitude of inadvertent modification of the stratospheric composition, atmospheric radiative fluxes and surface climate attendant upon increased emissions of particulates and gaseous contaminants in the stratosphere,

viewing with apprehension the increasing pressure for major decisions on the extent and mode of SST operations over Canada prior to the accumulation of basic knowledge and information on the consequences of such decisions, and

being mindful of the existence of a strong Canadian nucleus of scientific competence and a resource pool which could serve as the basis for meaningful studies (observation, experimental and theoretical), of stratospheric pollution,

recommends to the National Research Council of Canada and to the Atmospheric Environment Service, Department of the Environment, that:

- a) provision be made for additional manpower and facilities to be assigned to stratospheric pollution studies as a matter of urgency,
- b) relative priorities for assignment of existing resources be readjusted in acknowledgement of the importance to Canada of these studies.”

The Atmospheric Environment Service took up the challenge and expanded its programs in ozone and stratospheric studies. An Advisory Committee on

Stratospheric Pollution, representing the major scientific expertise and interests in the government-university community, was established to assist the AES in the formulation and review of research programs and in developing bi-national and international cooperation.

The AES two-dimensional modelling work was modified to include the effects of the hydrogen and nitrogen (and later the chlorine) systems on the ozone distribution, in a fully interactive manner.

Support for external research projects was increased and sufficient resources were allocated to launch Project STRATOPROBE in the summer of 1974. Multiple-experiment payloads, flown at levels near 30 km on SKYHOOK balloons, were designed to make simultaneous measurements of key stratospheric constituents important in the photochemical balance of the ozone layer. The twelve experiments normally carried on each AES flight involved the direct participation of five university research groups and several industrial companies. The results are expected to provide definitive answers to many aspects of the ozone problem.

This program has been in the vanguard of an international effort to understand the risks of uncontrolled stratospheric pollution. The world-wide concern in this area is expressed in the recent WMO statement on "Modification of the ozone layer due to human activities and some possible geophysical consequences."

The Canadian Meteorological Society is pleased that the scientific team has chosen to present its first results in our journal *Atmosphere* and wishes to congratulate all concerned.

P.E. Merilees
President

Meteorological and Ozone Data for the Project STRATOPROBE Balloon Flights of 8 and 22 July, 1974

S.E. Bain, C.L. Mateer and W.F.J. Evans

*Atmospheric Environment Service, 4905 Dufferin St.
Downsview, Ontario, M3H 5T4*

[Manuscript received 29 March 1976]

ABSTRACT

The meteorological conditions at the earth's surface and aloft for the two research balloon flights of Project STRATOPROBE on 8 July and 22 July, 1974, are presented and discussed briefly. Trajectories of the balloon flights at float level are traced. The

temperature and ozone profiles taken at Churchill before the launches and during the flights, which are necessary for the evaluation and interpretation of some of the experimental data, are also presented.

1 Introduction

In this paper, we present the meteorological conditions and ozone profiles associated with the first two flights of Project STRATOPROBE from Churchill, Manitoba, on 8 July (Flight 1) and 22 July (Flight 2), 1974. The ozone mixing-ratio and temperature profiles are required for the reduction of measurements of constituents such as nitric acid, and also for the interpretation of the measured nitric oxide, nitrogen dioxide, and nitric acid concentrations in terms of photochemical theory.

The second section of this paper summarizes the meteorological conditions on the launch dates. The third and subsequent sections present the temperature and ozone profiles derived from ozonesondes launched at intervals starting six hours prior to the launch of the large research balloons and ending approximately six hours after launch. Supplementary temperature data from rocketsondes and the NIMBUS 5 satellite are also included. The surface synoptic and the 10-mb height maps are included so that effects of meteorological transport on the theoretical interpretation of the constituent measurements may be considered.

2 Meteorological conditions

a *Flight 1*

The surface synoptic map for 0000 GMT 9 July 1974 is shown in Fig. 1(a). The surface weather conditions were ideal for this flight since a high pressure

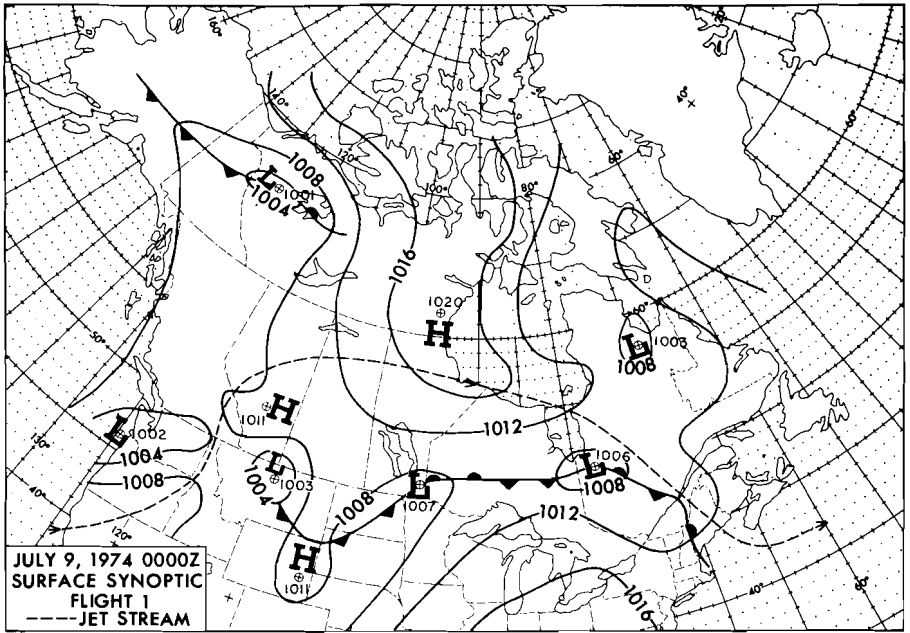


Fig. 1(a) Surface synoptic map for 0000 GMT 9 July 1974. Dashed line shows position of jet stream.

region with an associated north-south ridge extending into Northern Ontario had moved gradually southward to remain stationary just to the north of Churchill for several days. This high pressure region maintained a relatively constant pressure of 1020 mb bringing sunny skies and light surface winds to the launch site.

A pressing problem for this flight was the position and strength of the jet stream, since the strong turbulence and large wind shears near the jet can structurally damage a large volume research balloon. The launch was originally scheduled for 7 July 1974 but by then an extremely strong jet stream had moved directly over Churchill with maximum winds measured by radiosonde at 120 kt. The jet stream began to move southward the next day and by the beginning of the launch window at 2100 GMT on the afternoon of 8 July, the main core of the jet stream was just south of Churchill and the maximum winds aloft were from the NNW at 50 kt. The location of the jet core is indicated by the dashed line on the map in Fig. 1(a). The 10-mb height analysis for 1200 GMT 9 July 1974 is shown in Fig. 1(b). A study of this map indicates that the float level winds were approximately 20 kt from the ESE. The flight trajectory of the high altitude balloon from launch at 0103 GMT 9 July until termination at 0015 GMT the following day is also indicated on this map. This balloon which had a volume of $1.2 \times 10^5 \text{ m}^3$ attained a float altitude of approximately 13 mb.

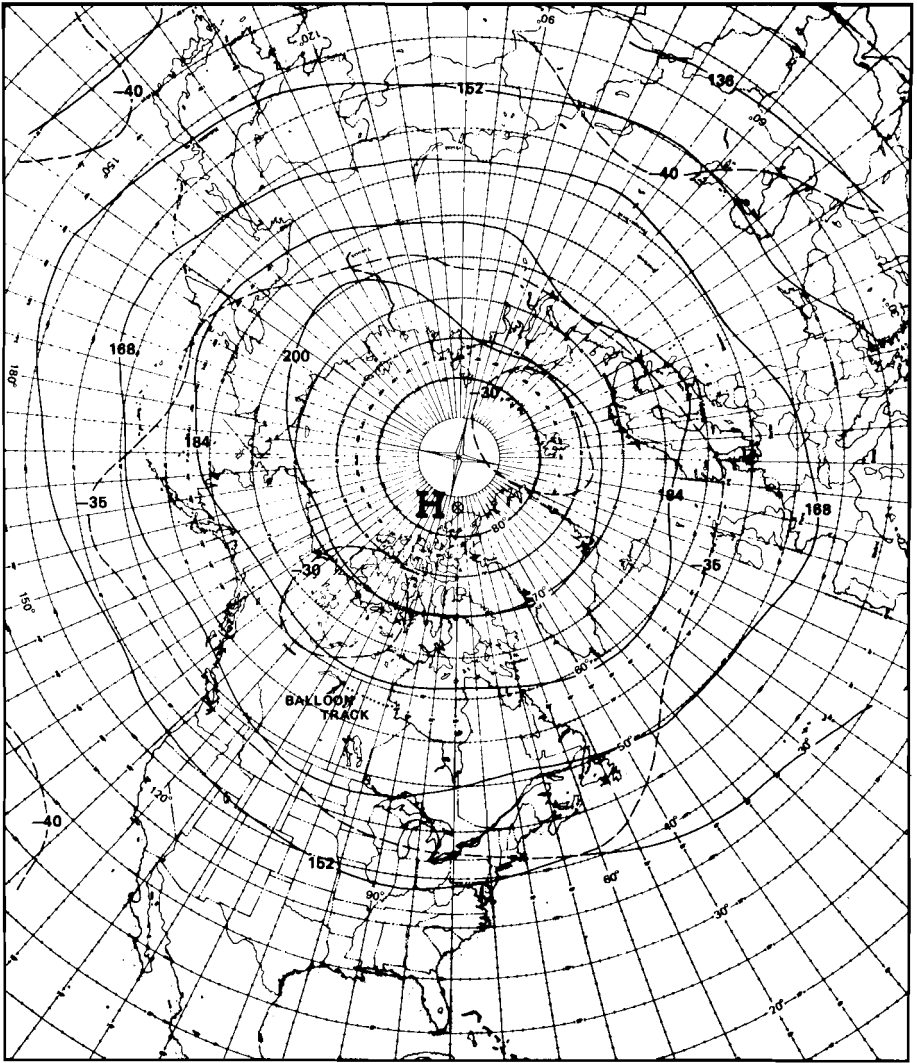


Fig. 1(b) 10-mb contour chart for 1200 GMT 9 July 1974. Dotted line west from Churchill shows balloon track.

The surface weather conditions at Churchill during this launch were:

Wind: SW 5 kt.

Temperature: 21°C.

Pressure: 1018 mb, steady.

b Flight 2

Fig. 2(a) shows the surface synoptic map for 0000 GMT 23 July 1974 which depicts the surface weather conditions close to the time of launch. The dominant feature affecting Churchill weather was the Low (988 mb) centred

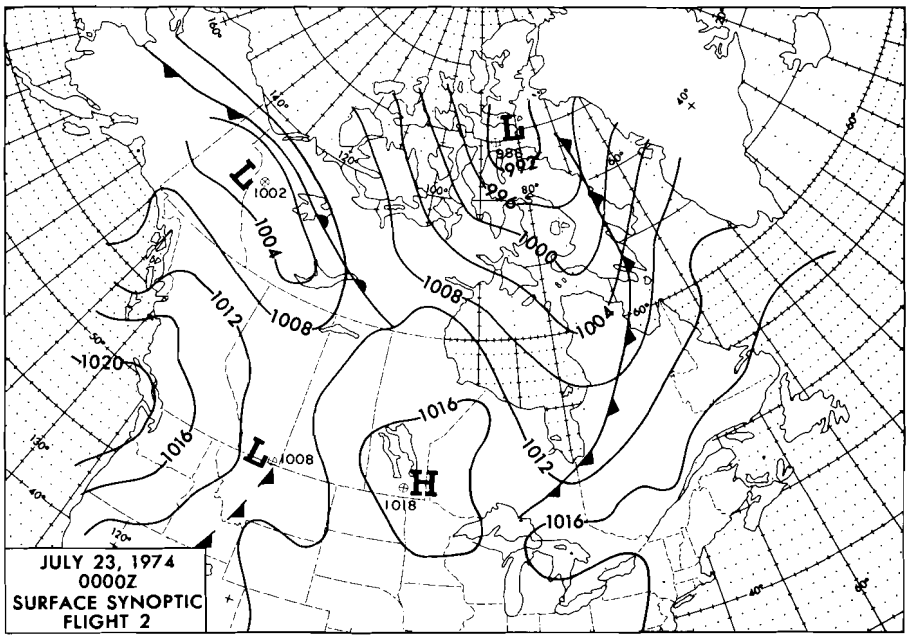


Fig. 2(a) Surface synoptic map for 0000 GMT 23 July 1974.

to the south of Devon Island with an extensive associated NW-SE trough reaching from Devon Island to just south of James Bay. This Low, which had been slowly weakening over a period of a few days, delayed the launch for two days, due to the associated poor weather conditions at Churchill. By early evening on the 21st, the ridge associated with the High (1018 mb) to the south of Lake Winnipeg pushed into the region bringing clear skies. Unfortunately, further delay was incurred due to the development of a strong surface gradient. However, on the 22nd, the gradient slackened sufficiently to permit a launch.

There were no significant jets at the 300-mb level during Flight 2, the strongest wind being 60 kt over Lake Winnipeg. Above Churchill itself the maximum winds aloft were less than 40 kt. From the 10-mb map in Fig. 2(b) for 1200 GMT 23 July 1974, it was determined that the winds along the float level flight path were from the SE at 20-30 kt. The trajectory of the second flight with a larger balloon of $3.3 \times 10^5 \text{ m}^3$ which floated at a higher maximum level of 6.3 mb is also indicated from launch at 2318 GMT 22 July until termination at 2156 GMT on 23 July. The surface weather conditions at Churchill during this launch were:

Wind: NE 5 kt.
 Temperature: 19°C.
 Pressure: 1014 mb, rising.

3 Temperature profiles

Figs. 3 and 4 show the vertical temperature profiles obtained from the

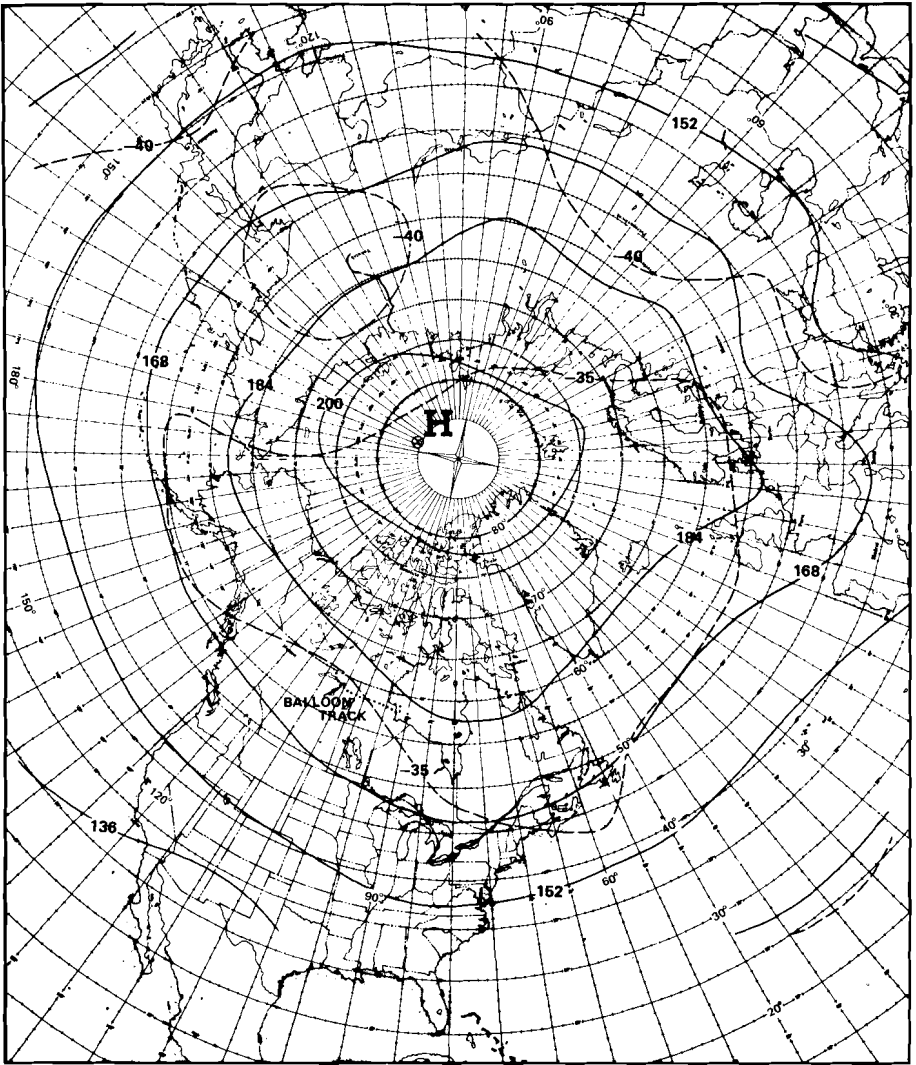


Fig. 2(b) 10-mb contour chart for 1200 GMT 23 July 1974. Dotted line west from Churchill shows balloon track.

ozonesondes launched during Flights 1 and 2, respectively. The solid dark line in all cases represents the U.S. standard atmosphere for July, 60°N.

The five soundings taken during Flight 1 do not deviate significantly from the standard atmosphere. However, for Flight 2 the soundings show a distinct inversion at 250 mb. From the inversion up to 45 mb the soundings are very close to the standard but at 45 mb the atmosphere becomes warmer than the standard, continuing so to the top of the soundings.

As additional information, we have included the temperature profiles

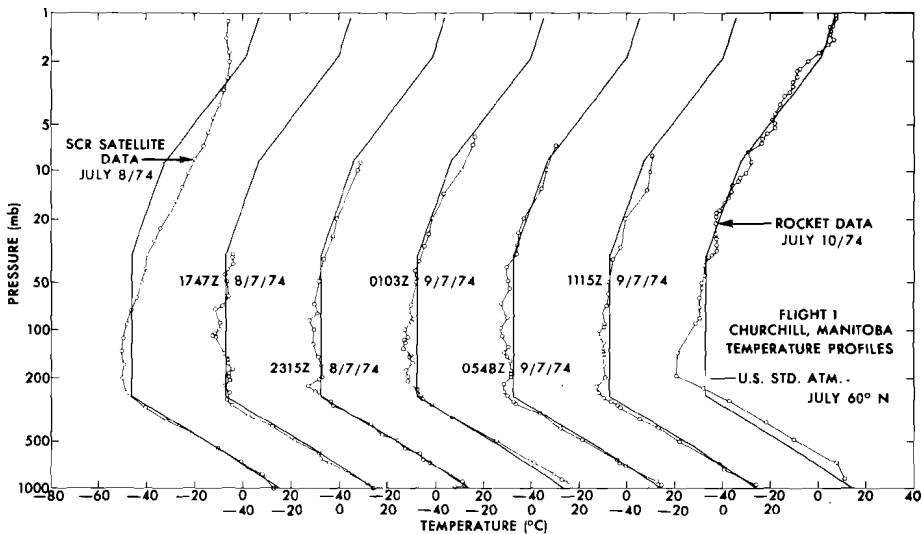


Fig. 3 Temperature profiles over Churchill on 8, 9, and 10 July 1974. Solid curves are U.S. Standard Atmosphere for 60°N in July.

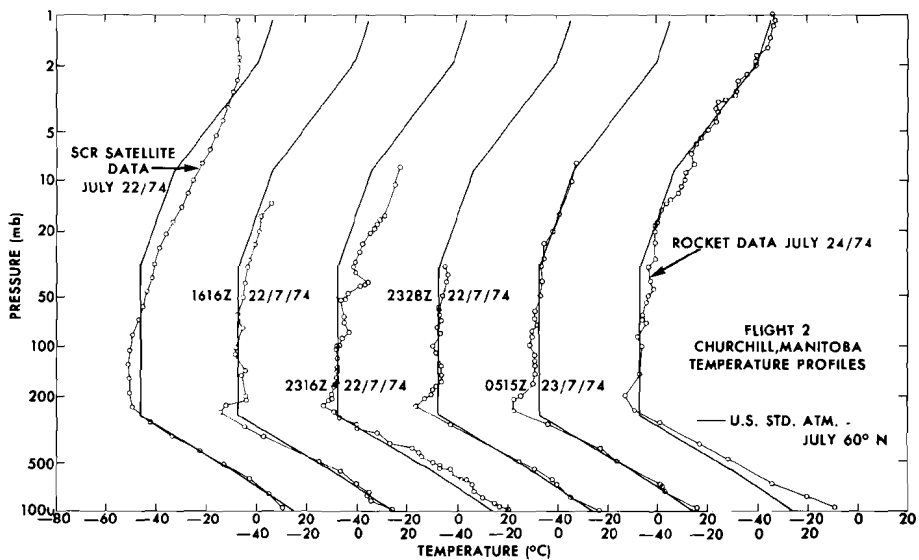


Fig. 4 Temperature profiles over Churchill on 22 and 23 July 1974. Solid curves are U.S. Standard Atmosphere for 60°N in July.

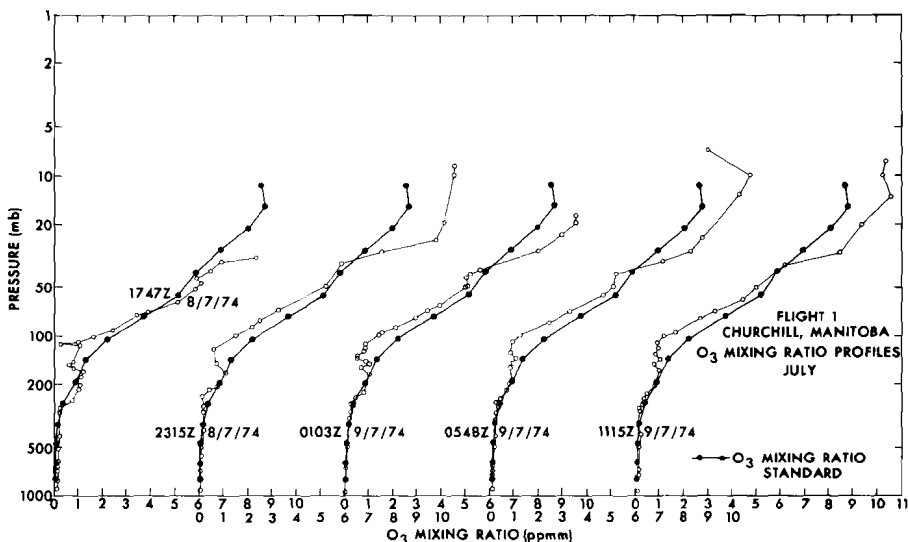


Fig. 5 Ozone mixing-ratio profiles over Churchill on 8 and 9 July 1974. Solid curves are July-August average from Hering and Borden (1965). (To convert to volume mixing ratio multiply by 0.60.)

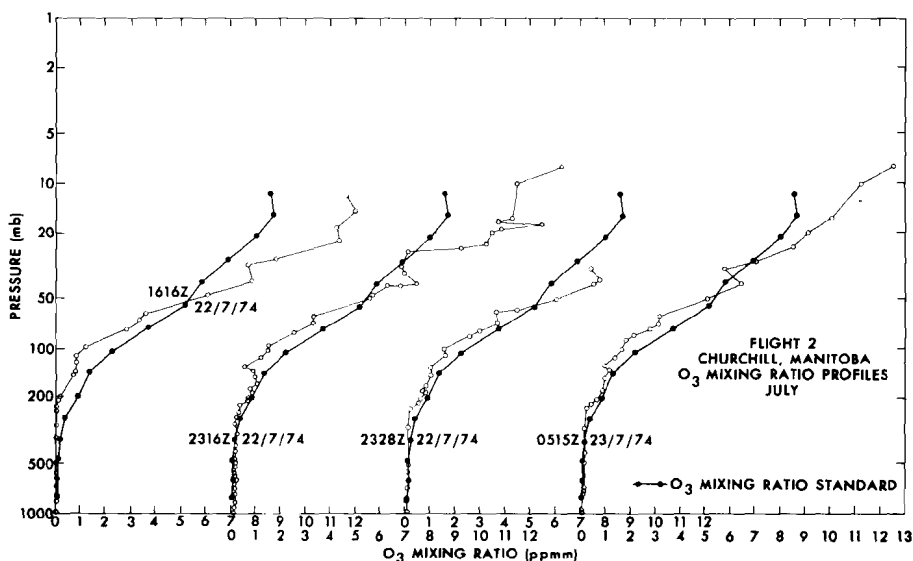


Fig. 6 Ozone mixing-ratio profiles over Churchill on July 22 and 23, 1974. Solid curves are July-August average from Hering and Borden (1965). (To convert to volume mixing ratio multiply by 0.60.)

obtained from rocketsonde data for 10 July and 24 July at Churchill and satellite inversion data from the SCR experiment on the NIMBUS 5 satellite. These data provide an extension of the radiosonde temperature data to higher levels. The obvious disagreement between the rocketsonde and satellite data is within the larger error of the satellite technique.

4 Ozone mixing-ratio profiles

Figs. 5 and 6 depict the vertical ozone mixing-ratio profiles for Flights 1 and 2, respectively. The solid dark line in each diagram represents the average ozone mixing-ratio profiles based on the July-August mean ozone densities calculated by Hering and Borden (1965) from 13 ozone soundings made at Churchill in 1963 and 1964.

The differences between the 1974 ozone soundings reported here and the average curve are typical of the variability to be expected at this latitude and season.

Acknowledgements

The authors wish to acknowledge the support of SED Systems Ltd., Saskatoon, the U.S. Office of Naval Research, and Raven Industries, North Dakota, for logistic support in the field operations; Mr. John Bellefleur and the staff of the Churchill Upper Air Station for taking the ozonesonde measurements, and Messrs. Sulev Sooviste and Larry Morrison for scaling and evaluating the ozonesonde data. We are indebted to Dr. E.J. Williamson, Oxford University, for providing evaluated temperature data from the NIMBUS 5 SCR experiment.

References

- | | |
|---|---|
| HERING, W.S. and T.R. BORDEN, 1965: Mean distribution of ozone density over North America, 1963-1964. USAF, Office of | Aerospace Research, Environmental Research Paper No. 162. |
|---|---|
-

The Measurement of Minor Stratospheric Constituent Concentrations by Far Infra-Red Emission Spectroscopy

T.A. Clark and D.J.W. Kendall

Physics Department, University of Calgary, Calgary, Alberta, T2N 1N4

[Manuscript received 9 February 1976]

ABSTRACT

Far infra-red stratospheric emission spectra recorded with a Michelson interferometer on board the AES balloon gondola during the 22–23 July 1974 flight from Churchill, Manitoba, are discussed and integrated column

densities of H_2O and O_3 derived for an altitude of 22 km. The possibility of detection of other constituents by present and future instrumentation is assessed.

1 Introduction

The far infra-red and submillimetre portions of the stratospheric emission spectrum are dominated by minor constituent emissions, particularly those of H_2O and O_3 . The major atmospheric components N_2 and O_2 are homopolar molecules with no electric dipole moment and do not exhibit pure rotational spectra in this region, while the two other relatively abundant constituents, the inert gas argon and the symmetric molecule CO_2 produce no far infra-red emission. The O_2 molecule does, however, possess a magnetic dipole moment, the weak rotational transitions of which produce a simple series of triplet lines through the far infra-red region which compete in intensity with those of H_2O and O_3 . Furthermore, their presence in the stratospheric spectrum leads to a method for minor constituent concentration determination by suitable normalization of the observed spectrum without the necessity for precise photometric calibration (Burroughs and Harries, 1970). This can be accomplished because the amount of O_2 at all altitudes in the stratosphere is both stable and well-known. Line strengths for these transitions can be calculated from the equations given for the dipole moment matrix elements by Tinkham and Strandberg (1955) (with minor corrections and modifications; see Gebbie *et al.*, 1969). These values have been verified by the laboratory measurements of Gebbie *et al.* (1969) to rather limited accuracy. Several groups have utilized this technique in the recent past to derive H_2O and O_3 concentrations as functions of latitude and altitude up to 15 km from aircraft measurements (Harries and Burroughs, 1971; Bussoletti and Baluteau, 1974). Many other minor but important constituents of the stratosphere show pure rotational spectra in this wavelength region, of sufficient strength to be detected in emission in the

stratosphere. Such molecular species as HNO_3 , N_2O , NO_2 have been detected at aircraft altitudes in the $10\text{--}35\text{ cm}^{-1}$ region by Harries *et al.* (1974a) and tentative concentration values obtained by utilizing line strength values derived from laboratory measurements by Fleming (1974).

These slowly varying emissions from uniformly distributed constituents in the stratosphere, in a spectral region where detector noise dominates all other sources of noise, are ideally suited to spectroscopic methods such as Michelson-Fourier spectroscopy in which the multiplex advantage and high instrumental throughput can be utilized. It is with this type of instrumentation that most of the advances in these measurements have been achieved in the past few years.

The present paper discusses the results obtained from a Michelson interferometer on one balloon flight of the AES of Canada gondola in July 1974 from Churchill, Manitoba (latitude 58.7°N , longitude 94°W) in the late evening hours, (0105 GMT 23 July 1974). A method is discussed for the normalization of the present spectra to the O_2 emissions when weak O_3 lines are contributing significantly to peak emissions in the O_2 and H_2O line positions. This method utilizes synthetic spectra derived from the programme compiled by McClatchey *et al.* (1973). Integrated column density values for H_2O and O_3 are derived by this method for spectra taken at 22 km during the above flight. The possibility of detection of other atmospheric constituents such as HCl , HNO_3 , NO_2 or N_2O is discussed in the context of the present results and some indication is given of the sensitivity of instrumentation used in flights during 1975, for which the data analysis is not yet completed.

These limiting values of minor constituents are compared to those expected from a combined absorption-emission experiment to be carried out with improved Michelson interferometers on a flight in 1976. A balloon-borne telescope successfully test-flown in 1975 will be utilized to provide the requisite solar steering in this experiment.

2 Experimental details

The Michelson interferometer used in the 1974 flights was a simple rapid-scanning instrument based on the NPL-Grubb-Parsons cube design equipped with plane mirrors and a $19\text{-}\mu\text{m}$ mylar beamsplitter. One mirror was mounted on a motor-driven precision-micrometer thread to produce the varying path difference between the divided beams. A toothed wheel and photo-cell system on the motor shaft provided mirror position information for digitization of the detector signal after the flight. The characteristics of the liquid-helium-cooled Ge(Ga) bolometer detector and its associated optics and filters are given in Table 1. Continuous scanning of the mirror produced characteristic signals (interferograms) whose highest frequency components (associated with the highest wave numbers of interest, $\sim 150\text{ cm}^{-1}$) corresponded to the approximate cut-off frequency of the detector element ($\sim 20\text{ Hz}$). The interferogram from this type of instrument represents the Fourier transform of the incident spectrum and post-flight computation of the inverse transform produces the emission spectrum.

TABLE 1. Instrument and flight details

<i>Detector</i>	Liquid-helium-cooled Ge(Ga) bolometer $NEP = 0.5 \times 10^{-13} \text{ W Hz}^{-1/2}$ (Infra Red Laboratories, Tucson, Arizona).
<i>Filters</i>	White polyethylene window, 4.8 mm (253K) Quartz wedge (77K) Black polyethylene 0.2 mm (77K) Mesh filter, cut-off 130 cm^{-1} (2K) PTFE blocking filter (2K) (C.P.S. Cambridge U.K.)
<i>Optics</i>	TPX lens 25 mm diameter $f/1.1$ (2K)
<i>Michelson Interferometer</i>	
<i>Beamsplitter</i>	Mylar $19 \mu\text{m}$ (Dupont Inc.)
<i>Mirror movement</i>	5.1 cm
<i>Time per scan</i>	70 s
<i>Viewing direction</i>	Zenith angle 75° , 180° from solar azimuth
<i>Flight</i>	
<i>Launch</i>	2318 GMT 22 July 1974
<i>Rate of Rise</i>	180 m/scan
<i>Height of Fig. 1 spectra</i>	21.5 km (47 mb) and 22.5 km (40.5 mb)
<i>Time of Data</i>	~ 0105 GMT 23 July 1974

The instrument was mounted with its field of view centered at a zenith angle of 75° in the anti-sun direction in azimuth, orientation in this direction being maintained by the solar steering device on the over-all gondola.

The detector characteristics were such that microphonic noise from the boiling helium severely degraded its signal-to-noise ratio until the λ point of the helium was reached at a pressure of 50 mb, after which time quiescent evaporation of the helium allowed the detector to operate at its design sensitivity. Good data were recorded from this altitude of 20.5 km for a period of 20 min after which the liquid helium supply unfortunately failed. A series of twelve good spectra were obtained in this time and have been analyzed to produce the present results.

3 Discussion of observed spectra

Fig. 1 shows two of the observed spectra between 20 and 130 cm^{-1} to a resolution of 0.2 cm^{-1} computed from 50-s sections of the interferogram records telemetered from the balloon. The reproducibility between these spectra taken in this short period by the rapid-scanning technique compares very favourably with that of other published spectra (Baluteau and Bussoletti, 1973) taken over much longer periods by phase-modulation methods and fully justifies the initial design decision. The expected positions and relative strengths of H_2O lines are indicated above these spectra while Q-branch and weak line positions of O_3 are shown below the spectra. The reference lines of O_2 are shown below those of O_3 . The quality of the data becomes relatively poor below 30 cm^{-1} because of poor instrument transmission and detector noise and above 130 cm^{-1} because of optical and electrical filter cut-off. The spectrum in the region around 47 cm^{-1} is superimposed upon a relatively wide but smooth peak which is thought to be an artifact of the instrument, although its

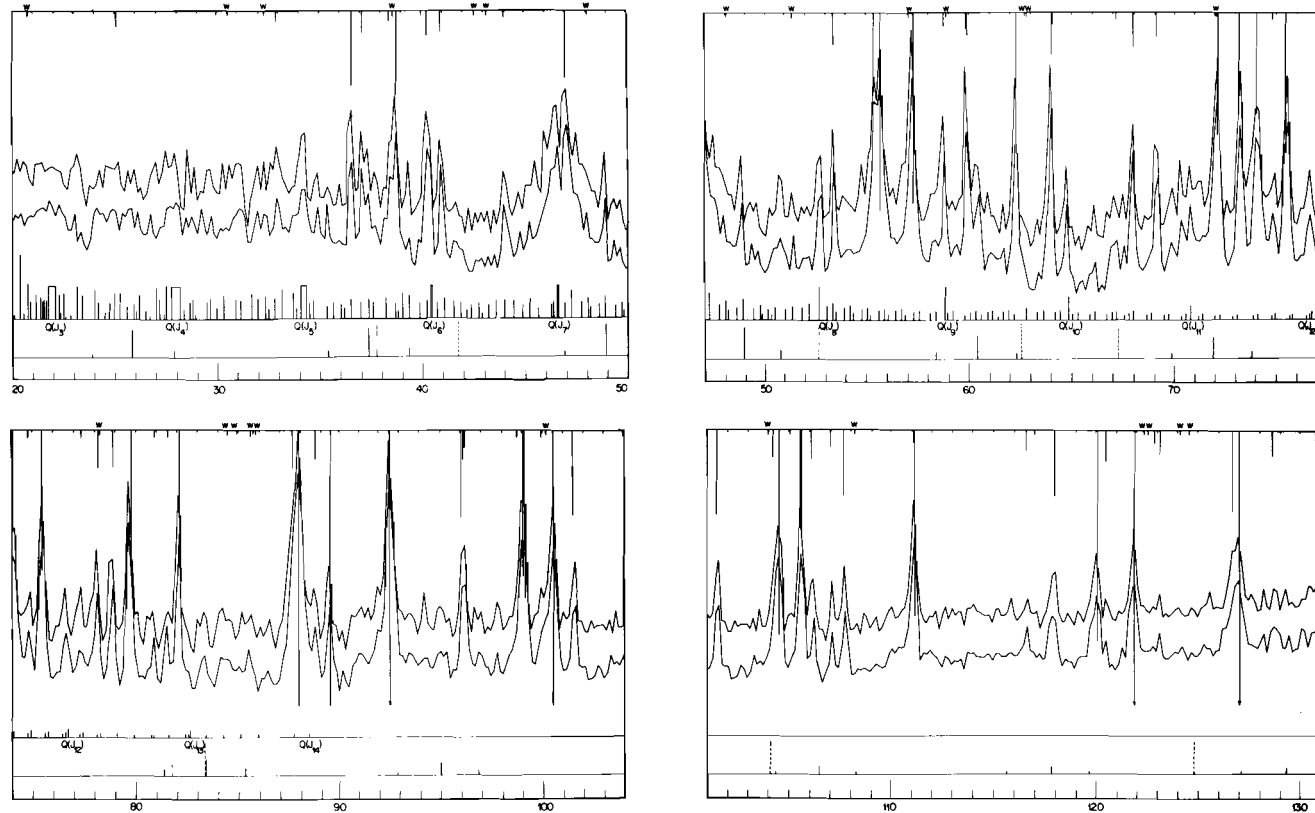


Fig. 1 Two spectra between 20 and 130 cm^{-1} to a resolution of 0.2 cm^{-1} , separated vertically to facilitate comparison. Line positions and relative strengths are indicated for the H_2O lines above the spectra while the O_3 Q-branch and weak line emissions are shown directly below the spectra. The reference O_2 lines are shown directly below the O_3 lines.

exact source is as yet unidentified. Except in these regions, the observed spectrum agrees extremely well with a calculated synthetic spectrum when allowance is made for instrumental transmission. The overall envelope on which the spectrum is superimposed has its origin in the fact that the central peaks of the interferograms overloaded the data telemetry. This background variation has little effect upon the analysis of limited portions of the spectrum for the determination of minor constituent concentrations, as has been shown by Harries and Burroughs (1971).

The dominant lines of this spectrum are from H_2O with several lines showing considerable width in the wings, and Q-branch emissions of O_3 which can be identified up to wave numbers of 80 cm^{-1} . The O_2 pure rotation lines are weaker than these other constituents but the strong central line of each triplet can be easily identified as far as 95 cm^{-1} except where strong blending occurs. Weak O_3 lines dominate the regions between lines as far as about 70 cm^{-1} making the identification of lines from other constituents relatively difficult in these regions. It is on the basis of these O_3 lines that a lower limit can be set on the sensitivity of this type of equipment for the detection of minor constituents.

No emissions from other minor constituents have been unambiguously identified in these spectra but several significant peaks are worthy of further consideration. Detailed comparison of selected portions of an average of four spectra with a single-layer calculation of a synthetic spectrum for H_2O , O_2 and O_3 at a temperature of 220K has led to several tentative identifications. Such a comparison of the averaged spectrum uncorrected for instrument transmission (varying relatively rapidly in this region) with the calculated emissivity over a limited wave number range containing two regions of interest is shown in Fig. 2. The synthetic spectrum has been convoluted with a sinc^2x function appropriate to an apodized interferogram (see Chantry, 1971).

The observed spectral shape near expected HCl emission at 41.7 cm^{-1} does not match the synthetic spectrum closely, whereas weak O_3 lines do match closely in nearby spectral regions. It is tempting to assign this observed emission to HCl although estimated column density on the basis of quoted line strength (Sanderson, 1967) is considerably above other measurements (e.g., Farmer, 1974). More definitive identification must await analysis of higher resolution spectra. The presence of the isotopic pairs of lines from HCl^{35} and HCl^{37} should serve to make this identification somewhat simpler than for other constituents.

A similar situation of high predicted column density also occurs in the case of NO_2 in which Q-branch emissions at 37.8 cm^{-1} are tentatively identified between the O_2 line at 37.3 cm^{-1} and the H_2O line at 38.8 cm^{-1} even when revised line strengths from Fleming's work given by Harries *et al.* (1974b) are used. There is some indication that aircraft data from these authors also leads to abnormally high NO_2 mixing ratios on the basis of this Q-branch emission.

Considerable structure is seen between strong lines beyond about 60 cm^{-1} which exceeds that predicted by the synthesis calculations and on the basis of coincidence between several predicted line positions and observed peaks it is

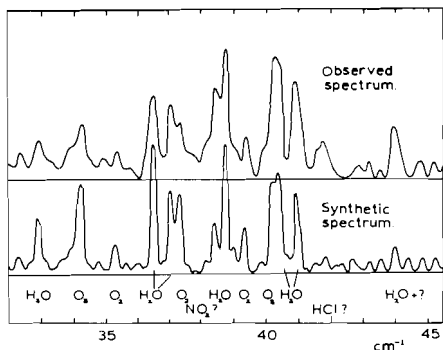


Fig. 2

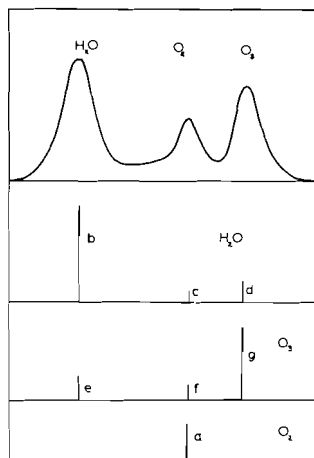


Fig. 3

Fig. 2 Expanded section of an average of four spectra between 32 and 45 cm^{-1} , compared to a calculated synthesis of the expected emissivity from an atmosphere at 220K, with column densities of 1.15×10^{18} molecules cm^{-2} for H_2O , 5×10^{18} molecules cm^{-2} for O_3 and 1.56×10^{23} molecules cm^{-2} for O_2 .

Fig. 3 Sketch of a typical spectral region containing lines from H_2O and O_2 and a Q branch of O_3 , with blended weak lines from O_3 and H_2O . Contributions at the peak from each constituent are assigned the letters a to g .

tempting to assign these to HDO and CO lines. Again, predicted intensities are considerably below the observed peak heights.

These results indicate that some part of the analysis procedure or one or other of the initial assumptions is suspect and this matter is being actively pursued at the present time. Should it be found that expected amounts of these constituents do in fact contribute the observed level of emission then the estimated limits for these constituents given later in this paper will require revision.

4 Method of normalization of the spectra

The determination of integrated column densities for H_2O and O_3 in the stratosphere from the observed spectra requires the correct normalization of spectra to the O_2 lines, whose line strengths are known and whose concentration can be easily determined. This normalization, while relatively easy to make for spectra taken at aircraft altitudes, where H_2O lines and Q -branch O_3 emissions are strong, is made difficult at balloon altitude because of the greater contribution to the overall spectrum from weak O_3 and H_2O lines, particularly in blends with stronger lines. It is necessary to allow for these weak-line contributions at the peak positions of strong lines. The following method utilizes synthetic spectra from the AFCRL programme (McClatchey *et al.*, 1973) to achieve a normalization.

A sketch of a typical spectral region of limited extent containing H_2O , O_2 and Q -branch peaks is shown in Fig. 3. The unknown contributions from the

three constituents at the peak positions of these three lines are indicated by lines below this spectrum and designated by the letters *a* to *g*. Assumptions made at this stage are that the equivalent black-body curve for the assumed atmospheric temperature does not vary significantly over the chosen wave number range and that the instrumental line width is considerably greater than the emission line width at this altitude, particularly the equivalent *Q*-branch width. Ratios of observed peak heights $R_1 = (b + e)/(a + c + f)$ and $R_2 = (d + g)/(a + c + f)$ for the H_2O and O_3 peaks compared to that of the O_2 peak can be obtained from the observed spectra. These ratios can be expressed in terms of auxiliary ratios $r_1 = c/b$, $r_2 = d/b$, $r_3 = e/g$ and $r_4 = f/g$ which can be obtained from synthetic spectra for individual constituents, these ratios being slowly varying functions of integrated column density. The ratios $x = b/a$ and $y = g/a$ represent the true ratios of peak heights of H_2O and O_3 *Q*-branch to the O_2 line, respectively. Thus, if r_1 , r_2 , r_3 , and r_4 can be determined by assumption of a reasonable value of integrated column density for each constituent (i.e., to the correct order of magnitude) then the required ratios x and y can be written as

$$x = \frac{(R_1 - r_3 R_2)}{D} \quad \text{and} \quad y = \frac{(R_2 - r_2 R_1)}{D}$$

where $D = (1 - r_4 R_2) (1 - r_1 R_1) - (r_4 R_1 - r_3) (r_1 R_2 - r_2)$. Values of integrated column density for each constituent can thus be obtained from these x and y values for the synthetic spectra.

Errors can arise in a number of ways in this method, not the least of which is the use of peak heights rather than integrated area under a line, and the assumption of order-of-magnitude values for constituent column densities for determining r_1 to r_4 . It is important that the correct instrument convolution function be used in the synthesis since the "feet" of this function (particularly for unapodized interferograms for which this function is $\text{sinc } x$) will substantially affect closely adjacent lines.

Nevertheless, the method is expected to produce reasonable values from which a detailed fit to the overall synthetic spectrum can be made when account is taken of the instrument transmission function. The comparison method gives vertical column density directly and the extent of the correction applied by this normalization procedure in the present spectra is found to be as high as 80% for H_2O and 40% for O_3 .

5 Results

Measurements on eight combinations of lines from these spectra have resulted in mean values of integrated column densities after application of the normalization procedure of $1.1(\pm 0.7) \times 10^{18}$ molecules cm^{-2} for H_2O and $5.0(\pm 1.8) \times 10^{18}$ molecules cm^{-2} for O_3 above 22 km, which compare favourably with other observations at this altitude and on this particular flight. The method depends critically on the correctness of the synthetic spectrum as well as upon other factors already mentioned. Initial indications are that at

least in the case of certain specific lines, the model is in error and that this might have contributed to the wide spread in values from which these average column densities were derived.

6 Estimation of limiting sensitivity for constituents of interest

In order to provide an assessment of the usefulness of the present technique and to produce design figures for future experiments both in emission and in solar absorption, a rough estimate has been made of the expected signal-to-noise ratio for various constituents on the basis of the present spectra. The noise level on the spectra was obtained by comparison of fluctuations both in peak heights and in relatively line-free regions between the twelve observed spectra. Line strengths of detected weak O_3 lines which were considered to be about twice this noise level were used to provide a limiting value for the equivalent width, which for weak lines is simply given by $W = Sag(\phi)$, where S is the line strength of the particular transition, a is the integrated column density in the vertical direction and g is a geometric factor dependent upon zenith angle ($g(\phi) = \sec \phi$ for $\phi \leq 80^\circ$). The equivalent width for these peaks, using $a = 5.0 \times 10^{18}$ molecules cm^{-2} obtained earlier, is found to be about $5 \times 10^{-3} \text{ cm}^{-1}$. Using this figure the limiting value of a can be estimated for any constituent, and the limiting mixing ratio found by assumption of a constant scale height between constituents equivalent to that of the overall atmosphere of $8 \times 10^5 \text{ cm}$. Thus a ratio of detectable mixing ratio m_d (to a S/N ratio of 2 in the spectrum) to presently accepted mixing ratio m can be derived and for the present situation $m_d = 9.25 \times 10^{-28}/S$ where S is the line strength for the chosen line of each constituent. The estimate for future emission experiments is made on the assumption that improved resolution (by a factor of 4) and improved S/N ratio ($\times 2$) will be achieved and that viewing down to 90° will also significantly increase detectability of these weak lines (by a factor of 2). Thus, an overall improvement of 16 is expected. For the absorption experiment, the solar intensity should be substantially higher than that from the atmosphere and a further gain of about a factor of 10 is included in the calculation. The limiting mixing ratios are listed in Table 2 for each of the constituents for which line strength estimates are available. These have come from the work of Fleming (1974) and Sanderson (1967) (HCl) and Rosenberg *et al.* (1972) and Fox (1971) (CH_4). Notwithstanding the uncertainties in the quantities used in this estimate, the values in Table 2 give a good indication of the usefulness of the technique and will help in design of future instrumentation. Fig. 4 shows graphically the ratio of typical m/m_d for each constituent and each category of experiment.

7 Conclusions

The present technique of far infra-red emission spectroscopy utilizing high efficiency Fourier spectroscopy and helium bolometric detectors has been shown in this initial test flight to give reproducible spectra from which constituent concentrations of H_2O and O_3 can be derived at balloon altitudes,

TABLE 2. Estimated limiting detectable mixing ratios for various molecular species

Molecular Species	Wave Number cm^{-1}	Typical Line Strength S cm^{-1} $(\text{molec cm}^{-2})^{-1}$	Detectable Mixing Ratio (m_d) (Conditions of Observation)			Typical Mixing Ratio
			Emission 75° $\Delta\nu = 0.2 \text{ cm}^{-1}$ $W = 5 \times 10^{-3} \text{ cm}^{-1}$ (1974)	Emission 90° $\Delta\nu = 0.05 \text{ cm}^{-1}$ $W = 5 \times 10^{-3} \text{ cm}^{-1}$ (Future)	Absorption 90° $\Delta\nu = 0.05 \text{ cm}^{-1}$ $W = 2.5 \times 10^{-4} \text{ cm}^{-1}$ (Future)	
H_2O	30.56 (weak)	0.143×10^{-20}	6.5×10^{-7}	4×10^{-8}	4×10^{-9}	$1-3 \times 10^{-6}$
O_3	54.214 (weak)	0.137×10^{-20}	6.75×10^{-7}	4.2×10^{-8}	4.2×10^{-9}	7×10^{-6}
HNO_3	~32	6.2×10^{-20}	1.49×10^{-8}	9.3×10^{-10}	9.3×10^{-11}	5×10^{-9}
HCl	41.7	1.5×10^{-18}	6.17×10^{-10}	3.9×10^{-11}	3.9×10^{-12}	1.5×10^{-10}
N_2O	~18	4.1×10^{-22}	2.26×10^{-6}	1.4×10^{-7}	1.4×10^{-8}	3×10^{-7}
CO	50-60	1.1×10^{-21}	8.4×10^{-7}	5.3×10^{-8}	5.3×10^{-9}	10^{-7}
NO_2	37.8	1.9×10^{-20}	4.9×10^{-8}	3×10^{-9}	3×10^{-10}	$2-6 \times 10^{-9}$
CH_4	94.2	1.2×10^{-23}	7.7×10^{-5}	4.8×10^{-6}	4.8×10^{-7}	8×10^{-7}
NO	~30	7.4×10^{-22}	1.25×10^{-6}	7.8×10^{-8}	7.8×10^{-9}	$\sim 10^{-9}$
SO_2	28.8	8.8×10^{-21}	1.1×10^{-7}	6.6×10^{-9}	6.6×10^{-10}	1.6×10^{-10}

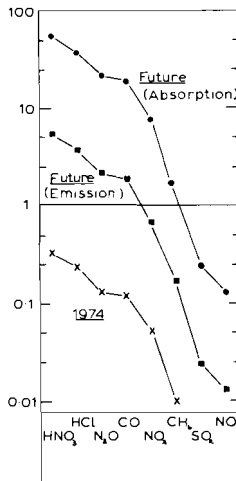


Fig. 4 Diagrammatic representation of the expected detectability of trace constituents, on the basis of weak O_3 line detection in the present experiment. The ratio of typical volume mixing ratio to the estimated measurable mixing ratio (m/m_d) is shown for each constituent in order of decreasing detectability.

when correct account is taken of weak lines contaminating H_2O and O_3 peaks in relatively low-resolution spectra. A recent report by Harries *et al.* (1976) of higher resolution data over a range of altitudes and zenith angles from 15 to 35 km indicates that reliable measures of mixing ratios for other constituents such as HNO_3 and NO_2 can be derived. Estimates of the potential detectability of future instrumentation show that this type of experiment should yield good estimates of constituent concentrations. In particular, it is demonstrated that it should be possible to obtain good measurements of pure rotational spectral lines of the environmentally important molecule HCl at two specific wavelengths in the far infra-red with equipment flown on the 1975 flight series and instruments being prepared for the combined emission/absorption flight in the 1976 flight season.

It is unfortunate that premature failure of the cryogenic coolant system prevented this instrument from operating through the important sunset and sunrise periods. New coolant vessels have resulted in considerably enhanced cryogen lifetimes and high-resolution data from redesigned Michelson interferometers mounted on a tilting arrangement for limb scanning should provide measurements of temporal and altitude changes of the minor constituents discussed earlier.

In view of the importance of the O_2 magnetic dipole emissions in the determination of concentrations in the stratosphere, further laboratory work is urgently needed to verify the theoretical line strength predictions for these lines, particularly beyond 65 cm^{-1} .

The combined technique of emission and solar absorption in future flights should provide more precise altitude profiles of these constituents since the solar pointing control accuracy is sufficient to provide beam widths through

the atmosphere of fractions of a degree and this is essential for the accurate derivation of altitude profiles when the constituent exists in narrow layers, as pointed out by Farmer (1974). The continuously scanning emission measurements will monitor important temporal changes during the vital sunset and sunrise periods.

Acknowledgements

It is a pleasure for the authors to thank the Atmospheric Environment Service and the National Research Council for the funding required to successfully carry out this experiment. The tireless assistance of Mr. R. Wytsma throughout the flight period is acknowledged, and the authors are grateful for the willing and important assistance rendered by SED Systems personnel during the whole pre-flight preparations.

References

- BALUTEAU, J.P., and E. BUSSOLETTI, 1973: High resolution spectra of the stratosphere between 30 and 200 cm^{-1} . *Nature*, **241**, 113-114.
- BURROUGHS, W.J., and J.E. HARRIES, 1970: Direct method of measuring stratospheric water vapour mixing ratios. *Nature*, **227**, 824-825.
- BUSSOLETTI, E., and J.P. BALUTEAU, 1974: Determination of $\text{H}_2\text{O}/\text{O}_2$ stratospheric mixing ratio from high resolution spectra in the far infrared. *I. R. Phys.*, **14**, 293-302.
- CHANTRY, G.W., 1971: *Submillimetre Spectroscopy*. Academic Press.
- FARMER, C.B., 1974: Infrared measurements of stratospheric composition. *Can. J. Chem.*, **52**, 1544-1558.
- FLEMING, J.W., 1974: High resolution far infrared studies of the absorption spectra of gases. N.P.L. Report on Materials Applications, No. 34.
- FOX, K., 1971: Theory of pure rotational transitions in the vibronic ground state of methane. *Phys. Rev. Letters*, **27**, 233.
- GEBBIE, H.A., W.J. BURROUGHS, and G.R. BIRD, 1969: Magnetic dipole rotation spectrum of O_2 . *Proc. Roy. Soc.*, **A310**, 579-590.
- HARRIES, J.E., and W.J. BURROUGHS, 1971: Measurements of submillimetre wavelength radiation emitted by the stratosphere. *Quart. J. Roy. Meteor. Soc.*, **97**, 519-536.
- , D.G. MOSS and N.R. SWANN, 1974a: H_2O , O_3 , N_2O and HNO_3 in the Arctic stratosphere. *Nature*, **250**, 475-476.
- , ——, N.R.W. SWANN, G.F. NEILL and P. GILDWARG, 1976: Simultaneous measurements of H_2O , NO_2 and HNO_3 in the daytime stratosphere from 15 to 35 km. *Nature*, **259**, 301.
- , N.W.B. STONE, J.R. BIRCH, N.R. SWANN, G.F. NEILL, J.W. FLEMING and D.G. MOSS, Jan. 1974b: Submillimetre wave observations of stratospheric composition. Proc. Int. Conf. on Structure, Composition and General Circulation of Upper and Lower Atmosphere, 275-291.
- MCCLATCHEY, R.A., W.S. BENEDICT, S.A. CLOUGH, D.E. BURCH, R.F. CALFEE, K. FOX, L.S. ROTHMAN and J.S. GARING, 1973: AFCRL atmospheric absorption line parameters compilation. AFCRL-TR-73-0096, Environmental Research Papers, No. 434.
- ROSENBERG, A., I. OZIER, and A.K. KUDIAN, 1972: Pure rotational spectrum of CH_4 . *J. Chem. Phys.*, **57**, 568.
- SANDERSON, R.B., 1967: Measurement of Rotational Line Strengths in HCl by Asymmetric Fourier Transform Techniques. *Appl. Opt.*, **6**, 1527-1530.
- TINKHAM, M., and M.V.P. STRANDBERG, 1955: Theory of the Fine Structure of the Molecular Oxygen Ground State. *Phys. Rev.*, **97**, 937-951.

Measurement of Stratospheric Nitrogen Dioxide from the AES Stratospheric Balloon Program

J.B. Kerr and C.T. McElroy

*Atmospheric Environment Service,
4905 Dufferin St., Downsview, M3H 5T4*

[Manuscript received 3 February 1976; in revised form 14 June 1976]

ABSTRACT

A spectrophotometer which is capable of measuring atmospheric nitrogen dioxide by remote sensing has been included on board the STRATOPROBE I and II balloon programs. The results obtained from the STRATO-

PROBE I flight from Churchill, Manitoba, on 22 July 1974, and preliminary results from the STRATOPROBE II flights from Yorkton, Saskatchewan on 17-18 August 1975, will be presented here.

1 Introduction

Nitrogen dioxide has strong absorption bands in the visible and near ultraviolet regions of the spectrum and for wavelengths between 430 and 450 nm the absorption varies rapidly with wavelength. This permits the measurement of atmospheric NO_2 by measuring its relative absorption of sunlight, using methods similar to those which are used to measure atmospheric ozone.

A program to measure atmospheric NO_2 was established in 1972 by Prof. A.W. Brewer at the University of Toronto. A spectrophotometer which was originally designed to measure ozone (Brewer, 1973) was adapted to measure NO_2 . The instrument is a modified 15-cm Ebert spectrophotometer which is capable of measuring simultaneously the light intensity at three wavelength intervals with a resolution of 0.5 nm. Earlier ground- and aircraft-based results have been formally reported (Brewer *et al.*, 1973, 1974). The program has been extended to be included in the AES stratospheric balloon projects during the summers of 1974 and 1975. Results from the 1974 program and some preliminary results from the 1975 program will be given here.

2 Method of measurement

The amount of NO_2 is determined by measuring the intensity of sunlight after it has been absorbed by atmospheric NO_2 . The intensity of sunlight at an isolated wavelength λ , after passing through the atmosphere, is given by:

$$\log_{10} I_{\lambda} = \log_{10} I_{0\lambda} - \alpha_{\lambda}X - \beta_{\lambda}m, \quad (1)$$

where $I_{0\lambda}$ is the intensity of sunlight outside the atmosphere at wavelength λ ,

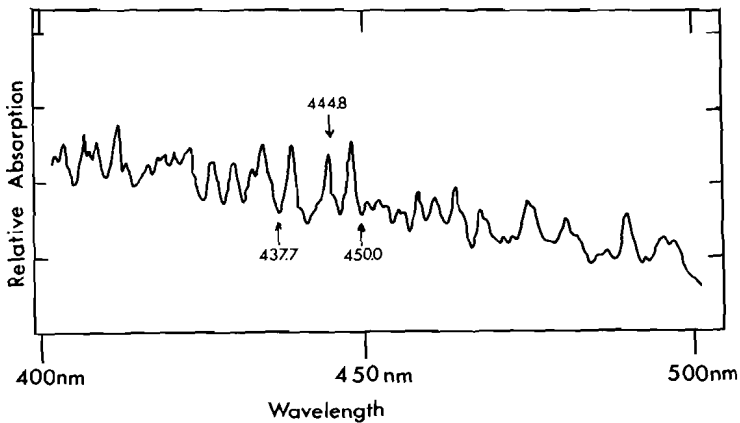


FIG. 1 The absorption spectrum of NO_2 (from Hall and Blacett, 1952) as measured at $25^\circ C$. The three wavelengths used in this work are indicated by arrows.

- α_λ is the decimal absorption coefficient of NO_2 (in cm^{-1}) at wavelength λ ,
- X is the optical depth (in cm at STP) of NO_2 in the path,
- β_λ is the Rayleigh scattering coefficient (per standard atmosphere) at wavelength λ , and
- m is the number of standard atmospheres in the optical path.

We measure light at three wavelengths in the NO_2 absorption spectrum with a resolution of 0.5 nm: $\lambda_1 = 437.7$ nm, $\lambda_2 = 444.8$ nm, and $\lambda_3 = 450.0$ nm. The NO_2 absorption at these three wavelengths, as indicated in Fig. 1, has a large variation with wavelength. The light intensity at each of the three wavelengths may be expressed in three equations similar to (1) with subscripts 1, 2, and 3 designating wavelengths λ_1 , λ_2 and λ_3 . It is now possible to form a combination of equations such as (1):

$$\log_{10} \frac{I_1}{I_2} - 1.46 \log_{10} \frac{I_2}{I_3} = \log_{10} \frac{I_{o1}}{I_{o2}} - 1.46 \log_{10} \frac{I_{o2}}{I_{o3}} - \Delta\Delta\alpha X$$

or
$$F = F_o - \Delta\Delta\alpha X \tag{2}$$

where
$$\Delta\Delta\alpha = (\alpha_1 - \alpha_2) - 1.46(\alpha_2 - \alpha_3) = -7 \text{ cm}^{-1}$$

and
$$1.46 = \frac{\beta_1 - \beta_2}{\beta_2 - \beta_3} = \text{weighting factor used to eliminate Rayleigh scattering.}$$

The weighting of light intensities given in (2) is such that F , our measured quantity, has maximum sensitivity to NO_2 and negligible sensitivity to Rayleigh scattering and all other effects which have slow monotonic wavelength dependence. Ozone absorbs at these wavelengths; however, its absorption is small and also nearly linear with wavelength. Using the absorption coefficients given by Vigroux (1953) and a typical ozone distribution, the effect of ozone on a measurement of F is about 4% that of NO_2 . This correction may be easily

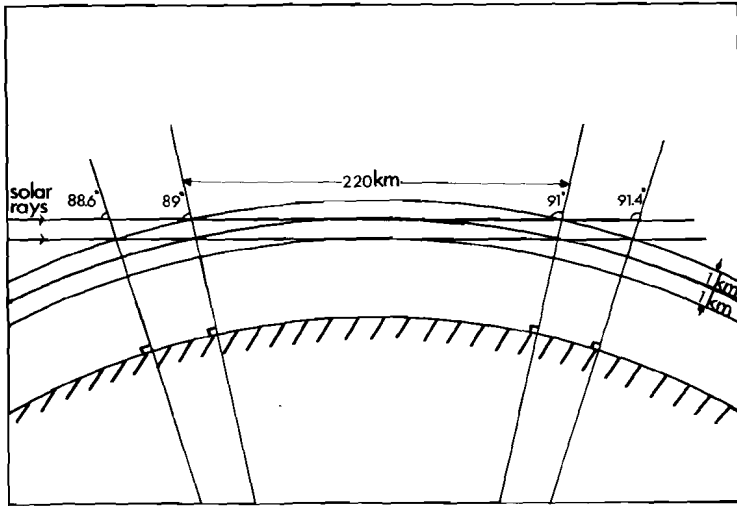


Fig. 2 The geometry of the tangent path technique. Tangent rays are approximately 220 km for 1-km-thick layers. A profile for NO_2 may be determined by comparing measurements at symmetric solar angles about 0° elevation. The effects of balloon-altitude changes during twilight may also be compensated.

applied to our measurements. We know of no other stratospheric constituent which absorbs light in such a way as to interfere with our measurements and we have carried out tests which indicate no interference caused by another stratospheric substance.

From our measurement of F we may deduce the amount of NO_2 in the solar path provided we know F_0 . From a balloon platform at 35 km it is possible to measure F_0 directly when the sun is higher than 20° elevation because the amount of NO_2 in the solar path is then negligible.

We have used our instrument to make laboratory measurements of $\Delta\alpha$ for NO_2 at room temperature and atmospheric pressure, and have found a value of -7.0 cm^{-1} . This value compares favourably with -5.91 cm^{-1} from Hall and Blacet (1952) and -8.17 cm^{-1} given by Johnston (1974). The absorption coefficient was found to be independent of pressure. Bass *et al.* (1976) have measured the effects of temperature on NO_2 absorption between 185 nm and 410 nm and for wavelengths at 410 nm they indicate about 10% less absorption at 235K than at room temperature. The effects of temperature on our $\Delta\alpha$ in the wavelength region between 430 nm and 450 nm have yet to be measured.

Vertical profiles of NO_2 may be measured quite accurately from a balloon during sunrise and sunset. This is accomplished by taking advantage of the very long tangential path lengths which result when the sunlight passes through the atmosphere below the balloon. For example, a ray tangent through a 1-km thick shell traverses a path of about 220 km through that shell. The geometry of this is shown in Fig. 2. The vertical profile is measured by first determining

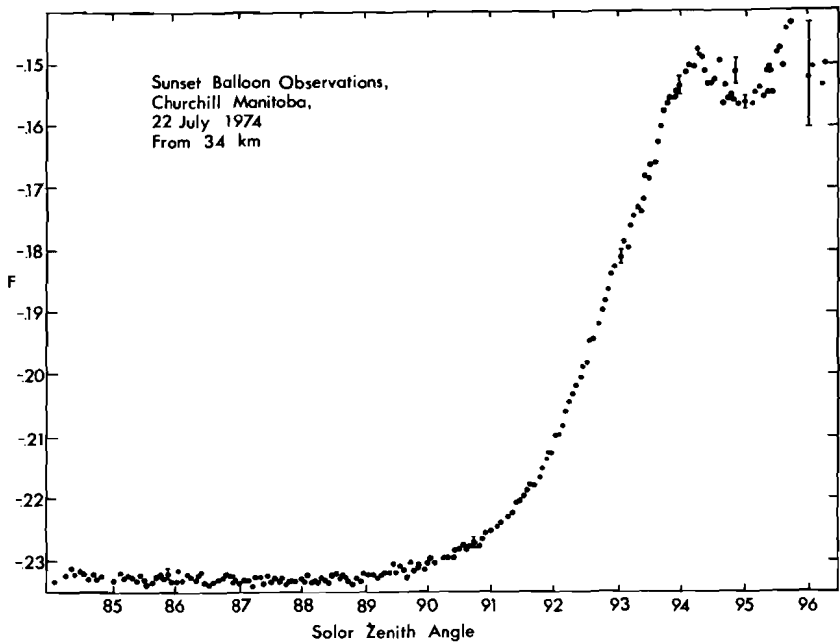


Fig. 3 The function F as a function of solar zenith angle as measured during sunset on July 22, 1974 from a height of 34 km. F increases during sunset because the sun's rays pass through atmospheric NO_2 . The shape of this curve is used to determine a unique vertical profile of NO_2 . Error bars indicate the error due to Poisson noise for an individual point.

the amount of NO_2 in the layer directly below the balloon and then proceeding to lower and lower layers.

3 Results

The usual timetable for the balloon flights allowed a late afternoon launch with the payload reaching float altitude about one hour before 0° solar elevation. Direct sun measurements were taken during sunset and during sunrise the next morning.

The evening measurements from the Churchill flight of 22 July 1974, are shown in Fig. 3. Meteorological conditions during the flight are given by Bain *et al.* (1976, this issue). The morning measurements of this flight are not available because of an instrument failure in the extreme cold overnight. This problem was rectified for subsequent flights. Fig. 3 shows the increase of F during sunset. This is caused by more and more NO_2 absorption as the sun's rays pass deeper and deeper through the earth's atmosphere. The error bars indicated in Fig. 3 are the single point errors which are estimated from the Poisson noise of photon counting.

The values of F in Fig. 3 were used to determine a unique vertical profile of NO_2 . Fig. 4 shows the reduced evening profile for the Churchill flight as

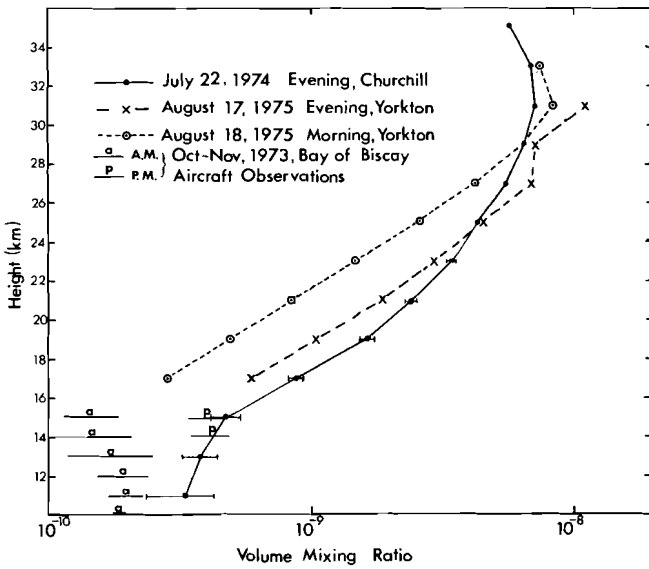


Fig. 4 Three measured profiles of NO_2 : sunset 22 July 1974; sunset 17 August 1975; and sunrise 18 August 1975. The range of aircraft measurements made with a different NO_2 instrument from a height of 15 km during October and November 1973 are also shown. The continuity between the aircraft measurements and the balloon measurements is quite consistent considering there is a spatial and time difference between the two sets of observations. This figure illustrates the difference between morning and evening NO_2 profiles. The estimated absolute error for all profiles is $\pm 20\%$. The error bars on the profile of 22 July indicate the estimated relative error due to Poisson noise.

well as the preliminary evening and morning profiles for the flight of 17–18 August 1975 from Yorkton, Saskatchewan. Also included in this diagram are previous measurements made from on board an aircraft at a height of 15 km during October and November 1973 (Brewer *et al.*, 1974).

In the reduction from the absorption as a function of zenith angle to NO_2 concentration as a function of height, corrections have been made to account for atmospheric refraction. The effect of refraction is to make the apparent position of the sun higher than its actual position. Consequently, the solar rays pass through the atmosphere at a higher tangent height than that which would be expected if refraction were neglected. Because the tangent rays are higher, the overall path length through the atmosphere is reduced. As a result, the concentration of NO_2 is corrected to larger values by about 5 to 10% between 10 and 15 km and less than that above 15 km.

The effects of the finite diameter of the sun have also been considered in the data reduction. As with refraction, the apparent position of the sun is raised. This is because the lower part of the sun is attenuated significantly more than the upper part. Incorporated into this correction is the fact that the limb of the sun is less bright than the centre of the solar disk. It was found that the

finite sun correction is about 15% of the correction due to atmospheric refraction.

The data in Fig. 4 illustrate one interesting feature. We have previously found that for lower altitudes there is usually a significant amount more NO_2 in the evening than in the morning, as indicated by the aircraft measurements. The results of the balloon measurements indicate that this diurnal variation is present but perhaps less pronounced at 30 km. The larger amounts of NO_2 at dusk may be explained by the slow dissociation of N_2O_5 into NO_2 and NO_3 during the day and the recombination of NO_2 and NO_3 to form N_2O_5 at night. A further discussion of this photochemical process is given by Evans *et al.* (1976, this issue).

In all, two morning and two evening profiles will be obtained from the 1975 program. It is hoped that these results and those of flights which are being planned for the future will contribute to a better understanding of the composition and photochemistry of our atmosphere.

Acknowledgements

We would like to thank those who have assisted us in this experiment. Professor A.W. Brewer of the University of Toronto has been very helpful with his suggestions and comments. SED Systems Ltd., designed, constructed, and operated the payload gondola during the STRATOPROBE programs. Raven Industries Ltd., provided the balloon launch services for the STRATOPROBE I program from Churchill. The National Center for Atmospheric Research provided the balloon launch services for the STRATOPROBE II program from Yorkton.

References

- BAIN, S.E., C.L. MATEER, and W.F.J. EVANS, 1976: Meteorological and ozone data for the project STRATOPROBE balloon flights of 8 and 22 July, 1974. *Atmosphere*, **14**, 147-154.
- BASS, A.M., A.H. LAUFER, and A.E. LEDFORD, JR., 1976: The absorption of NO_2 and N_2O_4 as a function of temperature (185 nm - 410 nm). *Journal of Research, N.B.S.*, in press.
- BREWER, A.W., 1973: A replacement for the Dobson spectrophotometer? *Pure and Applied Geophysics*, **106-108**, 919.
- , C.T. MCELROY, and J.B. KERR, 1973: Nitrogen dioxide concentrations in the atmosphere. *Nature*, **246**, p. 129.
- , ———, ———, 1974: Spectrophotometric nitrogen dioxide measurements. Proc. Third Conf. on the Climatic Impact Assess. Prog., U.S. Dept. of Trans., DOT-TSC-OST-74-15, p. 257.
- EVANS, W.F.J., J.B. KERR, D.I. WARDLE, J.C. MCCONNELL, B.A. RIDLEY, and H.I. SCHIFF, 1976: Intercomparison of NO , NO_2 , and HNO_3 measurements with photochemical theory. *Atmosphere*, **14**, 189-198.
- HALL, T.C. and F.E. BLACET, 1952: Separation of the absorption spectra of NO_2 and N_2O_4 in the range 2400-5000 Å. *J. Chem. Phys.*, **20**, 1745.
- JOHNSTON, H.S., 1974: Alternate interpretation of Umkehr data for nitrogen dioxide. Proc. Third Conf. on the Climatic Impact Assess. Prog., U.S. Dept. of Trans., DOT-TSC-OST-74-15, p. 264.
- VIGROUX, E., 1953. Contribution a l'étude expérimentale de l'absorption de l'ozone, *Ann. Phys.*, **8**, 709-762.
-

The Altitude Distribution of Nitric Acid at Churchill

W.F.J. Evans, C.I. Lin and C.L. Midwinter

*Atmospheric Environment Service
4905 Dufferin Street
Downsview, Ontario, M3H 5T4*

[Manuscript received 19 February 1976; in revised form 21 July 1976]

ABSTRACT

The altitude distribution of nitric acid vapour was measured from observations of atmospheric thermal emission in the $11.3\text{-}\mu\text{m}$ band during a balloon ascent launched at 2317 GMT on 22 July 1974 from Churchill, Manitoba (latitude 58.7°N). The total amount of nitric acid above the tropopause was 0.32 matmcm . The nitric acid

layer was peaked at 24 km with a maximum mixing ratio of 5.5 ppbv. This measurement is similar to other available measurements of nitric acid in terms of layer shape and peak concentrations. The total amount of 0.32 matmcm is consistent with aircraft measurements of the latitudinal variation of nitric acid.

1 Introduction

As part of Project STRATOPROBE, which had the objective of making coordinated measurements of key nitrogen constituents in the ozone layer chemistry, it was necessary to develop a technique to measure the altitude distribution of nitric acid from the same balloon payload as instrumentation designed to measure nitric oxide, nitrogen dioxide and ozone. The thermal-emission technique employed by Murcray *et al.* (1973) was chosen and an instrument was designed to make nitric acid profile measurements based on the same principle. Measurements of the atmospheric thermal-emission spectrum from Murcray *et al.* (1973) over the spectral region from 9 to $14\text{ }\mu\text{m}$ are shown in Fig. 1. The nitric acid band is located in the atmospheric window at $11.3\text{ }\mu\text{m}$ and is relatively free from interference by other atmospheric constituents. Five interference filters were used to cover this spectral region; the band-passes of these filters are also indicated in Fig. 1 in relation to the nitric acid emission feature at $11.3\text{ }\mu\text{m}$. Note the broad band pass of filter B ($11.0\text{ to }11.6\text{ }\mu\text{m}$) and the narrow band pass of filter D ($11.23\text{ to }11.39\text{ }\mu\text{m}$); these filters were used to measure the nitric acid emission feature. Filters A, C and E provide supplementary information on the atmospheric thermal-emission spectrum which has not been analyzed in this paper.

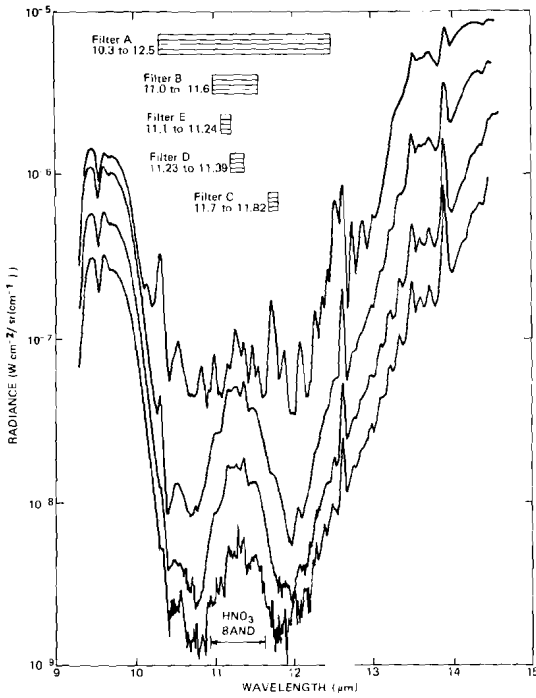


Fig. 1 The wavelength position of the bandpasses of the infrared interference filters in relation to the thermal-emission spectrum of nitric acid observed in the atmosphere by Murcay *et al.* (1973) at 3.4, 10.0, 20.1 and 24.7 km.

2 Theory of thermal emission measurements

Consider a layer i with:

T_i = temperature of layer i ,

P_i = mean pressure of layer i (expressed in atmospheres),

R_i = radiance at top of layer i ,

$B(T_i)$ = black body emission of layer i ,

ΔR_i = change in radiance across layer i ,

h_i = altitude of layer i ,

Δh_i = thickness of layer i ,

τ_i = transmission of layer i ,

ϵ_i = emissivity of layer $i = 1 - \tau_i$,

U_i = amount of nitric acid (atmosphere-cm),

Q_i = volume mixing ratio of nitric acid,

(S°/δ) = effective continuum absorption coefficient of the nitric acid band.

$$\frac{\downarrow R_i}{\text{layer } i \begin{matrix} T_i, P_i, U_i, Q_i, \Delta h_i \\ \epsilon_i, \tau_i \end{matrix}} \quad \frac{\downarrow R_i + \Delta R_i}{h_i}$$

The appropriate radiative transfer equation is:

$$(R_i \tau_i + \Delta R_i) - R_i = \epsilon_i B(T_i) \quad (1)$$

or $\Delta R_i = \epsilon_i B(T_i)$ since $\tau_i \approx 1.0$ for an optically thin layer. (2)

Thus $\epsilon_i = \Delta R_i / B(T_i)$. (3)

Now for weak absorption, $\epsilon_i = (S^0/\delta) U_i$. Here, the observed thermal emission of the layer is treated as the ideal black body radiation multiplied by the emissivity due to absorption by the amount of nitric acid in the layer.

$$\text{Inverting, } U_i = \Delta R_i/B(T_i) (S^0/\delta) \quad (4)$$

$$\text{and the volume mixing ratio } Q_i = U_i/(P_i \Delta h_i \cdot 273/T_i). \quad (5)$$

The effective band absorption coefficient was derived from the measurements at laboratory pressure and temperature by Goldman *et al.* (1971) with the expression

$$(S^0/\delta) = (S^1/\delta) (T^1/T_i)^{3/2}.$$

The appropriate room-temperature values of the band absorption coefficient, (S^1/δ) were 8.4 cm^{-1} and 11.3 cm^{-1} for the filter B measurements and filter D measurements, respectively.

The nitric acid band is located in a spectral region relatively free from interference by other atmospheric gases. Scattered solar radiation is negligible due to the long wavelength, and contributions from the water vapour continuum will be insignificant above the tropopause at 11 km due to the low mixing ratio of water vapour in the stratosphere.

3 Instrumentation

The five infrared interference filters were mounted on a continuously rotating wheel with one revolution every two minutes. A cross section diagram of the instrument is shown in Fig. 2. The total optical system is enclosed in a liquid nitrogen jacket with a capacity of 7 l. Extreme attention was paid to insulation design in order to obtain a long "hold time"; as a result, operation of the instrument is possible for more than 12 h under flight conditions.

Incident radiation enters the narrow aperture at the bottom of the cone of the copper jacket and is modulated by a 200-Hz Bulova tuning fork chopper. The radiation then passes through the filter wheel with the five interference filters mounted on it. The rotating filter wheel is driven by a set of gears from a fibreglass shaft attached to a d.c. Globe motor in the warm electronics section. The filtered radiation is then focussed onto a mercury cadmium telluride detector by a concave and flat mirror combination. The detector is operated with a 1 k Ω load resistor and a 4-volt bias. The signal is amplified by a low noise, low input impedance preamplifier. This is followed by two parallel linear and logarithmic amplifiers with a phase sensitive detector in each channel. The output filters have a 0.5-s time constant and the total instrument has a noise equivalent brightness of $10^{-8} \text{ W cm}^{-2} \text{ sr}^{-1} \mu\text{m}^{-1}$, which permits a signal to noise of ~ 30 on a typical observation of the total nitric acid layer.

The entire instrument is enclosed in a 30 cm \times 30 cm \times 60 cm block of foamed polyurethane with a 1.6-mm fibreglass shell. The instrument was mounted on the antisolar side of the STRATOPROBE 1 gondola with the optical axis at a zenith angle of 62.5° . Flight data were sampled at 7 samples/second by the pulse-code modulation telemetry system.

The instrument was calibrated radiometrically before and after flights with

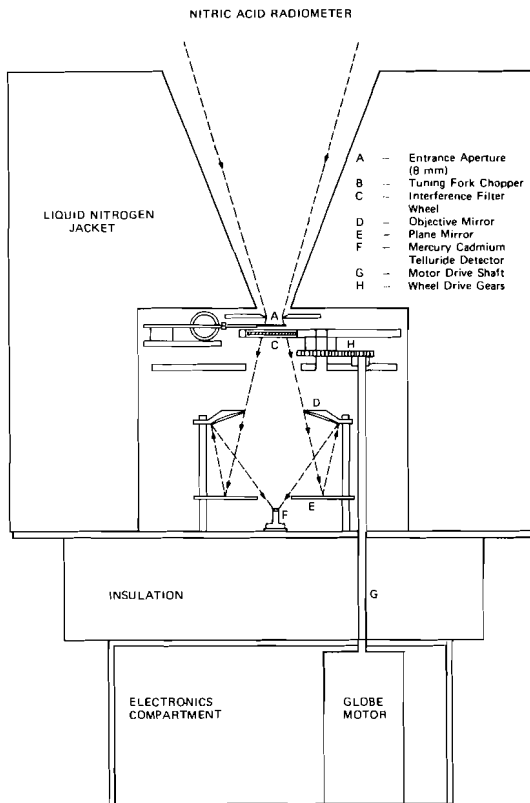


Fig. 2 A cross section view of the nitric acid radiometer.

a liquid nitrogen cooled “cold target” black body, the temperature of which could be varied from about 90 to 300 K in order to provide a range of radiance levels similar to those encountered in a balloon flight. The liquid nitrogen jacket is pressurized to maintain a constant detector sensitivity. The variation of detector sensitivity with pressure was measured in a high altitude simulation chamber; a small measured increase in instrumental sensitivity of 25% was corrected for in the data analysis.

4 Flight data

The present measurements were obtained from the ascent of the second STRATOPROBE I flight launched on 22 July 1974 at 2317 GMT from the airstrip at Churchill, Manitoba (latitude 58.7°N, longitude 94.3°W). The ascent to 34.5 km took approximately 120 min. The radiance data measured on this flight are shown in Fig. 3. A measurement by Murcay *et al.* (1973) from September 1970, at 33°N (small circles), is included for comparison. The radiance data measured by the 11.0 to 11.6 μm filter are indicated by the large open circles and the radiance data measured by the 11.2 to 11.4 μm filter are indicated by the solid triangular symbols.

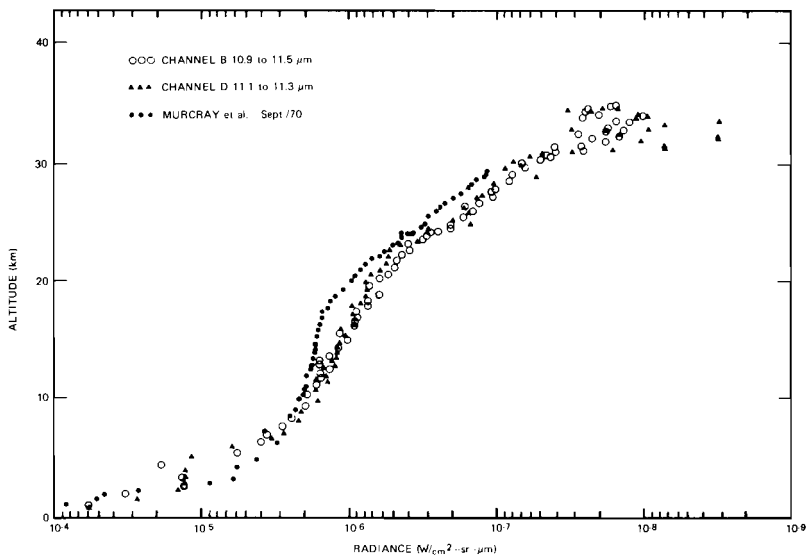


Fig. 3 The observed radiance profiles as a function of altitude for 22 July 1974 at Churchill.

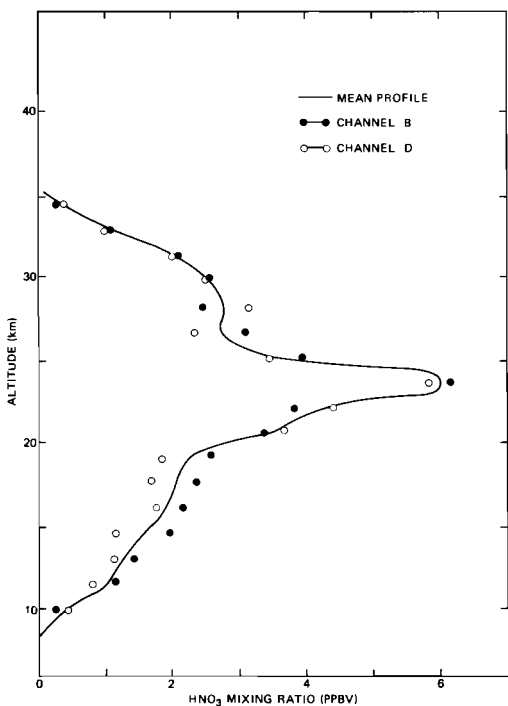


Fig. 4 The altitude distribution of nitric acid derived from the measured radiance profiles.

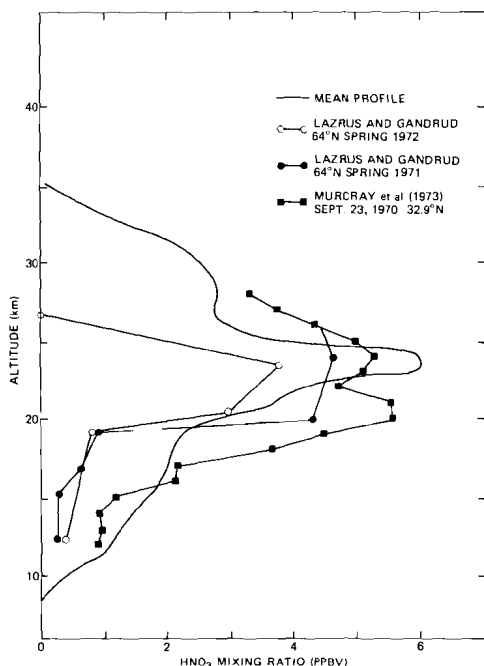


Fig. 5 A comparison of the nitric acid distribution measured at Churchill in July with other measurements of nitric acid distributions by Lazrus and Gandrud (1974) and Murcra y *et al.* (1973).

The tropopause was located at 11 km and is readily apparent in the radiance profiles as an inflexion at this altitude. The detailed temperature structure is given in Bain *et al.* (1976).

The observed radiance profiles were processed according to the expression in (5) to obtain the altitude distribution shown in Fig. 4. The radiosonde temperature profile data used to invert the radiance profile are given in Bain *et al.* (1976). The data from filter B yielded the profiles denoted by the closed circles while the analysis of the filter D data yielded the profile indicated by the open circles. The difference between the two profiles gives some indication of the relative error of the measurement, since the profiles were measured by two interference filter channels. An estimate of the relative error in the shape of the profile due to instrumental errors, such as detector noise, is ± 0.5 ppbv, roughly constant as a function of altitude. The absolute accuracy of the mixing-ratio profile due to uncertainty in the absolute radiometric calibration is estimated to be $\pm 30\%$. It should be noted that the layer peak is located at 24 km with a peak mixing ratio of 5.5 ppbv.

5 Comparison with other observations

A comparison of the nitric acid profile obtained at Churchill (58.7°N) on 22 July 1974 with measurements of the altitude distributions of nitric acid at high

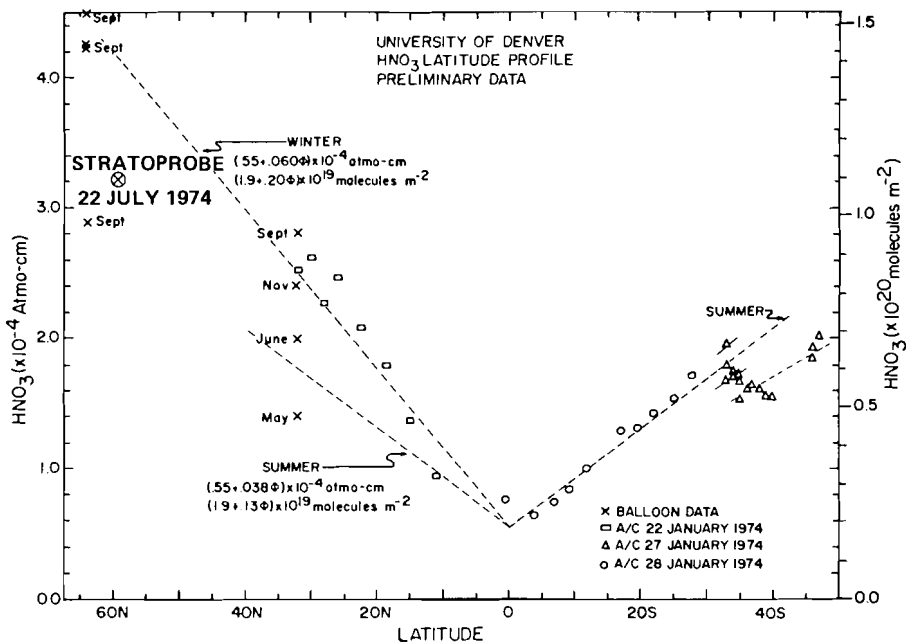


Fig. 6 The total column amount of nitric acid in relation to measurements of the latitudinal variation by Murcray *et al.* (1975).

latitudes in spring by Lazrus and Gandrud (1974) is shown in Fig. 5. A profile measured by Murcray *et al.* (1973) at 33°N in September, 1970 is also shown. It should be noted that the Lazrus and Gandrud (1974) measurements were made with an *in situ* sampling filter technique and generally indicate nitric acid concentrations a factor of two smaller than those measured by Murcray *et al.* (1973) with the thermal-emission technique. In any case, the altitude distribution observed in this paper appears to have the same general shape, similar peak altitude and peak concentrations as other measurements of nitric acid profiles. Vertical profile measurements taken exactly at 60°N in mid-summer by other experimenters are not available for comparison.

The total overhead amount of nitric acid measured was 0.32 matmcm; this is compared with recent results on the latitudinal dependence of total nitric acid from Murcray *et al.* (1975) in Fig. 6. The measured amount increases with latitude from 0.1 matmcm at the equator to more than 0.35 matmcm at 60°N. The measurement from this paper at 58.7°N in July is indicated by the large dot; it appears to be consistent with the overall latitudinal trend inferred by Murcray *et al.* (1975).

6 Summary and Conclusions

The distribution of the volume mixing ratio of nitric acid as function of altitude was measured at 58.7°N on 22 July 1974. Although no significant diurnal variation was expected, it should be noted that the measurement was made in

the late afternoon between 2317 and 0130 GMT. The nitric acid layer was peaked at 24 km with a maximum mixing ratio of 5.5 ppbv. The total amount above the tropopause was 0.32 matmcm. The measured distribution is consistent with other available measurements of nitric acid. A factor of two discrepancy between the thermal-emission technique and the *in situ* filter technique has been noted. A detailed comparison of the observed nitric acid distribution with theory is carried out by Evans *et al.* (1976).

Acknowledgements

The authors would like to acknowledge the major engineering contribution of SED Systems Ltd., who designed, constructed and provided field support for the payload gondola for the balloon flights of STRATOPROBE 1. SED Systems also operated the payload during the flights and provided the down-range telemetry station at Fort McMurray.

The balloon launch services were carried out by Raven Industries Ltd., as part of the 1974 SKYHOOK series administered by the Office of Naval Research. Range support and telemetry recording at Churchill were provided by the Space Facilities Branch of the National Research Council.

References

- BAIN, S., W.F.J. EVANS and C.L. MATEER, 1976: Meteorological and ozone data for the Project STRATOPROBE balloon flights of 8 and 22 July, 1974. *Atmosphere*, **14**, 147-154.
- EVANS, W.F.J., J.B. KERR, D.I. WARDLE, J.C. MCCONNELL, B.A. RIDLEY and H.I. SCHIFF, 1976: Intercomparison of NO , NO_2 and HNO_3 measurements with photochemical theory. *Atmosphere*, **14**, 189-198.
- GOLDMAN, A., T.G. KYLE and F.S. BONOMO, 1971: Statistical band model parameters and integrated intensities for the 5.9- μ , 7.5- μ , and 11.3- μ bands of HNO_3 vapor. *Appl. Opt.* **10**, 65-73.
- LAZRUS, A.L. and B.W. GANDRUD, 1974: Progress report on distribution of stratospheric nitric acid. Proc. Third CIAP Conf., Cambridge, Mass., Feb. 1974, DOT-TSC-OST-74-15, 161-167.
- MURCRAY, D.G., D.B. BARKER, J.N. BROOKS, A. GOLDMAN and W.J. WILLIAMS, 1975: Seasonal and latitudinal variation of the stratospheric concentration of HNO_3 . *Geophys. Res. Lett.*, **2**, 223-225.
- MURCRAY, D.G., A. GOLDMAN, A. CSOEKE-POECKH, F.H. MURCRAY, W.J. WILLIAMS and R.N. STOCKER, 1973: Nitric acid distribution in the stratosphere. *J. Geophys. Res.*, **78**, 7033-7038.
-

Altitude Profile and Sunset Decay Measurements of Stratospheric Nitric Oxide

B.A. Ridley, J.T. Bruin, H.I. Schiff and J.C. McConnell

Departments of Chemistry and Physics, York University, Downsview, Ontario

[Manuscript received 11 February 1976; in revised form 24 March 1976]

ABSTRACT

In July 1974 an NO/O_3 chemiluminescent instrument was used to obtain measurements of NO in the stratosphere during two balloon flights launched from Churchill ($59^\circ N$, $95^\circ W$). On the first flight, an altitude profile was obtained in which the NO volume mixing ratio was observed to increase from 0.3 to 2.7 ppbv between 19 and 29.5 km. On the second flight, the mixing ratio

was observed to increase from 0.25 to 2.7 ppbv between 19 and 29 km and to remain almost constant at about 2.7 ppbv from 29 to 34.5 km. On this flight, the sunset decay of NO was also obtained while the payload was at a constant float altitude of 34.5 km. These decay measurements are compared satisfactorily with the results obtained from a time dependent stratospheric model.

1 Introduction

The measurement of NO altitude profiles in the stratosphere provides an important means of assessing photochemical dynamical stratospheric models used to estimate the effect of anthropogenic perturbations on O_3 . However, the altitude profiles of a minor constituent such as NO depend on a complex interaction of chemistry and dynamics. Since most models parameterize dynamics with a single parameter, the eddy-diffusion coefficient, and use average insolation conditions because of the large differences in most chemical and flow time constants, agreement between measurement and theory cannot be expected to be very exact. Thus one ought to explore other methods of validating the models. One such method is to measure the diurnal variation dependence at a given location and altitude. Diurnal changes for NO occur on a much shorter time-scale than most atmospheric motions so that a test of agreement between models and measurement will be a test of specific chemistry uncomplicated by serious dynamic influences.

In this paper we present NO measurements which allow both of the above types of assessments to be made. *In-situ* measurements of the height profiles of NO and the first measurement of the change in NO concentration at a constant altitude through sunset are presented. Due to the apparent variability of NO profiles measured, no theoretical comparison is made since the models used to date cannot simulate such short-term profile variability. However the constant-altitude sunset data are compared with a time-dependent model calculation.

Simultaneous measurements of NO , NO_2 , HNO_3 and O_3 also provide a means to check models. Such measurements were also made during one of the flights described herein. An intercomparison of these results is given in another paper in this issue (Evans *et al.*, 1976).

2 Experimental

The NO/O_3 chemiluminescent instrument for *in-situ* NO sampling has been described in detail by Ridley and Howlett (1974). Experimental tests in the laboratory and during balloon flights to confirm the absence of sampling errors with the payload configuration used here have also been described (Ridley *et al.*, 1975a). Provision is made for on-board calibration of the instrument by the periodic addition of small known flows of NO to the ambient air flow from a high pressure cylinder containing a few ppm of NO in N_2 . Analysis of this flight cylinder by comparison with laboratory standards just before and after the balloon flights gave results which agreed to 5%. The estimated accuracy of the data presented below is $\pm 30\%$.

The balloons were launched from Churchill, $59^\circ N$, $95^\circ W$. Flight 1 occurred on 16 July 1974, using a 2.3×10^4 m³ balloon with the payload suspended some 30 m below. Measurements were made between 1700 and 2000 LT during ascent and float. Flight 2 occurred on 22 July 1974 using a 3.1×10^5 m³ balloon with the payload suspended about 100 m below. Measurements of the NO altitude profile and decay during sunset were made between 1930 and 2310 LT. Visible sunset occurred near 2308 LT. For Flight 2 there is an uncertainty of ± 0.5 km in the float altitude of the payload. Below about 29 km the uncertainty is much less.

3 Results

The NO mixing ratios obtained for solar zenith angles, χ , less than 90° are shown in Fig. 1. The corresponding number densities tabulated in Tables 1 and 2 were calculated from the mixing ratios using atmospheric data provided from radiosondes released from the Churchill Meteorological Station. The O_3 and temperature profiles shown in Fig. 2 were obtained from an ozonesonde released directly after the NO experiment was launched. O_3 , temperature and weather information for Flight 2 are reported by Bain *et al.*, (1976). The tropopause altitudes for flights 1 and 2 were both approximately 11 km.

For both flights, the NO mixing ratio increases quite strongly between about 19 and 29 km, a trend in agreement with earlier flights from New Mexico (Ridley *et al.*, 1975a). Flight 1 exhibits significantly higher mixing ratios between 20 and 28 km, though the two profiles converge at higher altitude. When $\chi \leq 90^\circ$, on either flight, there is little variation in the measured mixing ratio during the float duration. Over the nearly 2-h float period of Flight 1, the box in Fig. 1 indicates the extremes determined, whereas the average NO mixing ratio was 2.7 ± 0.2 ppbv. For Flight 2, the $\chi \leq 90^\circ$ measurement period was much shorter (~ 25 min) but the average was again 2.7 ± 0.2 ppbv.

During the float period of Flight 2, measurements of NO were made through

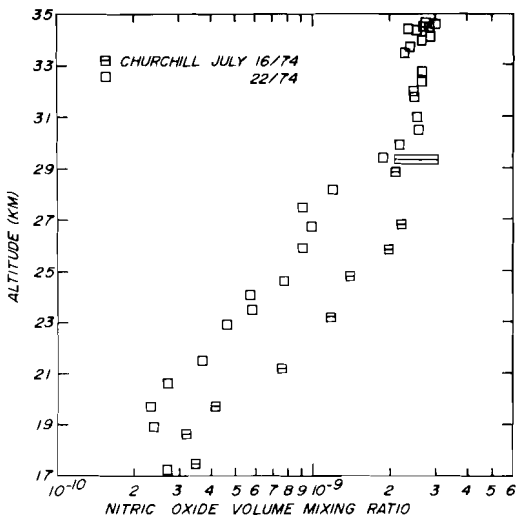
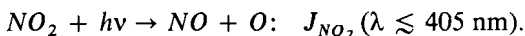


Fig. 1 High-sun NO mixing-ratio altitude-profiles obtained during the two balloon flights.

sunset. The open circles of Fig. 5 show the decay of NO , expressed as the ratio of NO during sunset to the average high sun ($\chi \leq 90^\circ$) value of 2.7 ppbv. The instrument operated for an additional 2.5 hours after visible sunset until the coolant and O_3 supplies were depleted but the NO mixing ratio remained below the detection limit of the instrument at this altitude (~ 0.06 ppbv). This confirms the expected absence of NO during night-time conditions.

4 Discussion

The principal reactions which govern the interconversion of NO_2 and NO are:



In the day-time stratosphere, the characteristic time-constant for the attainment of steady-state conditions is of the order of a few minutes, depending on the O_3 concentration and temperature, while the characteristic time constant for macro-transport is much longer. Consequently, the photochemical steady-state condition should be valid and

$$\frac{[NO_2]}{[NO]} = \frac{k_1[O_3]}{J_{NO_2} + k_2[O]}. \quad (1)$$

Since both the photolysis coefficient, J_{NO_2} , and $[O]$ decrease to zero in the absence of sunlight, this simple mechanism predicts conversion of NO to NO_2 at sunset and re-appearance of NO at sunrise. The decay of NO into NO_2 at sunset involves two time constants: (1) the time constant for conversion of NO into NO_2 , $t_1 = 1/k_1[O_3]$ and (2) the time constant for change of NO_2 into

TABLE 1. Nitric oxide data for flight of 16 July 1974

Altitude (km)	Number Density (cm^{-3})
17.5	9.4×10^8
18.6	7.2
19.6	8.2
21.2	11.0
23.2	13.0
24.8	12.0
25.8	15.0
26.8	14.9
28.8	11.0
29.4 ± 0.3	$13 \pm 1^*$

*average of 25 measurement cycles

TABLE 2. High-sun nitric oxide data for flight of 22 July 1974

Altitude (km)	Number Density (cm^{-3})	Altitude (km)	Number Density (cm^{-3})
17.2	7.9×10^8	30.5	9.7×10^8
18.9	5.5	31.0	9.1
19.7	4.6	31.8	7.7
20.6	4.7	32.0	7.5
21.5	5.6	32.4	7.6
22.9	5.6	32.8	7.1
23.5	6.4	33.5	5.4
24.1	5.8	33.7	5.5
24.6	7.1	34.0	5.9
25.9	7.0	34.1	6.0
26.7	6.7	34.4	5.3
27.5	5.4	34.4	4.9
28.2	6.5	34.5	5.7
29.4	8.5	34.5	5.7
29.9	9.1	34.6	6.0
		34.6	5.6

NO , $t_2 = 1/(J_{NO_2} + k_2[O])$. At sunset, if t_1 is of order a few minutes, then as t_2 (initially 2 minutes) becomes longer NO decreases, but because t_1 is still short NO and NO_2 remain in quasi-photochemical-steady-state and the decay is determined essentially by the time constant t_2 . However if t_1 is much longer than t_2 (e.g., $t_1 = 40$ min at 50 km) then much of NO will survive well-past sunset and the decay will depend only on t_1 , i.e., temperature and $[O_3]$.

The time constant t_2 is determined mainly by UV solar flux so that t_2 starts to increase before visible sunset.

5 Comparison of altitude profile data

Fig. 3 compares the high-sun Churchill data with measurements obtained during several flights from Holloman Air Force Base, New Mexico (Ridley

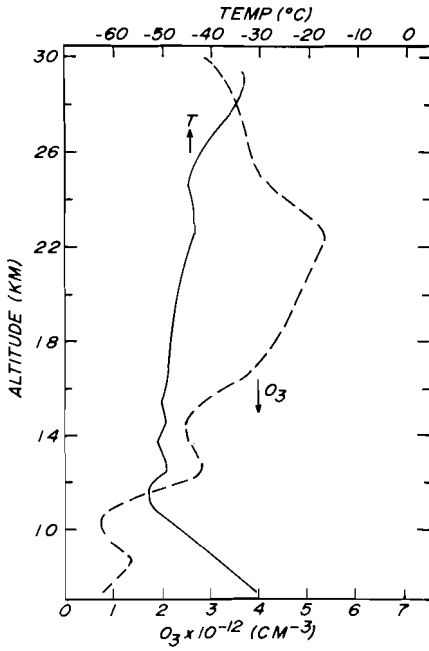


Fig. 2 Temperature and O_3 data for the flight of 16 July (Flight 1).

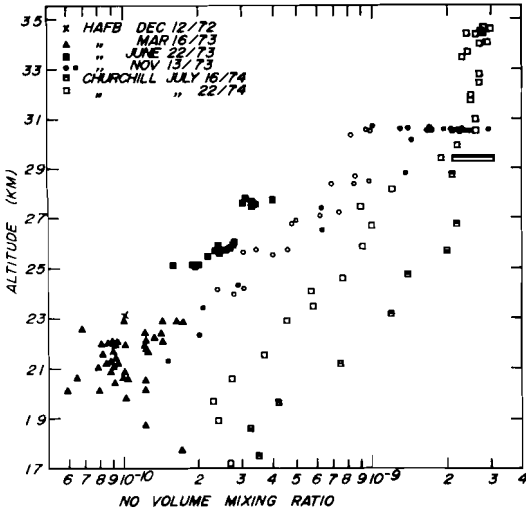


Fig. 3 Comparison of mixing-ratio altitude-profile data for Churchill and Holloman Air Force Base, New Mexico, balloon flights.

et al., 1975a). All of the New Mexico data were obtained during the morning after UV sunrise on the payload using either of two essentially identical instruments. Although the altitude profiles exhibit similar trends of increasing mixing ratio with altitude between about 20 and 30 km there are extreme differences in the measured mixing ratios of up to an order of magnitude in the 21–27-km region. These differences are in excess of the estimated inaccuracy of each particular experiment. Eq. (1) illustrates that the partitioning of NO_x into NO and NO_2 is quite sensitive to temperature through k_1 and to the O_3 density and a detailed analysis of all of the data to allow for these differences and the changes in J_{NO_2} will be reported at a later time. However, a qualitative comparison of just the ozone and temperature profiles for the Churchill flights and the New Mexico flights indicates that these factors cannot produce the order of magnitude change observed experimentally.

Loewenstein *et al.* (1975, 1976) have made a series of NO measurements from a high-altitude aircraft at 18.3 and 21.3 km to investigate both the seasonal and latitudinal dependence of NO . Their latitude data suggest little variation at 18.3 km between 30° and $60^\circ N$ for summer conditions. At 21.3 km an increase of about a factor of two is observed from 30° to $60^\circ N$. Their data also suggest a strong seasonal dependence of NO at both 18.3 and 21.3 km with about an order of magnitude increase from January to July between 33° and $48^\circ N$. The higher mixing ratios obtained for the present two northern flights tentatively support an increase in NO with increasing latitude if a straight comparison at geometric altitudes is made. However, an obvious seasonal effect is not distinguishable from the limited number of balloon flights reported here. Instead, the data suggest that substantial natural variability occurs.

Short-term variability is indicated by differences in the two Churchill profiles which were obtained only 6 days apart, with similar tropopause heights. Shorter-term variability still was observed during the two-hour float period of the November 13, 1973 flight. During the first part of the float period between 0910 and 0950 LT the NO mixing ratio increased from about 1.7 to 2.8 ppbv. Similar observations of a steady increase of NO after UV sunrise until about local noon have been made. (Ridley *et al.*, 1975b; Burkhardt *et al.*, 1975) This increase can be interpreted as a result of photolysis of N_2O_5 formed during the night. However, during the subsequent hour of the float period of the flight of Nov. 13 the NO decreased from 2.8 to about 1.0 ppbv. This short-term decrease does not have a ready photochemical explanation and is therefore most likely a result of natural variability. Substantial variability has also been observed with long-path IR absorption techniques by Ackerman *et al.* (1975). They observed an increase by factors of about 4 and 6 at the highest and lowest comparable altitudes on flights made one year apart from the same location. Short-term variability is also exhibited in the data reported by Loewenstein *et al.* (1974, 1975). Murcay *et al.* (1974), and Lazrus and Gandrud (1974) have also observed considerable variation in HNO_3 , the predominant NO_x species below about 27 km.

Fig. 4 shows the data of Fig. 3 relative to the altitude above the tropopause.

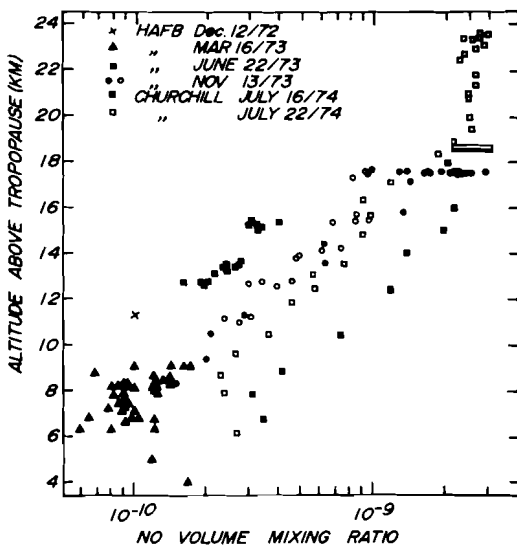


Fig. 4 Same data as Fig. 3 but plotted w.r.t. height above the tropopause.

Over-all, there is some convergence of the Churchill and New Mexico data. The interpretation of such a plot for two different latitudes is not readily made. Since O_3 , temperature, transport and insolation all may change with latitude, the differences are not due to a simple general lowering of the tropopause as northern latitudes are approached. However, the agreement noted may suggest that both latitudinal and seasonal variations should be investigated with respect to the tropopause as well.

Due to the variability of NO , discussed above, it is difficult to make a detailed comparison of the measurements with models, other than to note that the models appear to represent some mean value of NO . No present model, either 1-, 2- or 3-dimensional, is able to simulate the variability of NO noted above.

6 Sunset data

In Fig. 5 the measured decay of NO during sunset is compared with the results of a time-dependent photochemical model. This model includes all reactions and up-dated rate coefficients which have time constants short enough to be of importance in the diurnal variation. The calculation is for the particular date, location and payload altitude of Flight 2. The solid curve of Fig. 5 is the calculated ratio of $NO_x/NO_{x=90^\circ}$ for the actual temperature and ozone conditions determined for Flight 2. The remaining curves and symbols, as explained in the caption of Fig. 5, illustrate that the computed $NO_x/NO_{x=90^\circ}$ sunset ratio is fairly insensitive to reasonable ozone and temperature changes. The agreement between the calculated and measured ratio is quite good. For the altitude, temperature and ozone conditions prevailing during the experiment, t_1 is of order a few minutes. Thus, as discussed earlier, the NO decay is determined primarily by t_2 . A plot of t_2 is shown in Fig. 5. Changing O_3 and/or temperature

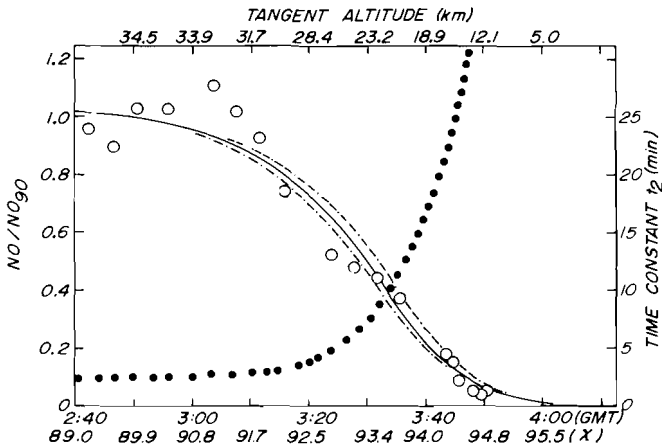


Fig. 5 The sunset decay of nitric oxide versus GMT time and solar zenith angle at the constant float altitude of $34.5 \pm .5$ km, on Flight 2 (22 July).

Solid circles: Time constant $t_2 = \frac{1}{J_{NO_2+k_2}[O]}$ as calculated from model (a) below.

Open circles: The calculated ratio of the measured nitric oxide mixing ratio to the average high sun ($\chi \lesssim 90^\circ$) measured value of 2.7 ppbv.

Full line: Model calculation (a) using the measured O_3 temperature data and for the location of the payload at an altitude of 34 km.

Dash-dot line: Model calculation (b); same as (a) except that the O_3 concentration was arbitrarily increased by 30%.

Double-dash dot line: Model calculation (c); same as (a) except that the temperature was decreased by 10° C.

will change the absolute amount of NO but not the shape of the NO profile as the sun sets.

Burkhardt *et al.* (1975) have reported measurements of NO during sunset at 33° N in May 1974 which show features of NO disappearance similar to those of the present results. Their measurements, however, are complicated by a rather severe loss (~ 7 km) of payload altitude during sunset and by the lack of simultaneous O_3 measurements. In spite of this, the same time-dependent model used here can reproduce their results reasonably well if a typical ozone profile is used, a reasonable total NO_x profile is adopted, and allowance is made for the loss of balloon altitude.

7 Summary

The sunset decay of nitric oxide observed experimentally has been shown to be well-accounted for by a straightforward time-dependent photochemical model. The data also confirm the expected absence of NO during night-time conditions. The observed differences in the two NO profiles are not as readily explained. However, the variation does introduce a qualification in the interpretation of simultaneous measurements of NO_x species obtained by a mixture of *in-situ* and remote-sensing techniques. The latter measurements are, of

course, averages over a much larger scale and over atmospheric paths that extend farther and farther from the payload as the sun sets.

Acknowledgement

It is a pleasure to acknowledge the help given by L.C. Howlett of Utah State University, N. Foulds and his group from SED Systems Ltd., Saskatoon, and the launch and recovery crew from Raven Industries and the Department of Naval Research. We are also grateful to Wayne Evans of the Atmospheric Environment Service and to the operators of the Churchill Meteorological Station for obtaining the ozone profile for Flight 1. Support for Flight 1 was kindly provided by the National Research Council of Canada and for Flight 2 by the Atmospheric Environment Service of Canada.

References

- ACKERMAN, M., J.C. FONTANELLA, D. FRIMOUT, A. GIRARD, N. LOUISNARD and C. MULLER, 1975: Simultaneous measurement of NO and NO_2 in the stratosphere. *Planet. Space Sci.* **23**, 651.
- BURKHARDT, E.G., C.A. LAMBERT and C.K.N. PATEL, 1975: Stratospheric nitric oxide: measurements during daytime and sunset. *Science*, **188**, 1111-1113.
- BAIN, S., C.L. MATEER and W.F.J. EVANS, 1976: Meteorological and ozone data for the Project STRATOPROBE balloon flights of 8 and 22 July, 1974. *Atmosphere*, **14**, 147-154.
- EVANS, W.F.J., J.B. KERR, D.I. WARDLE, J.C. MCCONNELL, B.A. RIDLEY and H.I. SCHIFF, 1976: Intercomparison of NO , NO_2 and HNO_3 measurements with photochemical theory. *Atmosphere*, **14**, 189-198.
- LAZRUS, A.L. and B.W. GANDRUD, 1974: Distribution of stratospheric nitric acid vapour. *J. Atmos. Sci.*, **31**, 1102-1108.
- LOEWENSTEIN, M., J.P. PADDOCK, I.G. POPPOFF and H.F. SAVAGE, 1974: NO and O_3 measurements in the lower stratosphere from a U-2 aircraft. *Nature*, **249**, 817-818.
- and H. SAVAGE, 1975: Latitudinal measurements of NO and O_3 in the lower stratosphere from 5° to $82^\circ N$. *Geophys. Res. Lett.*, **2**, 448-450.
- , ——, and R.C. WHITTEN, 1976: Seasonal variation of NO and O_3 at altitudes of 18.3 and 21.3 km. Submitted to *J. Atmos. Sci.*
- MURCRAY, D.G., A. GOLDMAN, W.J. WILLIAMS, F.H. MURCRAY, J.N. BROOKS, R.N. STOCKER and D.E. SNIDER, 1974: Stratospheric mixing ratio profiles of several trace gases as determined from balloon-borne infrared spectrometers. Paper presented at Int. Conf. on Structure, Composition and Gen. Circ. of the Upper and Lower Atmos. and Possible Anthropogenic Perturbations. Int. Union of Geod. and Geophys., Int. Ass. of Atmos. Phys., Aust. Acad. of Sci., U.S. Dept. of Transp., Melbourne, Australia, Jan. 14-25, 1974.
- RIDLEY, B.A. and L.C. HOWLETT, 1974: An instrument for nitric oxide measurements in the stratosphere. *Rev. Sci. Instrum.*, **45**, 742-746.
- , H.I. SCHIFF, A. SHAW and L.R. MEGILL, 1975a: In situ measurements of stratospheric nitric oxide using a balloon-borne chemiluminescent instrument. *J. Geophys. Res.*, **80**, 1925-1929.
- , J.T. BRUIN, M. MACFARLAND, H.I. SCHIFF and J.C. MCCONNELL, 1975b: Diurnal measurements of stratospheric NO . Paper presented at the Amer. Geophys. Union 1975 Fall Annual Meeting, San Francisco, California, December 8-12.

Intercomparison of NO, NO₂ and HNO₃ Measurements with Photochemical Theory

W.F.J. Evans, J.B. Kerr and D.I. Wardle

*Atmospheric Environment Service, 4905 Dufferin St.,
Downsview, Ontario, M3H 5T4*

J.C. McConnell, B.A. Ridley and H.I. Schiff

*Centre for Research in Experimental Space Science, York University,
Downsview, Ontario, M3J 1P3*

[Manuscript received 30 April 1976; in revised form 21 July 1976]

ABSTRACT

The simultaneous measurements of NO, NO₂ and HNO₃ mixing-ratio profiles carried out on the STRATO-PROBE balloon flight of 22 July 1974 have been simulated with a time-dependent model using the measured temperature and ozone profiles. The calculated ratios of NO/NO₂, HNO₃/NO₂ using currently accepted photochemistry are consistent with the measured ratios within the experimental errors of the measurements. The measured NO₂/NO ratio is almost a factor of two smaller than predicted, although the discrepancy is still within the experimental errors. A remarkable proportionality in the NO₂ and O₃ profiles has been noted

and is unexplained. A time-dependent simulation has been employed to convert the measurements into diurnally-averaged profiles suitable for intercomparison with two-dimensional stratospheric models and a comparison with constituent profiles from Prinn *et al.* (1975) is carried out as an example. The NO_y mixing ratio, formed from the sum of the NO, NO₂ and HNO₃ measurements is similar to the NO_y mixing ratio from several one- and two-dimensional models used to predict the effects of SST's on the ozone layer. The odd nitrogen mixing ratio is roughly constant from 20 to 35 km at 11 ppbv.

1 Introduction

The stratospheric models which are used to predict the effects of future fleets of SST's, freon usage and increased fertilizer production on the stratospheric ozone layer are extremely dependent on the exact photochemical reaction set used to model the distributions of minor nitrogen constituents. In addition, previous measurements of single species such as nitric oxide or nitric acid have indicated wide variability.

In 1973, the Atmospheric Environment Service organized a project to ob-

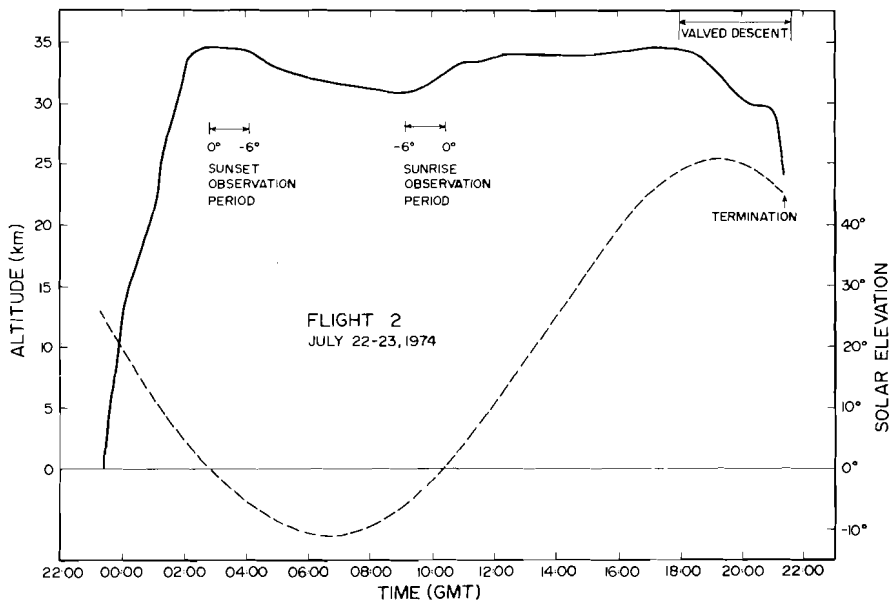


Fig. 1 The time-altitude profile of the STRATOPROBE 1 flight launched at 2317 from Churchill, Manitoba, on 22 July 1974.

tain a set of simultaneous measurements of nitric oxide, nitrogen dioxide and nitric acid in order to verify the currently accepted photochemical schemes for the nitrogen chemistry of the ozone layer. These measurements are reported in papers by Ridley *et al.* (1976, this issue), Kerr and McElroy (1976, this issue) and Evans *et al.* (1976, this issue). In order to interpret the photochemical relationships between the nitrogen constituents, it is essential to measure the ozone distribution accurately and to measure the temperature profile, both for the number density and for the calculation of rate constants which are temperature dependent. The ozone and temperature measurements, together with the general meteorological conditions, are reported by Bain *et al.* (1976, this issue).

2 Balloon-flight measurements

The measurements were made during a high altitude research balloon flight on 22 July 1974 launched from Churchill, Manitoba (latitude 58.7°N , longitude 94.1°W). The altitude of the balloon as a function of time is shown in Fig. 1. The measurements of the altitude profiles of nitric acid, ozone and nitric oxide were taken during the balloon ascent; during the two-hour measurement period the solar zenith angle varied from 75° at 15 km to 84° at 30 km. Remote-sensing measurements of nitrogen dioxide were made during sunset by long-path solar absorption; hence the inverted NO_2 profile corresponds to a solar zenith angle of 90° and this time difference from the NO and HNO_3 measurements must be accounted for in the comparison with theory by the use of a time-dependent photochemical model. It should also be noted

TABLE 1. Atmospheric parameters for the simulation

Altitude (km)	Temperature (K)	Number Density (cm^{-3})	Ozone Concentration (cm^{-3})
0	288	0.2575 E + 20	0.1555 E + 12
2	281	0.2072 E + 20	0.6260 E + 12
4	269	0.1665 E + 20	0.1006 E + 13
6	254	0.1355 E + 20	0.6553 E + 12
8	239	0.1090 E + 20	0.5931 E + 12
10	224	0.8720 E + 19	0.5795 E + 12
12	221	0.6479 E + 19	0.2622 E + 13
14	226	0.4675 E + 19	0.2373 E + 13
16	223	0.3494 E + 19	0.2322 E + 13
18	224	0.2567 E + 19	0.4187 E + 13
20	225	0.1886 E + 19	0.4901 E + 13
22	227	0.1381 E + 19	0.5341 E + 13
24	229	0.1013 E + 19	0.4163 E + 13
26	230	0.7503 E + 18	0.4351 E + 13
28	234	0.5492 E + 18	0.3716 E + 13
30	238	0.4042 E + 18	0.2735 E + 13
32	241	0.2998 E + 18	0.2210 E + 13
34	245	0.2236 E + 18	0.1688 E + 13
36	249	0.1666 E + 18	0.1117 E + 13
38	255	0.1241 E + 18	0.7169 E + 12
40	260	0.9320 E + 17	0.4628 E + 12
42	266	0.7040 E + 17	0.3002 E + 12
44	270	0.5358 E + 17	0.1965 E + 12
46	274	0.4100 E + 17	0.1293 E + 12
48	274	0.3001 E + 17	0.8124 E + 11
50	275	0.2496 E + 17	0.5807 E + 11
52	275	0.1952 E + 17	0.3903 E + 11
54	274	0.1530 E + 17	0.2635 E + 11
56	274	0.1190 E + 17	0.1761 E + 11
58	270	0.9383 E + 16	0.1190 E + 11
60	266	0.7398 E + 16	0.8091 E + 10

that the NO_2 measurements were made in a somewhat different air mass, since the tangent point of the sunset NO_2 measurements is ~ 200 km west of the balloon location.

Table 1 gives the ozone and temperature profiles employed in the inter-comparison; these are composite profiles derived from a series of four ozonesondes flown 6 h before, during, 6 h after and 12 h after the launch time of the STRATOPROBE I payload which included the ozonesonde experiment as part of the scientific package. Data from a rocketsonde fired from Churchill on 23 July 1974 were used to extend the temperature profile up to 60 km.

The measured profiles for NO , NO_2 and HNO_3 are shown in Fig. 2 along with the O_3 profile which has been divided by 10^3 . The NO_2 and O_3 profiles are remarkably similar in shape, which will be discussed in Section 4.

3 Theoretical simulation

A one-dimensional time-dependent model was employed to simulate the temporal variation of the major nitrogen constituents for the conditions of the

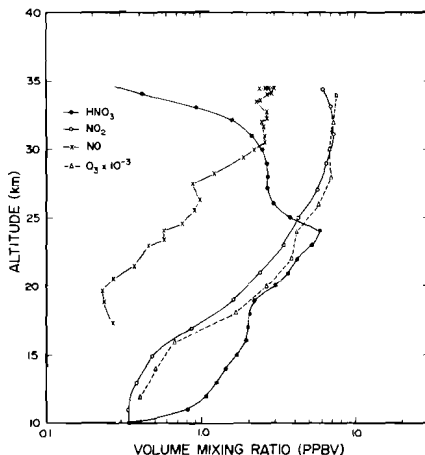


Fig. 2 The measured ozone, nitric oxide, nitrogen dioxide and nitric acid profiles.

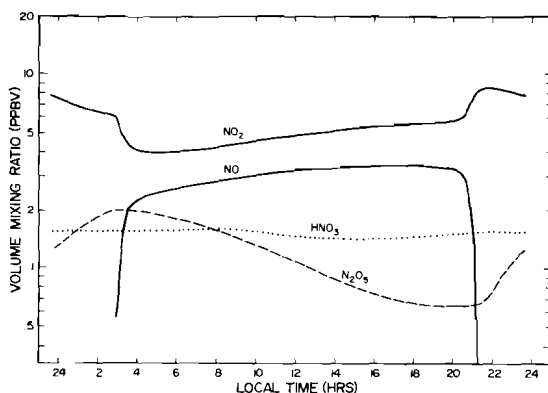


Fig. 3 The calculated diurnal variations of NO , NO_2 , N_2O_5 and HNO_3 at 30 km as simulated for the conditions of the 22 July flight.

balloon-flight measurements. The time variations in the mixing ratios of NO , NO_2 , N_2O_5 , and HNO_3 over a 24-hour period at an altitude of 30 km are shown in Fig. 3. This demonstrates the necessity of using a calculation which includes the effects of changing solar elevation angle to interpret measurements of NO and NO_2 ; HNO_3 has little diurnal variation below 30 km. This also indicates that the optimum time to measure N_2O_5 would be just before dawn when the concentrations could be as high as 2 ppbv.

The model is an extension to the time-dependent case of earlier work by McConnell and McElroy (1973). The main characteristics important to this simulation will be outlined. The chemical rate coefficients and photodissociation parameters employed are those recommended by CIAP in Monograph 1 (1975). In particular, the rate constant for HNO_3 formation from NO_2 and OH used the new parameterization by Tsang (1974). A value of 5×10^{-11}

was used for the reaction rate $OH + HO_2$; this is critical to the determination of OH concentrations and effects the ratios of HNO_3 to NO and NO_2 .

4 Ratios of the nitrogen constituents

Fig. 4 shows the ratio of NO_2 to NO formed from the measured profiles of Fig. 2. Under photochemical steady-state conditions at fixed solar angle this ratio would be given by the expression:

$$R_{NO_2/NO} = k_{NO+O_3}[O_3]/(J_{NO_2} + k_{NO_2+O}[O]). \quad (1)$$

However, since the NO measurements were taken at varying solar angles around 80° and the NO_2 measurement at 90° , the theoretical ratio was calculated from the time-dependent model output at the times corresponding to the solar zenith angles of the actual observations.

The error limits indicated for the measured ratio correspond to $\pm 30\%$ for the NO measurement and $\pm 20\%$ for the NO_2 measurement. The simulated ratio should also be considered to have a range of error of $\sim \pm 20\%$ associated with it, corresponding to $\pm 10\%$ in the ozone densities and $\pm 2^\circ C$ in the temperature measurements. Another limitation to the theoretical simulation is that albedo effects have not been included because of the complexity of this effect, although this effect would tend to decrease the calculated ratio.

The observed ratio has a similar altitude variation to the simulated NO_2/NO ratio, but is a factor of 1.8 larger at most altitudes. The discrepancy could be resolved in several ways. Measurements of the NO_2 concentrations may be too large, or measurements of NO too small by a factor of up to 1.8. Alternatively, the value currently accepted for the rate constant at ~ 220 K for the $NO + O_3$ reaction may be in error, although the difference from theory is only slightly less than the combined estimated error of the two measurements.

If transport effects were unimportant, the ratio HNO_3/NO_2 would be given approximately by the expression:

$$R_{HNO_3/NO_2} = \frac{k_{OH+NO_2}[OH][M]}{J_{HNO_3} + k_{OH+HNO_3}[OH]}. \quad (2)$$

(Note that this approximate expression neglects the presence of N_2O_5 which produces some variation in this ratio at night as shown by the time-dependent model simulation in Fig. 3). In Fig. 5, this simulated ratio has been taken from the HNO_3 profile corresponding to the range of solar angles encountered during the ascent measurement and the NO_2 profile at solar angle $\chi = 90^\circ$. The model was run for 100 days to achieve reproducible diurnal variations from day to day. It should be noted that there will probably be transport effects on the observed ratio at altitudes below 20 km and these have not been accounted for. In making the comparison between the simulated and measured ratios, estimated errors of $+56\%$ and -38% , due respectively to the $\pm 20\%$ accuracy of the NO_2 measurements and the $\pm 25\%$ accuracy of the HNO_3 measurements, should be considered. The simulated ratio is in good agreement with the measured ratio at most altitudes; the shape, as well as the mag-

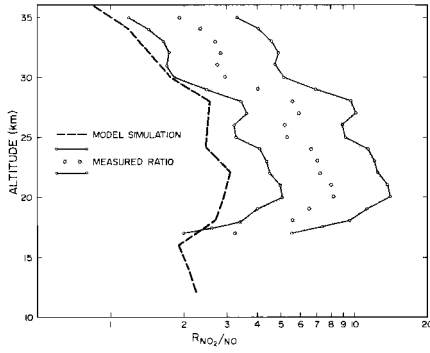


Fig. 4 A comparison of the measured and simulated ratios for NO_2/NO , as a function of altitude.

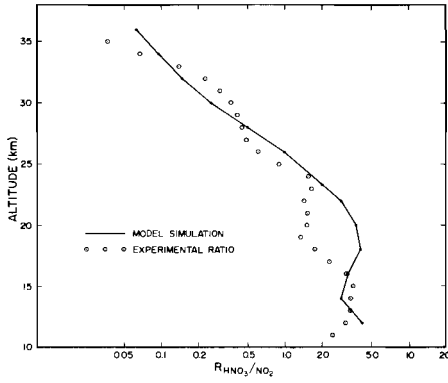


Fig. 5 A comparison of the measured and simulated ratios for HNO_3/NO_2 as a function of altitude.

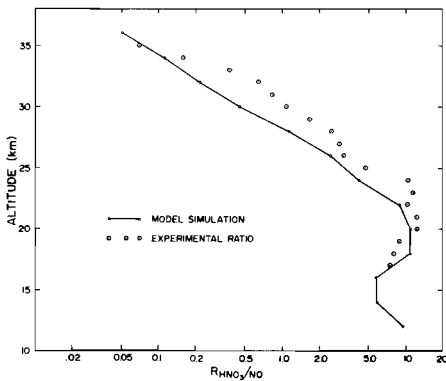


Fig. 6 A comparison of the measured and simulated ratios for HNO_3/NO .

nitude, is similar to the measured ratio. It should be noted that this ratio is very sensitive to the hydroxyl concentrations in the model; these correspond to a "moderate" OH model since a value of 5×10^{-11} was employed for the rate coefficient of the reaction between OH and HO_2 . A range of a factor of 3 is available in the OH concentrations since the laboratory value for the rate coefficient is only constrained to the range 2×10^{-11} to 2×10^{-10} . However, the upper limit has recently been lowered to 5×10^{-11} by the atmospheric measurements of Anderson (1976), which indicate large hydroxyl concentrations close to the upper limit permitted by laboratory measurements of the rate constant.

The third ratio which can be obtained from the experimental measurements is the ratio HNO_3/NO shown in Fig. 6. This ratio can be obtained from the previous ratios by the expression:

$$R_{HNO_3/NO} = R_{HNO_3/NO_2} \cdot R_{NO_2/NO}$$

The model-simulated ratio has a similar altitude variation to the observed ratio and is only slightly smaller at most altitudes. Although the HNO_3 profile has little diurnal variation, this ratio has a significant time variation due to diurnal changes in NO concentrations at some altitudes.

As was noted earlier, the altitude distributions of NO_2 and O_3 in Fig. 2 are similar in shape. A detailed examination shows that the ratio of the observed concentrations for the two constituents is approximately constant with a small variation between 0.7×10^{-3} and 1.0×10^{-3} . The same feature is reproduced in the time-dependent model simulation with the proportionality factor about 40% smaller. A cursory examination of several two-dimensional models indicates a similar behaviour in the summer hemisphere and suggests that this is a photochemical effect. An exact explanation of this proportionality is lacking, but it may prove to be a useful empirical means to estimate the amount of NO_2 present at a specific location and time when only ozone measurements are available.

A quantity which is unaffected by diurnal variations and which is expected to be relatively uniformly mixed in the stratosphere is the mixing ratio of odd nitrogen which, aside from N_2O_5 , is approximately equal to the quantity often designated as $NO_y = NO + NO_2 + HNO_3$.

The measured HNO_3 , NO_2 and NO mixing-ratio profiles have been converted to the same solar zenith angle (80°) by using the time-dependent model and summed to obtain the NO_y mixing-ratio profile for 22 July 1974 at $59^\circ N$. In Fig. 7, this may be compared with the odd nitrogen mixing-ratio profile from the two-dimensional model of Vupputuri (1975) (curve C) and the two-dimensional model of Prinn *et al.* (1975) (curve B). On the right-hand side of this figure, the results from one-dimensional models of Crutzen and Isaksen (1976) and McConnell and McElroy (1973) are included. (The tropopause height of 16 km for $30^\circ N$ has been aligned with the observed tropopause height of 11 km at $59^\circ N$ to facilitate the comparison.) There is a significant difference in solar insolation.

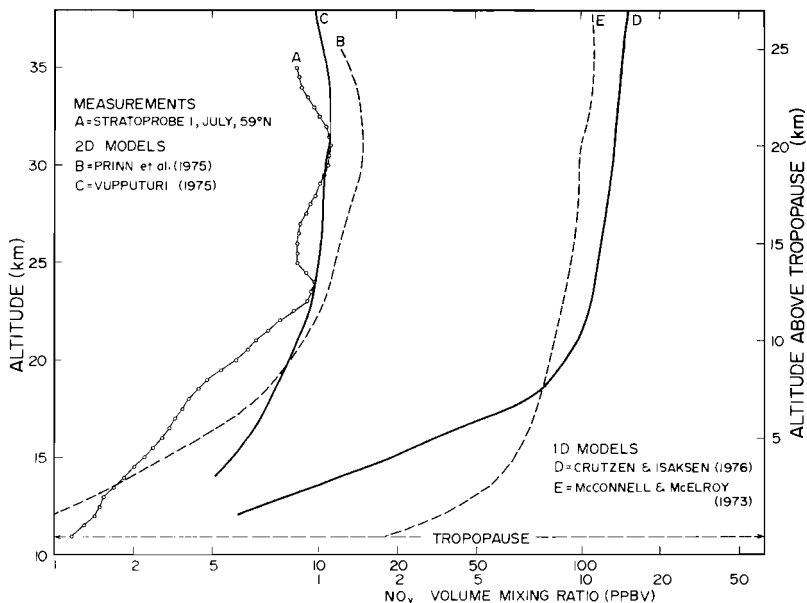


Fig. 7 The measured total odd nitrogen (NO_y) mixing ratio as derived from the individual constituent profile measurements in comparison with the NO_y altitude distribution from several one- and two-dimensional models of the stratospheric ozone layer.

All the models indicate mixing ratios which are approximately constant from 20 to 40 km and in the range 10 to 15 ppbv. The measured profile indicates an odd nitrogen mixing ratio of ~ 11 ppbv, approximately constant with altitude above 20 km. The Prinn *et al.* (1975) profile for $60^\circ N$ in July is very similar in shape, but 20% greater than the measurements from Churchill.

The NO_y mixing ratio at $43^\circ N$ in May 1974 has been estimated by Ackerman *et al.* (1975) from simultaneous measurement of NO and NO_2 combined with estimates for HNO_3 obtained from Murcray *et al.* (1973). Their estimate of 12 ± 2 ppbv, roughly constant over the altitude range from 20 to 35 km, is consistent with our measurement of 11 ppbv, approximately constant with altitude above 20 km.

In order to make a proper comparison of the measured profiles with the NO , NO_2 , and HNO_3 profiles from a two-dimensional diurnally-averaged model such as that of Prinn *et al.* (1975) it is necessary to convert the observed profiles which were measured at a particular time of day (solar zenith angle) into equivalent diurnal-average profiles. In the past, modellers have often attempted to compare their diurnally-averaged model profiles directly with constituent profiles measured at a specific time (such as sunset); however, this type of intercomparison can only be made properly with the use of a separate time-dependent model (or at minimum an equilibrium calculation which accounts for the changing photodissociation rates as a function of solar zenith angle).

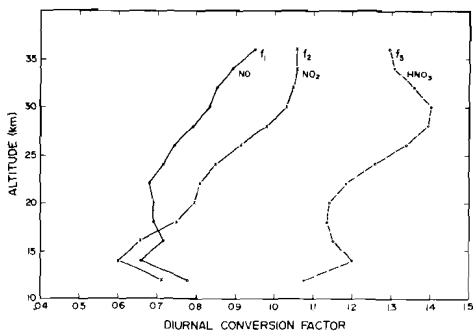


Fig. 8 Correction factors for the conversion of the observed concentration profiles into diurnally-averaged concentration profiles.

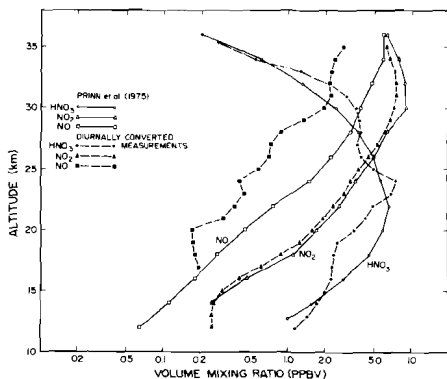


Fig. 9 A comparison of the diurnally converted mixing-ratio profiles of NO , NO_2 and HNO_3 with the corresponding predicted distributions from the model of Prinn *et al.* (1975).

Fig. 8 shows the conversion factors f_1 , f_2 , and f_3 to be applied to the observed profiles of NO , NO_2 , and HNO_3 , respectively, in order to convert them into diurnally-averaged concentration profiles suitable for intercomparison with two-dimensional model calculations which employ diurnally-averaged photochemistry. These conversion factors were calculated from a comparison of a steady-state run of the model with time-dependent concentrations for the actual times of the measurements.

Note that the maximum correction is less than a factor of 1.5 for NO , less than 1.6 for NO_2 , and less than 1.4 for HNO_3 . This indicates the size of the error that can be made by comparing measurements directly with diurnally-averaged model profiles.

In Fig. 9 the diurnally-converted altitude distributions of NO , NO_2 and HNO_3 are compared with the corresponding profiles from Prinn *et al.* (1975). The agreement with our converted profiles is excellent and we take this to imply that the Prinn *et al.* (1975) model presents a parameterization of the nitrogen photochemistry of the stratospheric ozone layer sufficiently good for ozone-depletion simulations. (It should be noted that the Prinn *et al.* model employs a rate constant of 2×10^{-10} for the $OH + HO_2$ reaction and does not include N_2O_5 in the nitrogen chemistry.)

5 Conclusions

Altitude mixing-ratio distributions of NO , NO_2 , and HNO_3 have been measured on the same balloon flight together with the ozone and temperature profiles. This is sufficient information to test the currently recommended photochemistry of active nitrogen constituents. The measured ratios of NO_2/NO , HNO_3/NO_2 and HNO_3/NO have been successfully simulated to better than a factor of two at most altitudes using a fully time-dependent photochemical model. This demonstrates that the nitrogen photochemistry employed in cur-

rent models is a reasonable representation of the actual atmospheric chemical processes.

The measured altitude distributions of NO , NO_2 and HNO_3 have been converted into the equivalent diurnally-averaged profiles to facilitate intercomparison of the results with two-dimensional models which, up to now, have used diurnally-averaged photochemistry. The profiles of Prinn *et al.* (1975) are in reasonable agreement with the converted versions of the measured nitrogen constituent profiles. By combining the NO , NO_2 , and HNO_3 measurements, the total odd nitrogen mixing-ratio distribution has been inferred. This demonstrates a mixing ratio of ~ 11 ppbv roughly constant from 20 to 35 km, in agreement with most models, and particularly similar to the profile from Prinn *et al.* (1975) for $60^\circ N$, July.

References

- ACKERMAN, M., J.C. FONTANELLA, D. FRIMOUT, A. GIRARD, N. LOUISNARD and C. MULLER, 1975: Simultaneous measurements of NO and NO_2 in the stratosphere. *Planet. Space Sci.*, **23**, 651.
- ANDERSON, J.G., 1976: The absolute concentration of OH ($X^2\pi$) in the Earth's stratosphere. *Geophys. Res. Lett.* **3**, 165.
- BAIN, S.E., C.L. MATEER and W.F.J. EVANS, 1976: Meteorological and ozone data for the Project STRATOPROBE Balloon Flights of 8 and 22 July, 1974. *Atmosphere*, **4**, 147-154.
- CIAP Monograph 1, 1975: The natural stratosphere of 1974. Scientific Panel on the Natural Stratosphere, Chairman E.E. Reiter, Table 5.39.
- CRUTZEN, P.J. and I.S.A. ISAKSEN, 1976: The impact of the chlorocarbon industry on the ozone layer. *J. Geophys. Res.*, **81**, in press.
- EVANS, W.F.J., C.I. LIN and C.L. MIDWINTER, 1976: The altitude distribution of nitric acid at Churchill. *Atmosphere* **14**, 172-179.
- KERR, J.B. and C.T. MCELROY, 1976: Measurement of stratospheric nitrogen dioxide from the AES Stratospheric Balloon Program. *Atmosphere* **14**, 166-171.
- MCCONNELL, J.C. and M.B. MCELROY, 1973: Odd nitrogen in the atmosphere. *J. Atmos. Sci.*, **30**, 1464-1480.
- MCELROY, M.B., S.C. WOFSEY, J.E. PENNER and J.C. MCCONNELL, 1974: Atmospheric ozone: possible impact of stratospheric aviation. *J. Geophys. Res.* **31**, 287.
- MURCRAY, D.G., A. GOLDMAN, A. CSOEKE-POECKH, F.H. MURCRAY, W.J. WILLIAMS and R.N. STOCKER, 1973: Nitric acid distribution in the stratosphere. *J. Geophys. Res.* **78**, 7033-7038.
- PRINN, R.F., F.N. ALYEA and D.M. CUNNOLD, 1975: Stratospheric distribution of odd nitrogen and odd hydrogen in a two-dimensional model. *J. Geophys. Res.* **80**, 4997.
- RIDLEY, B.A., J.T. BRUIN, H.I. SCHIFF and J.C. MCCONNELL, 1976: Altitude profile and sunset decay measurements of stratospheric nitric oxide. *Atmosphere*, **14**, 180-188.
- TSANG, W., 1974: Rate constants for the reaction $OH + NO_2 + M \rightarrow HNO_3 + M$, chemical kinetics data survey. Internal report, Nat. Bur. of Stand., Washington, D.C.
- VUPPUTURI, R.K.R., 1975: Seasonal and latitudinal variation of N_2O and NO_x in the stratosphere. *J. Geophys. Res.* **80**, 1125.

Solar Ultraviolet Flux Measurements

D.J. McEwen and H.T. Meredith

*Institute of Space and Atmospheric Studies,
University of Saskatchewan, Saskatoon, Sask. S7N 0W0*

[Manuscript received 4 May 1976]

ABSTRACT

Solar ultraviolet fluxes were measured with a ¼-metre Ebert spectrometer flown as part of an Atmospheric Environment Service balloon payload from Fort Churchill on 8 July 1974. The spectral region from 1820 to 3150Å was scanned each 7.5 s with 1.5Å resolution from 1256 to 0025 UT on 10 July. These measurements covered a range of solar

zenith angles from 37° (noon) to 69° with the balloon initially at a float altitude of 28.6 km. Fluxes in the window region 1900 to 2200Å were analyzed to determine ozone content above the balloon. Values from 0.069 to 0.11 cm NTP were obtained at heights over a range from 28.6 to 25.3 km.

1 Introduction

A ¼-metre Ebert spectrometer was flown on two Atmospheric Environment Service balloon flights in July 1974 from Fort Churchill, Manitoba. The purpose of this experiment was to record the solar spectrum from 1820 to 3150Å and to measure the stratospheric absorption of this solar radiation. Accurate knowledge of the deposition of this energy in the stratosphere and the photodissociation rates of oxygen and other molecules such as freons are essential in determining the effect of pollutants on depletion of the ozone layer.

2 Instrumentation

The spectrometer used was a ¼-metre Ebert-type spectrometer with an EMR-542F solar blind photomultiplier. Fig. 1 shows an external view of the instrument. It was of rugged construction originally designed for rocket studies of vacuum ultraviolet auroral emissions but equally suitable for balloon work. It utilized a 50-mm square grating, ruled 2400 lines/mm and blazed for peak efficiency at 1500Å. The instrument scanned over the 1820 to 3150Å spectral region each 7½ s by means of a stepping motor which advanced the grating in 0.005-degree steps at the rate of 250 steps/s. The photon counts accumulated during each 4-ms interval were telemetered to the ground and recorded on tape. Curved slits 0.1 mm wide and 29 mm high were used giving a spectral resolution of approximately 1.5Å.

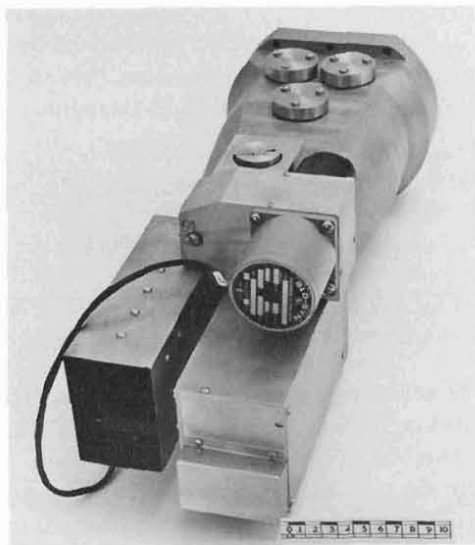


Fig. 1 Spectrometer showing entrance baffle on the front and the detector with amplifier adjacent.

The instrument was mounted on the balloon gondola with a servo-control system which kept the instrument pointed at the sun throughout the daytime portion of the balloon flights. A quartz diffusing screen with an effective transmission of about 0.4 was placed in the front of the entrance baffle. This eliminated the need for pointing accuracy any greater than $\pm 2^\circ$.

The spectrometer was calibrated with a standard quartz iodide lamp over its useful range of 3150 to 2500Å and with a deuterium lamp from 2500Å to 1900Å. These calibrations were made after the balloon flights. While the shape of the spectral output of the deuterium lamp was quite reproducible, the absolute flux was not accurately known. The resulting absolute calibration, in view of these factors, is estimated to be accurate to about $\pm 25\%$ only.

Peak sensitivity of the whole instrument was in the region 2100–2300Å falling off by an order of magnitude at the high end of the scan at 3150Å.

3 Flight data

Solar spectra were obtained during the first balloon flight throughout the day from 1256 GMT 9 July to 0025 GMT 10 July 1974. These spectra covered the range of solar zenith angles $\psi = 68^\circ$ through $\psi = 37^\circ$ to $\psi = 66^\circ$. During this daytime period the balloon floated at a near constant height of 28.6 km, dropping to 25.3 km in the late afternoon.

A second balloon carrying the spectrometer was flown on 23 July but failure of the high voltage supply about two hours after lift-off, when the balloon had just reached 19.8 km, prevented obtaining any useful data on that flight. Accordingly, all of the spectral measurements discussed in this paper are from the first balloon flight of 9 July.

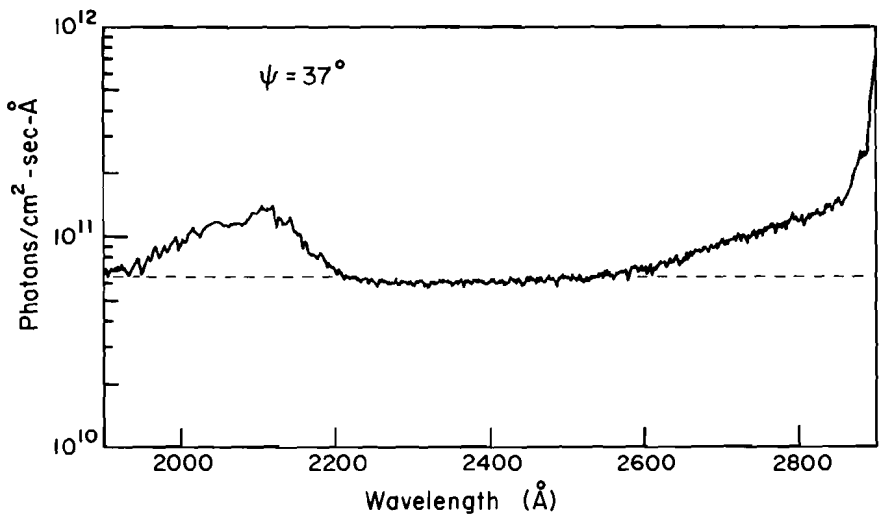


Fig. 2 Typical solar spectrum from 1900 to 2900Å above a background of scattered light and interference shown by the dashed line, for solar zenith angle of 37° and balloon height of 28.4 km.

Fig. 2 shows a portion of a typical solar spectrum obtained for the range 1900 to 2900Å. Below 1900Å no measurable solar flux reached the balloon level, while above 2900Å the flux rapidly increased with wavelength and gave counting rates ($> 10^6$ Hz) which were beyond the linear capability of the photomultiplier detector. This spectrum was recorded near noon at a solar zenith angle of 37° and is the average of 20 successive $7\frac{1}{2}$ -s scans. Interference from the telemetry transmitter gave a relatively constant background counting rate of about 3700 Hz and this shows up as noise in the 2200–2600Å region where the absorption of solar flux is complete. The scattered light contribution to this background was small.

Solar radiation was recorded in the 1900–2200Å “window region”. Throughout the 2200–2600Å spectral region absorption by ozone (Hartley bands) above the balloon is complete. Below 1900Å, there is complete absorption of radiation by molecular oxygen (Schumann-Runge bands).

The solar flux incident on the earth’s atmosphere has been measured by Broadfoot (1972) and others and is fairly reliably known over this wavelength region. The absorption coefficients of ozone throughout the whole spectral range from 3100Å to 2000Å were first measured by Inn and Tanaka (1953) and have since been studied and confirmed by Grigg (1968). Using these data and measurements of solar flux at balloon level it is possible to calculate the total amount of ozone in the path from the balloon to the sun, using either the spectral region 2800–2900Å or 2100–2200Å. The latter region was chosen since the response of the instrument was fairly flat there and hence the results are potentially of high accuracy. In these calculations, the effect of Rayleigh scattering and absorption by O_2 were neglected as the changes in those coefficients were small over the 2100 to 2200Å interval, compared to

TABLE 1. Measured ozone above balloon

Time GMT 9 July 1974	Solar Zenith Angle	Balloon Altitude (km)	Ozone (cm NTP)
1615	45.5°	28.6	0.069
1747	38.4°	28.6	0.064
1932	37.2°	27.4	0.082
2026	39.9°	26.5	0.094
2039	41.6°	25.9	0.11
2250	48.5°	25.3	0.091

the change in absorption coefficients for ozone, and it was the shape of the spectrum, or slope, that was used to calculate the amount of ozone in the path.

The results of these determinations of ozone content above the balloon are shown in Table 1 for a selection of balloon levels and solar zenith angles throughout the day of the flight. They have been converted to the equivalent ozone content vertically above the balloon by dividing the amount measured in the slant path to the sun by the secant of the solar zenith angle. The increasing amount of ozone measured above the balloon, 0.069 to 0.11 cm NTP, was due undoubtedly to the decreasing height of the balloon as the day progressed. The measured value of 0.069 cm of ozone above 28.6 km can be compared with the value of 0.1 cm above that height extracted from ozone densities reported by Mateer and Godson (1960) for Edmonton, a comparable latitude, in summer.

Fig. 3 shows an expanded portion of the solar spectrum in the region 1900 to 2300Å and illustrates the potential of such measurements from balloon for obtaining precise values of ozone density through most of the ozone layer. The absorption above 2100Å is due almost entirely to ozone. Ozone content in the slant path to the sun from the solid line spectrum is calculated to be 0.082 cm. A spectrum obtained by Simon (1974) with a rather similar spectrometer is shown for comparison. A marked difference in absorption is seen, due to the fact that their balloon was 10 km higher and above much of the ozone layer. Ozone in the optical path above that balloon was calculated from their spectrum to be 0.011 cm. The observed spectrum is seen to be a very sensitive function of ozone content. Measurements in this spectral region can thus give very precise values of ozone density through most of the ozone layer, provided the spectrometer is carried up through the ozone layer near mid-day when the solar zenith angle is small. At the balloon height of about 28.6 km, solar radiation in the window region has been almost entirely absorbed when the solar zenith angle exceeds 60°. Cann *et al.* (1976, this issue) have carried out a computer simulation of solar spectra from 2050 to 2150Å over a range of solar zenith angles (40° to 80°) for comparison with observed spectra.

The appearance of the solar spectrum observed below 2100Å is determined largely by molecular oxygen in the optical path, due to absorption in the Schumann-Runge system. Absorption peaks can be seen in Fig. 3 from the

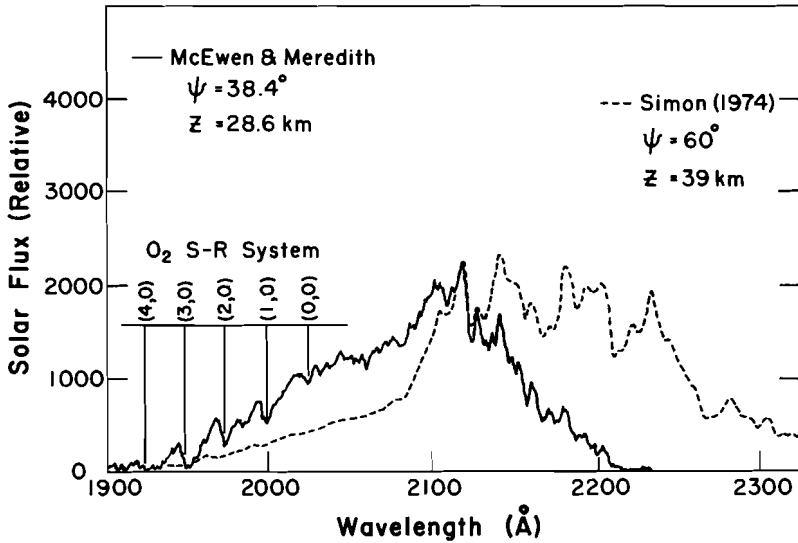


Fig. 3 Expanded portion of solar spectrum from 1900-2300Å. A spectrum obtained by Simon (1974) is shown for comparison. The Schumann-Runge O_2 absorption bands are identified.

(0,0) band head at 2025Å and succeeding Schumann-Runge bands to the (4,0) band at 1924Å. This spectral region has not been investigated in any detail, particularly at high resolution, although its importance in the photochemistry of the stratosphere is recognized. The comparison spectrum (Simon, 1974) shows much more absorption due to the longer slant path through the atmosphere but has no spectral detail since the spectral resolution was only 6Å.

4 Summary

Solar spectra were obtained over the range 1900 to 2900Å in a balloon flight from Fort Churchill in July 1974. Accuracy of the absolute fluxes is estimated to be $\pm 25\%$. It is seen that the measured flux for the range 2100 to 2200Å is a very sensitive function of ozone content above the balloon and can be used to obtain reliable ozone profiles under controlled balloon-flight conditions.

Further effort will be devoted to improving the calibration of the spectrometer. The instrument will be flown as an integral part of further Atmospheric Environment Service balloon studies of photochemistry of the stratosphere and significant minor constituents.

Acknowledgements

The authors wish to thank Miss G. Petty for her assistance in data processing and in calibration of the spectrometer. They are grateful to Dr. W.F.J. Evans for his continued interest and assistance in the project and to the Atmospheric Environment Service for financial support through a research contract. Integra-

tion of the instrument into the balloon payload was most competently done by SED Systems Ltd.

References

- BROADFOOT, A.L., 1972: The solar spectrum 2100-3200Å. *Astrophys. J.*, **173**, 681-689.
- CANN, M., R.W. NICHOLLS, W.F.J. EVANS and D.J. MCEWEN, 1976: Theoretical simulation of solar ultraviolet fluxes measured on the 8 July 1974 STRATOPROBE I flights. *Atmosphere*, **14**, 205-213.
- GRIGG, M., 1968: Absorption coefficients of ozone in the ultraviolet and visible regions. *J. Chem. Phys.*, **49**, 857-859.
- INN, E.C.Y. and Y. TANAKA, 1953: Absorption coefficient of ozone in the ultraviolet and visible regions. *J. Opt. Soc. Amer.*, **43**, 870-873.
- MATEER, C.L. and W.L. GODSON, 1960: The vertical distribution of atmospheric ozone over Canadian stations from Umkehr observations. *Quart. J. Roy. Meteor. Soc.*, **86**, 512-518.
- SIMON, P., 1974: Balloon measurements of solar fluxes between 1960 and 2300Å. Proc. of the Third Conf. on the CIAP, Cambridge, Massachusetts.
-

Theoretical Simulation of Solar Ultraviolet Fluxes Measured on the 8 July 1974 STRATOPROBE I Flights

M.W.P. Cann and R.W. Nicholls

*Centre for Research in Experimental Space Science, York University,
Downsview, Ontario, M3J 1P3*

W.F.J. Evans

*Atmospheric Environment Service
4905 Dufferin St., Downsview, Ontario, M3H 5T4*

and

D.J. McEwen

Physics Department, University of Saskatchewan, Saskatoon, Sask.

[Manuscript received 15 June 1976; in revised form 21 July 1976]

ABSTRACT

Solar ultraviolet fluxes in the wavelength region 1900 to 2300Å were measured during the first balloon flight of Project STRATOPROBE on July 8, 1974, over a range of solar zenith angles at a float altitude of 28.6 km. High-resolution computer simulations of the measured spectra were made for a range of solar zenith angles of

40° to 80° over the wavelength region 2050 to 2150Å, and comparisons made with the observed spectra at 40° and 47°. Qualitative agreements were obtained but there were significant discrepancies between the simulated and experimentally obtained fluxes. Sources of the discrepancies are discussed.

1 Introduction

The solar flux transmitted into the stratosphere in the 2100-Å window region of the spectrum has special significance at the present time because of general concern over the inadvertent disturbance of the ozone layer by man. Activities which may seriously affect the photochemistry in this layer include the release and upward diffusion of chlorofluorocarbons used in refrigeration and aerosol spray cans, upward diffusion of N_2O from chemical fertilizers and the release of oxides of nitrogen by high altitude commercial SST fleets.

The radiation in the 2100-Å region is responsible for the production of ozone through the photodissociation of molecular oxygen and also for the photodissociation of $CFCl_3$ and CF_2Cl_2 . The accurate simulation of this flux is thus essential to photochemical transport models used to model the global

ozone layer and depletion of ozone due to injections of NO_x and chlorine compounds. An early experimental study of the ultraviolet flux in the atmosphere was carried out by Brewer and Wilson (1965) but with inconclusive results.

The purpose of the ultraviolet experiment on Project STRATOPROBE was to obtain measurements of the solar flux at various altitudes and solar zenith angles in conjunction with measurements of temperature and ozone in order to determine how well the actual atmospheric fluxes could be simulated. The measured spectra are reported by McEwen and Meredith (1976, this issue). In this paper we report a high spectral resolution calculation of the spectral transmission of the atmosphere which we use in conjunction with solar flux measurements, made at altitudes above significant absorption, to simulate the solar flux at the balloon float altitude of 28.6 km.

2 Basis of the calculations

The atmosphere was divided into a number of layers of unequal thickness and each layer was assigned mean values for temperature, pressure and species concentrations. For a layer of thickness L , the transmission $T(\nu)$ at frequency ν is given by

$$\begin{aligned} T(\nu) &= \exp(-\tau(\nu)) \\ &= \exp\left(-L \sum_i N_i \sigma_i(\nu)\right) \end{aligned} \quad (1)$$

where $\tau(\nu)$ is the optical depth, N_i the number density of species i , and $\sigma_i(\nu)$ is the absorption cross-section for species i at frequency ν . For a molecular absorber,

$$\sigma_i(\nu) = \frac{8\pi^3}{3hc} \cdot \nu \cdot \sum_{v',v''} R_e^2(\bar{F}_{v',v''}) \cdot q_{v',v''} \cdot \sum_{J',J''} S_{J',J''} \cdot b(\nu), \quad (2)$$

where $R_e(\bar{F}_{v',v''})$ is the electronic transition moment, $q_{v',v''}$ is the Franck-Condon factor, $S_{J',J''}$ is the Hönl-London factor for the J' to J'' transition and $b(\nu)$ is the line shape factor or profile. Summations are over all lines in the band (v',v'') which contribute at a frequency ν .

For molecular Rayleigh scattering the extinction cross-section is (Penndorf, 1957)

$$\sigma(\nu) = \frac{8\pi^3}{3} \cdot \nu^4 \cdot \frac{(n^2 - 1)^2}{N^2} \cdot \frac{6 + 3\rho}{7 - 7\rho} \quad (3)$$

where N is the total number density of air molecules, n the refractive index at frequency ν and ρ is the depolarisation factor. In equations (2) and (3) the frequency ν is expressed as the wave number, e.g., cm^{-1} .

It is clear from the above equations that in order to calculate the spectral transmission $T(\nu)$, information is needed on species number densities, N_i , temperature and also pressure as a function of altitude (temperature and pressure control the line intensities and shapes). Information is also required on the line positions and transition probability parameters for Eq. (2); more detailed information may be found in a paper by Cann *et al.* (1976).

In order to obtain the spectral transmission, the optical depth was first calculated for each layer, according to Eqs. (1) to (3) and then summed. Taking the negative exponent of this gives the transmission $T(\nu)$ for the atmosphere above the balloon float altitude. Then, if $I_0(\nu)$ is the solar flux incident on the atmosphere, the flux at balloon float altitude is given by

$$I(\nu) = I_0(\nu) \cdot T(\nu). \quad (4)$$

3 Atmospheric model

The model used was based on the U.S. Standard Atmosphere (1966) for 60°N in July supplemented by the high altitude (above 120 km) model for summer, with an exospheric temperature of 600K, and modified by ozonesonde data acquired at the time of the research balloon flight. The series of ozonesonde flights carried out in coordination with the experiment provided temperature and ozone concentration data up to 35 km (Bain *et al.* (1976), this issue). Above 35 km the ozone and temperature data are more uncertain. The ozone profile above 45 km was taken from a series of high altitude ozone profiles inferred from $O_2(^1\Delta)$ rocket measurements from Churchill in July and August in previous years (Evans and Llewellyn, 1970). Between 35 and 45 km, an interpolation of the two different profiles was employed. It is hoped that the high altitude ozone profile for this flight can be improved when the NIMBUS IV BUV data have been processed. A table of the model used for the spectroscopic calculations is given by Cann and Nicholls (1975).

4 Spectroscopic data

The absorption and extinction processes included in the calculation were: absorption by the ozone continuum, O_2 Herzberg continuum ($A^3\Sigma_u^+ \leftarrow X^3\Sigma_g^-$), O_2 Schumann-Runge lines ($B^3\Sigma_u^- \leftarrow X^3\Sigma_g^-$) and Rayleigh scattering by air molecules. The ozone absorption data of Griggs (1968) were used: the effect of temperature has not been reported in the literature but one may assume this to be small for the continuum region. Absorption cross-sections in the O_2 Herzberg continuum were calculated using the Franck-Condon density principle, Cann *et al.* (1976).

The contributions from lines of the O_2 Schumann-Runge bands were computed to high accuracy using a line-by-line technique. The pre-dissociation broadening, well-known in this band system, is only poorly known for the weak bands in the 2050–2150 Å spectral range; an estimate was included, however, along with pressure and Doppler broadening using the well-known Voigt line profile. A total of 371 spectral lines were included.

5 Atmospheric transmission calculations

A detailed study in which test cases run for a 0.5-Å spectral region for 26, 25 and 10 layers showed that in fact 8 atmospheric layers were adequate for computing the spectral transmission down to the balloon float altitude of 26.8 km, accurate to well within the limits set by the data and spectroscopic constants

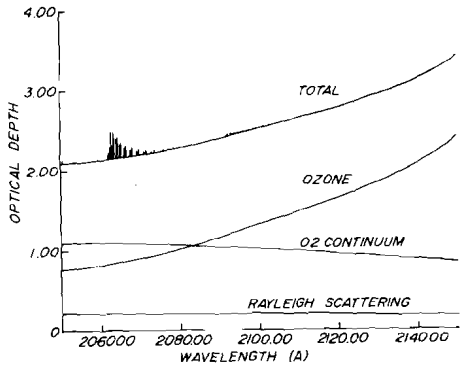


Fig. 1 Relative contributions to the atmospheric optical depth above 26.8 km for a solar zenith angle of 40° .

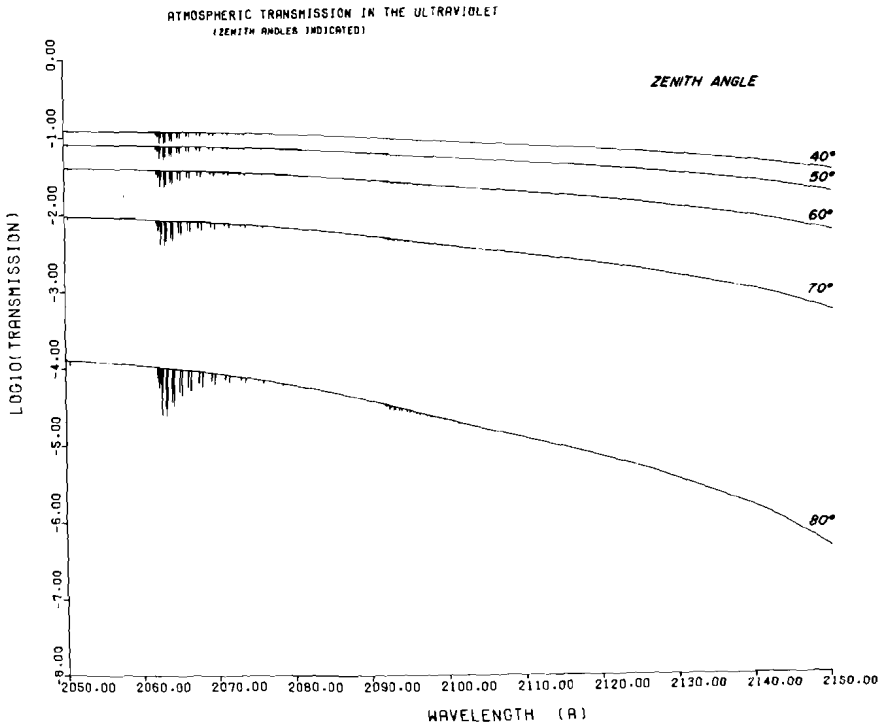


Fig. 2 High-resolution ultraviolet atmospheric transmission down to 26.8 km for solar zenith angles from 40° to 80° .

used – these layers were specified for a spherical atmosphere. Tabulated layer specifications are given by Cann and Nicholls (1975).

In Fig. 1, the various contributions to the atmospheric absorption are shown for the simulation conditions at an altitude of 28.6 km and a solar zenith angle of 40° . Ozone is the major source of absorption above 2085 Å while the O_2 continuum is dominant below this wavelength. O_2 Schumann-Runge bands are

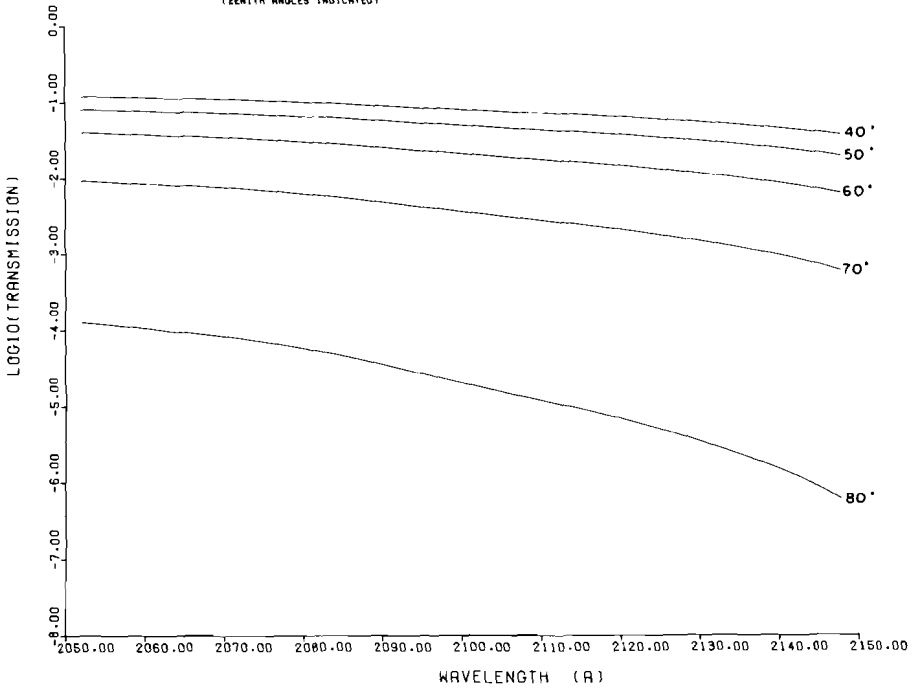


Fig. 3 Ultraviolet atmospheric transmission degraded by a 2 Å instrumental slit function for solar angles from 40° to 80°.

present in the 2095-Å and 2065-Å regions, but do not contribute significantly to the absorption. The contribution from Rayleigh scattering is also small. This demonstrates that, for practical purposes in models, the absorption can be conveniently calculated using only O_3 absorption and the O_2 Herzberg continuum absorption over the wavelength range from 2050 to 2150 Å. This is not true at shorter wavelengths where the Schumann-Runge bands of the $v'' = 0$ progression appear and become important. The errors in the ozone and Rayleigh scattering extinction coefficients are about 5%. The O_2 continuum should be accurate to 10% but the line absorption contribution is only accurate to around 30%.

Fig. 2 shows the calculated transmissions for various zenith angles from 40 to 80°; the logarithm (base 10) of the transmission is shown as a function of wavelength. This figure demonstrates that the transmission varies from 10% to 0.01% at 2050 Å over this range of solar angles and should permit a good evaluation of the accuracy of solar flux simulations, even at a constant float altitude. The eventual aim of this work is to check the accuracy of solar flux simulation in models as a function of altitude, both in high-resolution and parameterized calculations. Fig. 3 shows the same transmission curves degraded with a 2 Å instrumental slit width for the same range of zenith angles; the very weak oxygen lines no longer show.

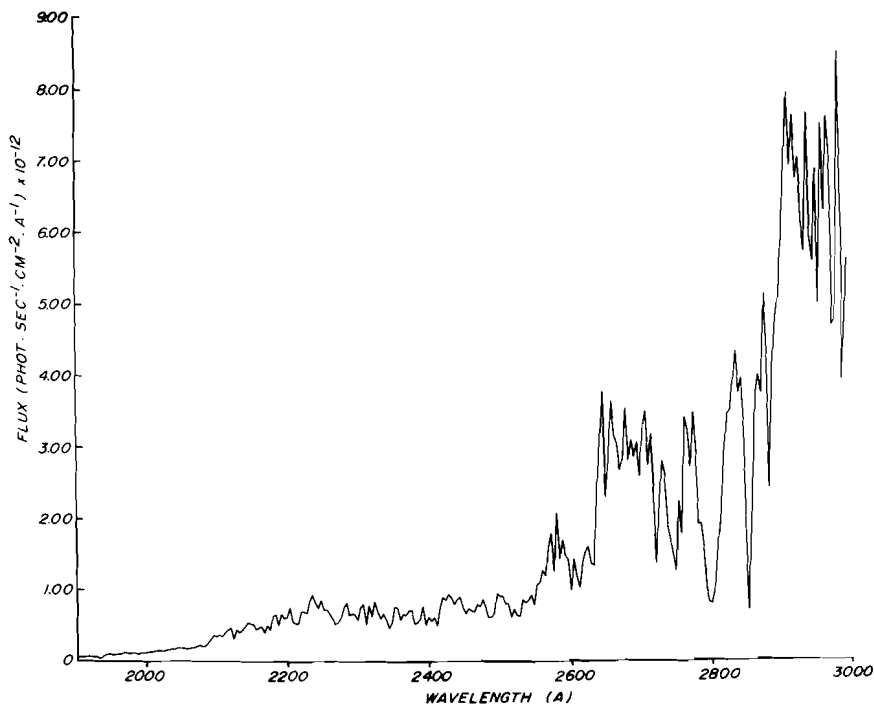


Fig. 4 Solar spectrum incident on the atmosphere (Brinkmann *et al.*, 1967). Resolution is 4 Å.

6 Comparison between observed and simulated solar spectra

A NRL solar spectrum earlier reported by Brinkmann *et al.* (1967) is shown in Fig. 4. Since the spectral lines in the terrestrial absorption spectrum do not contribute significantly to the atmospheric absorption (see above) there is no fine structure in the transmission spectrum. Hence the transmissions shown in Fig. 3 may be multiplied by the spectrum in Fig. 4 to give the expected solar spectrum at 28.6 km (Eq. (4)). This has been done for solar zenith angles of 40° and 47° and compared with the experimental results in Figs. 5 and 6, respectively. In Fig. 5 the measured and simulated spectra have similar appearance but the latter is less intense by a factor about 2.5, which is greater than the estimated calibration error of the spectrometer ($\pm 25\%$). In Fig. 6 the measured flux is again larger than the simulated flux, although the 47° experimental spectrum has a poorer signal-to-noise ratio than the 40° spectrum. The attenuation due to the larger air mass at 47° is about the same for the experimental and simulated spectra so that the former spectrum is again larger than the latter by a factor about 2.5. The discrepancies in the absolute fluxes between the experimental and the simulated spectra can be largely, if not entirely, explained by the various uncertainties in both sets of spectra. Ozone densities are a major source of uncertainty although the column

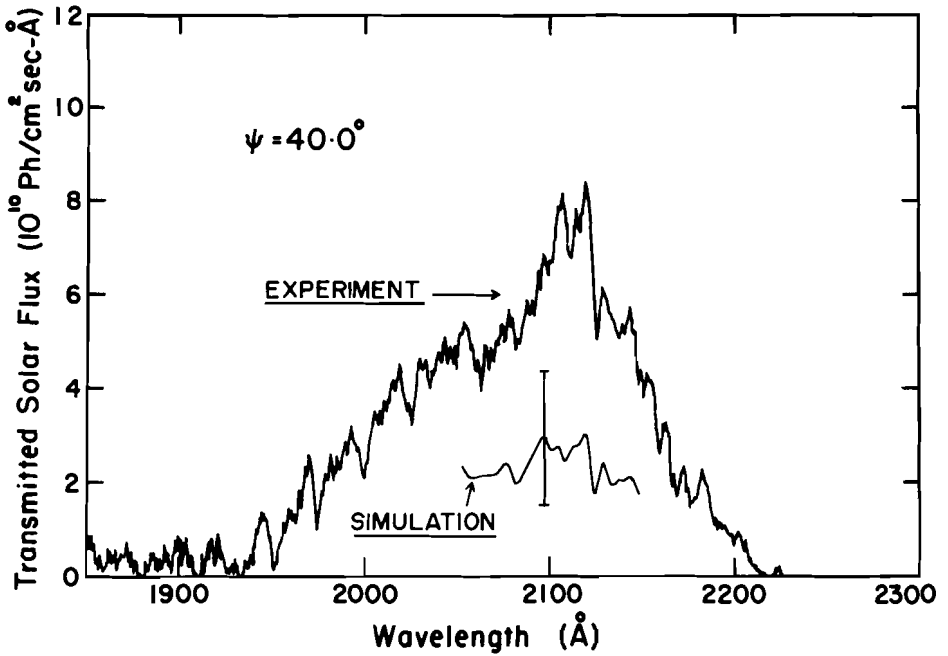


Fig. 5 A comparison between the observed and simulated solar flux spectrum for a solar zenith angle of 40° at an altitude of 28.6 km. Error bars at 2100 Å show the effect of $\pm 30\%$ changes in the ozone densities.

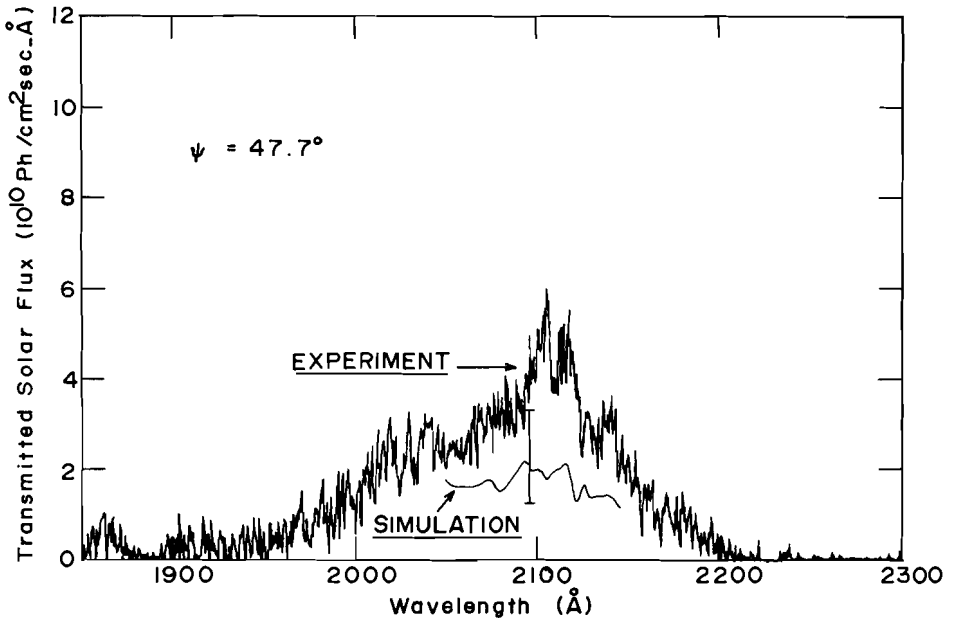


Fig. 6 A comparison between the observed and simulated solar flux spectrum for a solar zenith angle of 47° at an altitude of 28.6 km. Error bars at 2100 Å show the effect of $\pm 30\%$ changes in the ozone densities.

density along the optical path inferred by McEwen and Meredith (1976) (e.g., $2.4 \times 10^{18} \text{ cm}^{-2}$ for 40°) is effectively the same as that used in the simulation spectrum ($2.36 \times 10^{18} \text{ cm}^{-2}$). The error bars at 2100 Å in Figs. 5 and 6 show the effect of $\pm 30\%$ uncertainty in the total amount of ozone along the optical path. As noted in Section 3, ozone densities were measured only up to 35 km at the time of the balloon flight. Densities at higher altitudes were obtained from the literature (Evans and Llewellyn, 1970). If the ozone densities for altitudes > 40 km are reduced by a factor 2, which is not unreasonable, then the simulated photon flux in Fig. 5 (40°) is further raised by about $0.3 \times 10^{10} \text{ photons sec}^{-1} \text{ cm}^{-2} \text{ Å}^{-1}$. A combination of these two factors, raising the simulated flux, with the instrument calibration error ($\pm 25\%$) lowering the experimental flux, almost brings the experimental and simulated fluxes into coincidence. Further, the NRL solar spectrum used here could easily have an absolute error of $\pm 25\%$, as is shown by comparisons in the recent review by Simon (1975). In addition, some variation with solar sunspot cycle may be expected.

Continuation of this work will include a careful scrutiny of the assumptions and procedures concerned. Future work will be conducted using more recent solar data at higher resolution; this last is necessary when the line structure of the strong Schumann-Runge bands are important, *i.e.*, at lower wavelengths.

7 Summary

A simulation of the expected solar flux spectrum in the wavelength range 2050 to 2150 Å has been carried out using realistic high-resolution atmospheric transmission calculations for the observed temperature and ozone concentrations for the STRATOPROBE I balloon flight of 8 July 1974 from latitude 59°N and a NRL solar spectrum. A comparison between simulated and measured spectra at solar angles of 40° and 47° shows unexpectedly high experimental results but these are in approximate agreement with the simulations when all sources of uncertainty are included. The purpose of this initial simulation was to evaluate the feasibility and limitations of this experiment. A final objective is to simulate the observed spectra as a function of altitude under known ozone, temperature and number-density conditions.

The calculation will be extended down to 1900 Å for future work using a more recent, and higher resolution, solar spectrum. Efforts are required to improve the absolute calibration of the flight spectrometer as well as the accuracy of the ozone and temperature profiles above the balloon float level. The future availability of ozone BUV satellite data should improve the accuracy of the ozone profile. The accuracy with which we can execute this type of experimental comparison limits the extent to which the production terms for ozone in stratospheric models can be verified. The photodissociation of chlorofluorocarbons in the stratosphere is also affected by this same flux in the 2100 Å window.

Acknowledgements

The authors wish to thank Miss G. Petty for her assistance in data processing and Mr. H.T. Meredith for his excellent work in both field support and calibration of the spectrometer.

References

- BAIN, S.E., C.L. MATEER and W.F.J. EVANS, 1976: Meteorological and ozone data for the Project STRATOPROBE balloon flights of 8 and 22 July, 1974. *Atmosphere* **14**, 147-154.
- BREWER, A.W. and A.W. WILSON, 1965: Measurement of solar ultra-violet radiation in the stratosphere. *Quart. J. Roy. Meteor. Soc.*, **91**, 452-461.
- BRINKMANN, R.T., A.E.S. GREEN and C.A. BARTH, 1967: Atmospheric scattering of the solar flux in the middle ultraviolet. *Appl. Optics* **6**, 373-383.
- CANN, M.W.P. and R.W. NICHOLLS, 1975: Calculation of the spectral transmission of the earth's atmosphere in the ultraviolet. York University, CRESS Spectroscopic Report No. 7, March.
- , ——— and W.F.J. EVANS, 1976: High resolution atmospheric calculations down to 94,000 ft in the spectral range 2000-2400 Å. To be published.
- EVANS, W.F.J. and E.J. LLEWELLYN, 1970: Molecular oxygen emission in the air-glow. *Ann. Geophys.* **26**, 167.
- GRIGGS, M., 1968: Absorption coefficients of ozone in the ultraviolet and visible regions. *J. Chem. Phys.* **49**, 857.
- MCEWEN, D.J. and H.T. MEREDITH, 1976: Solar ultraviolet flux measurements. *Atmosphere* **14**, 199-204.
- PENNDORF, R., 1957: Tables of refractive index for standard air and Rayleigh scattering coefficient for the spectral region between 0.7 and 20 μ . *J. Opt. Soc. Amer.* **47**, 176.
- SIMON, P., 1975: Nouvelles mesures de l'ultraviolet solaire dans la stratosphère, *Aeron Acta* No. 145.
- U.S. GOVERNMENT, 1966: *U.S. Standard Atmosphere, Supplements 1966*. ESSA/NOAA/USAF. U.S. Government Printing Office, Washington, D.C.
-

The Steady-State Structure of the Natural Stratosphere and Ozone Distribution in a 2-D Model Incorporating Radiation and O-H-N Photochemistry and the Effects of Stratospheric Pollutants

R. Krishna Rao Vupputuri

*Atmospheric Environment Service, 4905 Dufferin St.,
Downsview, Ontario, M3H 5T4*

[Manuscript received 13 August 1975; in revised form 20 April 1976]

ABSTRACT

A mean meridional circulation model of the stratosphere, incorporating radiative heating and photochemistry of the oxygen-hydrogen-nitrogen atmosphere, is used to simulate the meridional distributions of O_3 , HO_x , N_2O , NO_x , temperature and the three components of mean motion for the summer and winter seasons under steady-state conditions. The results are generally in good agreement with the available observations in the normal stratosphere. The model has been applied to assess the effects of water vapour and nitrogen oxide perturbations resulting from aircraft emissions in the stratosphere. It is found that a fleet of 500 Boeing-type SST's, flying at 20 km and $45^\circ N$ in the summer hemisphere and inserting NO_x at a rate of 1.8 megatons per year, has the effect of reducing the global total ozone by 14.7%. Similar calculations for 342 Concorde/TU-114's, cruising at 17 km and injecting NO_x at a rate of 0.35 megatons per year, show a global-average total-ozone reduc-

tion of 1.85%. Although water vapour is considered important, because of its ability to convert NO_2 into HNO_3 , the direct effect on global-average total-ozone reduction resulting from the 100% increase in the stratospheric water content is less than 1%. The changes in the chemical structure (HO_x , NO_x), temperature, and mean motions associated with the ozone reduction are also investigated in the case of the 1.8-megaton-per-year NO_x perturbation. It is shown that the reduced meridional temperature gradient in the middle and upper stratosphere resulting from the NO_x perturbation leads to the weakening of the tropical easterly jet in the summer hemisphere and mid-latitude westerlies in the winter season.

The sensitivity of the model solutions to an alternate choice of input parameters (diffusion coefficients and solar photodissociation data) is tested and the main deficiency of the model is pointed out.

1 Introduction

Ozone has long been recognized as one of the most important trace substances occurring naturally in the earth's atmosphere. Because of its intense absorption properties in the ultraviolet part of the solar spectrum, it not only protects

life at the ground from the sun's harmful ultraviolet radiation, but it also provides the dominant source of thermal energy to drive the circulation in the stratosphere.

A few years ago environmentalists voiced concern that a fleet of high-flying aircraft might reduce the ozone balance by exhausting substantial amounts of water vapour and nitrogen oxides into the stratosphere, and that serious consequences on the earth's biological system and its climate would follow. This concern over man's impact on the environment led to the initiation of the Climatic Impact Assessment Program (CIAP) in the United States in 1971. Over its three operational years, the program has contributed significantly to our knowledge of ozone photochemistry and of the radiative and transport properties of the stratosphere. For example, the important photochemical reactions leading to the formation and destruction of ozone, and the odd hydrogen and nitrogen compounds have been identified and their reaction rates have been confirmed. Numerical model calculations incorporating the water vapour and/or nitrogen oxide reactions in the ozone photochemistry have shown these reactions to reduce stratospheric ozone significantly (Johnston, 1971; Crutzen, 1972; Hesstvedt, 1973; Rao and Christie, 1973; Stewart, 1973; Rao-Vupputuri, 1974a, b; Chang, 1974; McElroy *et al.*, 1974; Whitten and Turco, 1974; Shimazaki and Ogawa, 1974; Cunnold *et al.*, 1974; Hunten, 1974; Widhopf, 1974), although the calculated percentage decreases of ozone by artificial NO_x differ depending on the dimensionality and the complexities of photochemical-dynamical considerations of the model.

The problem of assessing both the effects of natural concentrations of HO_x and NO_x and their perturbation by a potential high altitude fleet on the ozone balance and other meteorological elements is a complex one. First of all, it should be emphasized that in the stratosphere the concentrations of O_3 , HO_x and NO_x are mutually interdependent through the oxygen-hydrogen-nitrogen photochemical system. In addition, the temperature structure, and consequently the large-scale motions, are largely determined by the ozone distribution through radiative heating while the motions themselves influence the distributions of radiatively active gases such as ozone and other minor constituents. It is thus evident that only by treating these non-linear interactions in a numerical model can one properly describe the behaviour of naturally occurring trace substances and evaluate their perturbation effects in the stratosphere.

One-dimensional vertical diffusion models usually include very comprehensive photochemical schemes and provide important first approximations to the background concentrations of the minor constituents in the stratosphere. However, it is well-known that in the stratosphere the large-scale quasi-horizontal eddy mixing and mean meridional motions also play a significant role in determining the overall concentrations of certain trace gases such as O_3 , N_2O , HNO_3 . This is particularly so in the lower stratosphere where the photochemical time-scales for these chemical species are large compared to the transport time-scales.

There are also a number of two-dimensional models which include fairly

comprehensive photochemical schemes and allow horizontal, as well as vertical, transports. Unfortunately, most of these models specify the temperature structure and mean meridional motions and, in so doing, neglect the coupling between temperature and the radiatively active minor constituents.

The more sophisticated three-dimensional general circulation models of the troposphere and stratosphere are so complex that they must leave out some of the important coupling effects between chemistry and dynamics because of computer limitations. Although a simplified three-dimensional model (based on quasi-geostrophic conditions) incorporating the interaction between dynamics and ozone photochemistry has been reported (Cunnold *et al.*, 1974) the model still uses simplified chemistry and does not calculate the structure of the chemical trace species affecting the ozone distribution.

Despite the limitations imposed by having to parameterize the large-scale eddy processes it has been shown recently (Rao, 1973) that the major interactions between atmospheric composition, temperature and transport processes can be incorporated in a two-dimensional model.

The objectives of this paper are: first, to investigate the seasonal and latitudinal structure of the normal stratosphere with respect to temperature, ozone HO_x (HO , HO_2), N_2O , NO_x (NO , NO_2 , HNO_3) and the mean circulation, taking into account their mutual interrelationships; and second, after comparing the computed results with available observational data and testing the validity of the model for the normal stratosphere, to assess the effects of HO_x , NO_x , resulting from a hypothetical fleet of high-flying aircraft.

2 Transport model

The stratospheric transport model used for the study is the two-dimensional mean circulation model developed by Rao (1973). It runs from 10 to 55 km in the vertical and from summer pole to winter pole in the horizontal. The grid spacing is approximately 3 km in the vertical and 10 degrees latitude in the meridional direction.

The model equations are those governing the zonal momentum and heat balance and the continuity of the net mass and ozone, and they are averaged with respect to time and longitude.

The eddy fluxes of heat and ozone are parameterized using a mixing length representation on a sloping surface in the meridional plane (Reed and German, 1965). The eddy fluxes of momentum in the horizontal direction, however, are related to the meridional thermal gradients (Williams and Davies, 1965). The diffusion coefficients k_{yy} , k_{yz} , k_{zz} were derived from heat flux and temperature data in the stratosphere after the study of Reed and German. The radiational heating and cooling is incorporated in a form which allows for the major interactions among ozone, temperature and mean circulation.

The boundary conditions applied are such that both temperature and ozone mixing ratio are specified at the lower and upper boundaries and zero horizontal flux is assumed at both poles. The seasonal values of zonal winds are specified at 10 km and the vertical component of mean motion based on

thermal equilibrium (Murgatroyd and Singleton, 1961) is used at the top boundary. Further, both the zonal wind and the north-south component of the mean motion are assumed to be antisymmetric with respect to the poles. The sensitivity of the numerical solution to each of these boundary conditions has been tested and documented by Rao (1973).

It should be noted that the values of k_{yw} , k_{yz} , and k_{zz} reported by Reed and German (1965) are generally overestimated in comparison with the new values computed by Luther (1973) using more recent data on heat fluxes, temperatures and wind variances (Oort and Rasmusson, 1971). In view of this apparent discrepancy, a sensitivity test on the model results has been performed using a new set of diffusion coefficients.

3 Photochemical model

The primary mechanism by which ozone is produced in the earth's atmosphere is by the photodissociation of molecular oxygen and the subsequent recombination of atomic oxygen and molecular oxygen in the presence of neutral particles (Chapman, 1930). However, it is destroyed not only by photodissociation and by recombination with atomic oxygen but also by catalytic chain reactions involving, among other substances, water and nitrogen products. The principal chemical and photochemical reactions leading to the formation and destruction of ozone, the odd hydrogen and the odd nitrogen particles, in an interactive manner, are listed in Table 1. The choice of reactions and rate coefficients is based on the simplified sets of chemical reactions prepared by Johnston (1973). The reaction rates are the revised NBS values (Garvin and Hampson, 1974), and these are recommended by CIAP for incorporation into transport models. The additional reactions involving hydrogen and nitrogen compounds and their implications for the ozone layer have been discussed rather extensively in the recent literature (Hampson, 1964; Hunt, 1966; Crutzen 1969, 1971; Leovy, 1969; Johnston, 1971, 1973; Hesstvedt, 1973; Brasseur and Nicolet, 1973; Rao and Christie, 1973; Rao-Vupputuri, 1975; and others). Based on reactions R1 to R30 the photochemical tendency equations for O_3 , HO_x , NO_x and N_2O could be written in a form that is more suitable for a transport model. Thus we have¹:

$$\frac{d\chi}{dt} = AJ_1 - BJ_4\chi^2 - \chi\{CJ_4\chi(NO_2) + D\chi(HO) + EJ_4\chi(HO)\}, \quad (1)$$

$$\frac{d\chi(HO_x)}{dt} = FJ_5\alpha_3\chi + J_{20}\chi(HNO_3) - G\chi^2(HO_x) - \{H\chi(NO_2) + I\chi(HNO_3)\}\chi(HO_x), \quad (2)$$

$$\frac{d\chi(NO_x)}{dt} = \frac{2K_{14}\chi(N_2O)J_5\alpha_3\chi}{K_7} - \frac{2K_{17}J_{15}\chi^2(NO_x)}{R_3(K_{17}\chi(NO_x) + \alpha R_3K_{16})} + 2\chi(N_2)J(N_2) \frac{\alpha R_3K_{16} - K_{17}\chi(NO_x)}{K_{17}\chi(NO_x) + \alpha R_3K_{16}}, \quad (3)$$

¹From here onwards all the chemical species will be expressed in units of volume mixing ratio, except for ozone which will be expressed in units of mass mixing ratio.

TABLE 1. The important photochemical reactions and reaction rates affecting the concentrations of ozone and other trace species in the stratosphere

Reactions	Rate Coefficients (cgs Units)
R1 $O_2 + hv \xrightarrow{\lambda < 0.25 \mu m} O + O$	J_1 (Solar flux dependent)
R2 $O + O_2 + M \longrightarrow O_3 + M$	$K_2 = 1.07 \times 10^{-34} e^{510/T}$
R3 $O + O_3 \longrightarrow O_2 + O_2$	$K_3 = 1.9 \times 10^{-11} e^{-2300/T}$
R4 $O_3 + hv \xrightarrow{\lambda < 1.1 \mu m} O_2 + O$	J_4 (Solar flux dependent, see text)
R5 $O_3 + hv \xrightarrow{\lambda < 0.31 \mu m} O_2 + O(^1D)$	J_5 (Solar flux dependent)
R6 $O(^1D) + O_3 \longrightarrow O_2 + O_2$	$K_6 = 2.5 \times 10^{-10}$
R7 $O(^1D) + M \longrightarrow O + M$	$K_7 = 5.4 \times 10^{-11}$
R8 $NO_2 + hv \xrightarrow{\lambda < 0.41 \mu m} NO + O$	J_8 (Solar flux dependent, see text)
R9 $NO + O + M \longrightarrow NO_2 + M$	$K_9 = 3.96 \times 10^{-33} e^{940/T}$
R10 $NO_2 + O \longrightarrow NO + O_2$	$K_{10} = 9.1 \times 10^{-12}$
R11 $NO + O_3 \longrightarrow NO_2 + O_2$	$K_{11} = 9 \times 10^{-13} e^{-1200/T}$
R12 $N_2O + hv \xrightarrow{\lambda < 0.34 \mu m} N_2 + O$	J_{12} (Solar flux dependent, see text)
R13 $N_2O + O(^1D) \longrightarrow N_2 + O_2$	$K_{13} = 1.1 \times 10^{-10}$
R14 $N_2O + O(^1D) \longrightarrow NO + NO$	$K_{14} = 1.1 \times 10^{-10}$
R15 $NO + hv \xrightarrow{\lambda < 0.19 \mu m} N + O$	J_{15} (Solar flux dependent, see text)
R16 $N + O_2 \longrightarrow NO + O$	$K_{16} = 1.02 \times 10^{-14} T e^{-3150/T}$
R17 $N + NO \longrightarrow N_2 + O$	$K_{17} = 2.7 \times 10^{-11}$
R18 $O(^1D) + H_2O \longrightarrow 2HO$	$K_{18} = 3.5 \times 10^{-10}$
R19 $O(^1D) + CH_4 \longrightarrow HO + CH_3$	$K_{19} = 4.0 \times 10^{-10}$
R20 $HNO_3 + hv \xrightarrow{\lambda < 0.55 \mu m} HO + NO_2$	J_{20} (Solar flux dependent, see text)
R21 $HO + O_3 \longrightarrow HO_2 + O_2$	$K_{21} = 1.6 \times 10^{-12} e^{-1000/T}$
R22 $HO + O \longrightarrow O_2 + H$	$K_{22} = 4.2 \times 10^{-11}$
R23 $HO_2 + O_3 \longrightarrow HO + 2O_2$	$K_{23} = 1.0 \times 10^{-13} e^{-1250/T}$
R24 $HO_2 + O \longrightarrow HO + O_2$	$K_{24} = 8.0 \times 10^{-11} e^{-500/T}$
R25 $H + O_2 + M \longrightarrow HO_2 + M$	$K_{25} = 2.1 \times 10^{-32} e^{290/T}$
R26 $H + O_3 \longrightarrow HO + O_2$	$K_{26} = 2.6 \times 10^{-11}$
R27 $HO_2 + HO_2 \longrightarrow H_2O_2 + O_2$	$K_{27} = 3 \times 10^{-11} e^{-500/T}$
R28 $HO + HO_2 \longrightarrow H_2O + O_2$	$K_{28} = 2.0 \times 10^{-11}$
R29 $HO + NO_2 + M \longrightarrow HNO_3 + M$	$K_{29} = \frac{8.5 \times 10^{-13} e^{360/T}}{\{[M] + 1.5 \times 10^{18}\}}$
R30 $HO + HNO_3 \longrightarrow H_2O + NO_3$	$K_{30} = 1.3 \times 10^{-13}$

$$\frac{d\chi(N_2O)}{dt} = -J_{12}\chi(N_2O) - \frac{(K_{13} + K_{14})J_5\alpha_3\chi\chi(N_2O)}{K_7}, \quad (4)$$

where:

$$A = 2 \left(\frac{\rho_2}{\rho_{air}} \right) \frac{m_3}{m_2},$$

$$B = \frac{2}{(\rho_2/\rho_{air})[M]} \left(\frac{K_3}{K_2} \right) \frac{m_2}{m_3},$$

$$[M] = P/RT_m,$$

$$C = \frac{2K_{10}}{\alpha[M]K_2},$$

$$\alpha = [O_2]/[M],$$

$$D = 2K_{21}[M],$$

$$E = \frac{2K_{22}}{\alpha[M]K_2},$$

$$F = \frac{2K_{18}\chi_E(H_2O)}{K_7},$$

$$\alpha_3 = m/m_3,$$

$$G = \frac{2K_{27}[M]\beta^2 + 2K_{28}[M]\beta}{(\beta + 1)^2},$$

$$H = \frac{(K_{29}[M])[M]}{(\beta + 1)},$$

$$I = \frac{K_{30}[M]}{(\beta + 1)},$$

$$\beta = \frac{\chi(HO_2)}{\chi(HO)} = \frac{\alpha K_2 K_{21}[M]^2 + K_{22}J_4}{\alpha K_2 K_{23}[M]^2 + K_{24}J_4},$$

$$\frac{\chi(HO_x)}{\chi(HO)} = 1 + \beta,$$

$$R_1 = \frac{\chi(NO_2)}{\chi(NO)} = \frac{\alpha K_{11}K_2[M]^2\alpha_3\chi}{\alpha K_2[M]J_8 + K_{10}J_4\alpha_3\chi},$$

$$R_2 = \frac{\chi(HNO_3)}{\chi(NO_2)} = \frac{(K_{29}[M])[M]\chi(HO)}{J_{20} + K_{30}[M]\chi(HO)},$$

$$R_3 = \frac{\chi(NO_x)}{\chi(NO)} = 1 + R_1 + R_1R_2,$$

$$\chi_E(H_2O) = \chi(H_2O) + 2\chi(CH_4).$$

χ is the mass mixing ratio of ozone.

m, m_2, m_3 are the molecular masses of air, oxygen and ozone, respectively.

$[O_2], [M]$ are the number densities of molecular oxygen and air, respectively.

ρ_2 is the density of molecular oxygen.

P is the pressure.

T is the temperature.

R is the gas content.

$\chi_E(H_2O)$ is the effective water vapour mixing ratio.

In deriving (1) to (3) it is assumed that the individual trace constituents in each of the odd oxygen, hydrogen and nitrogen systems are in photochemical equilibrium among themselves. This assumption is generally valid in the stratosphere except near the winter pole in the case of HNO_3 . Since the winter polar region represents only a small fraction of the mass in the present model atmosphere, the neglect of transport on the HNO_3 distribution will not seriously alter the NO_x results.

In order to close the photochemical system we still require two more equations for H_2O and CH_4 . In this study the concentration of water vapour and methane are specified from the measurements of Mastenbrook (1974) and Ehhalt and Heidt (1973) instead of treating them as variables in the model.

As one can see from (1) to (4) the constituent mixing ratios of O_3 , HO_x , NO_x and N_2O are not only mutually interdependent among themselves, but they are also coupled to the radiative and transport properties of the stratosphere through the ozone continuity equation. In view of these non-linear effects it is more appropriate to solve the continuity equation for ozone, HO_x , NO_x and N_2O simultaneously, thus allowing for the feedback effects of temperature variation on reaction rates. In this respect the present experiment is different from the other 2-D models (Widhopf, 1974; Prinn *et al.*, 1975) which ignore the coupling effects between temperature, mean meridional motions and trace constituents which are important in the stratosphere.

Additional boundary conditions on the hydrogen and nitrogen species are required to solve the continuity equations for HO_x , N_2O and NO_x in conjunction with the ozone, temperature, zonal momentum and mass continuity equations. We assume zero horizontal flux at the poles and zero vertical flux at the top boundary for all the hydrogen and nitrogen species. At the lower boundary the N_2O mixing ratio is prescribed from the measurements by Schutz *et al.* (1970) while an average tropospheric value for NO_x (Junge, 1963) is adopted. Because observational data are lacking, the lower boundary condition for HO_x is interpreted from one-dimensional model results.

There appears to be some question as to the validity of the lower boundary condition on the NO_x mixing ratio which is based on the average tropospheric value (3 parts per billion by volume). Recent measurements around the tropopause indicate NO_x ($NO + NO_2 + HNO_3$) mixing ratios considerably less than the average tropospheric value. Because of this uncertainty on the NO_x lower boundary value, a comparative test has been performed with a reduction of 50%.

4 Solar fluxes and photodissociation parameters

In order to compute photodissociation rates and solar heating by ozone in the model, we require spectral data on solar intensities outside the atmosphere, absorption cross-sections and quantum yields for the chemical species under consideration and the scattering cross-section for air. The data on solar fluxes, absorption cross-sections and quantum yields for ozone and molecular oxygen and the scattering cross-section for air were taken from Byron-Scott (1967) and the method of computing J_1 , J_4 (the dissociation rates for oxygen and ozone) and the solar heating by ozone was described by Rao (1973). The spectral domain considered covers the wave-number range 13500 to 59375 cm^{-1} (1684.2–7407 Å). It includes modified spectral data published by Brewer and Wilson (1965) within the 41237–55555 cm^{-1} (1800–2425 Å) range.

A more recent data compilation of solar fluxes and absorption cross-sections

tions by Ackerman *et al.* (1970) shows that the values of solar intensity and the absorption cross-sections for molecular oxygen are much higher than the values tabulated by Brewer and Wilson, especially around 2200 Å (the values differ roughly by a factor of 3 in solar fluxes and 2 in the case of the cross-sections of O_2). In view of these discrepancies, the sensitivity of the latitudinal distribution of the total ozone column has been tested by using the two sets of spectral data.

We also require additional spectral data on the absorption cross-sections of N_2O , NO , NO_2 and HNO_3 to compare J_{12} , J_{15} , J_8 and J_{20} . The photodissociation cross-sections of N_2O are taken from Bates and Hays (1967) and for NO_2 and HNO_3 the values reported by Johnston and Graham (1973) are used.

It is difficult to determine the photodissociation rates of NO , since one requires a detailed knowledge of the absorption spectrum in the Schumann-Runge bands of molecular oxygen. Recently Cieslik and Nicolet (1973) have attempted to calculate J_{15} in the stratosphere using the detailed cross-sections of molecular oxygen determined by Ackerman *et al.* (1970) and these values are used in the present calculations.

As far as the production of atomic nitrogen $\{2[N]J(N_2)\}$ by cosmic rays is concerned, a value of 5 molecules $cm^{-3} s^{-1}$ is chosen arbitrarily, based on the study by Brasseur and Nicolet (1973). More recently, however, Nicolet (1975) has shown that the production of NO by cosmic rays varies considerably with latitude, height and solar activity in the lower stratosphere. In the light of this new evidence a case experiment has been performed to test the effect of latitude-height variations of NO production rates on the model results for the conditions of solar minimum (maximum NO production rates).

5 Discussion of results

a Natural Stratosphere

Two different types of experiments were carried out to determine the steady-state meridional structure of the temperature, the three components of mean motion, ozone, HO_x , N_2O and NO_x for summer and winter in the stratosphere. The first experiment was a computation for an uncontaminated background atmosphere incorporating radiative-photochemical processes in an oxygen-hydrogen-nitrogen atmosphere. The second experiment was identical to the first except the calculations included the deposition of stratospheric pollutant gases resulting from a hypothetical fleet of high-flying aircraft. In addition, the first experiment was repeated to test the sensitivity of the model results to the uncertainties in the diffusion and chemical rate coefficients, solar spectral data, boundary conditions and production of odd nitrogen by cosmic rays.

Figs. 1 to 7 give the meridional distribution of ozone, temperature, HO , N_2O , NO , NO_2 and HNO_3 (solid lines) which were derived in a self-consistent manner under the combined influence of radiation, $O-H-N$ photochemistry and transport processes, in the first experiment. Also derived as a part of the simultaneous solution were the three components of mean circulation, the results

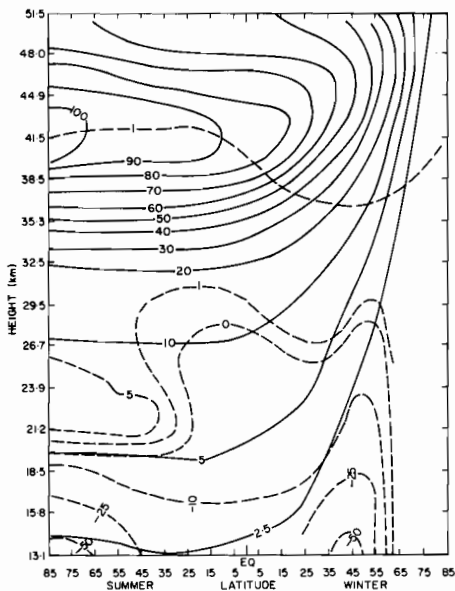


Fig. 3 Meridional cross-section representing the distribution of HO (units 10^5 particles cm^{-3}) in the normal stratosphere (solid lines) and percentage change in the HO concentration (dashed lines) in the same experiments as in Fig. 1. Negative values represent increase.

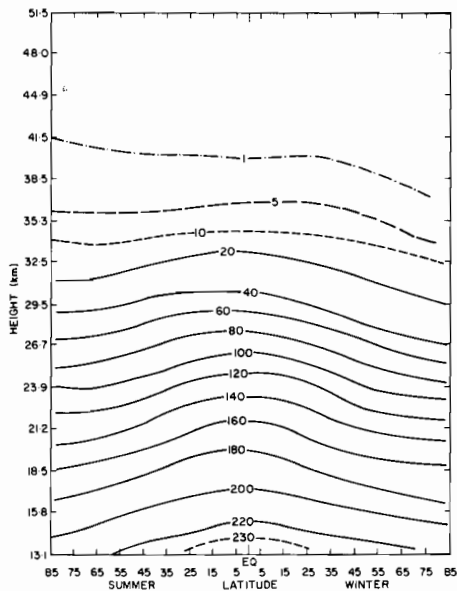


Fig. 4 Meridional cross-section representing the distribution of N_2O mixing ratio in the normal stratosphere derived in the same experiment as in Fig. 1. ($O-H-N$ atmosphere, experiment 1). Units are ppbv.

the high latitudes or it could be related to the overprediction of NO_x and consequent excessive destruction of ozone at high latitudes in the summer hemisphere.

Consistent with the ozone distribution, the computed meridional temperature field is also in good agreement with the observations reported by Cunnold *et al.* (1974) for summer and winter. However, there are differences in details between the model results and observations with respect to the equator-to-pole temperature gradients and the height of the stratopause level in the summer hemisphere, which could be related to the uncertainties in the transport characteristics through diffusion coefficients and boundary conditions.

The predominant chemical process leading to the formation of HO_x (HO and HO_2) radicals in the normal stratosphere is the reaction between H_2O and the electronically excited oxygen atom $O(^1D)$, with additional contributions from the reaction between CH_4 and $O(^1D)$. The CH_4 contribution was taken into account in the definition of effective water vapour without going into complex CH_4 photochemistry. The termination reactions R27 to R30, on the other hand, act as sinks for HO_x radicals. However, the ultimate distribution of HO_x in the atmosphere is determined by the mutual interactions among

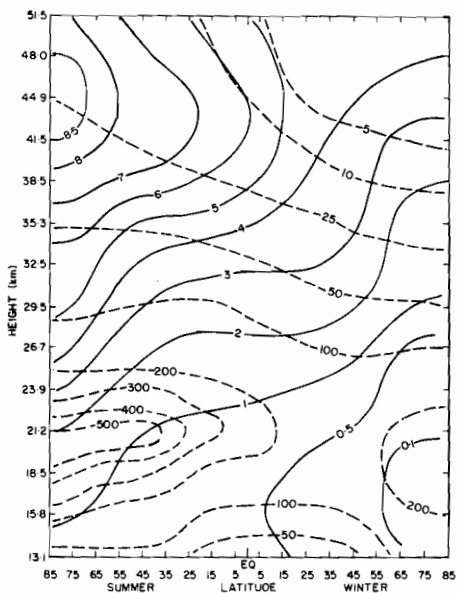


Fig. 5 Meridional cross-section representing the distribution of NO (ppbv, solid lines) in the normal stratosphere and the percentage increase in the NO mixing ratio (dashed lines) in the same experiments as in Fig. 1.

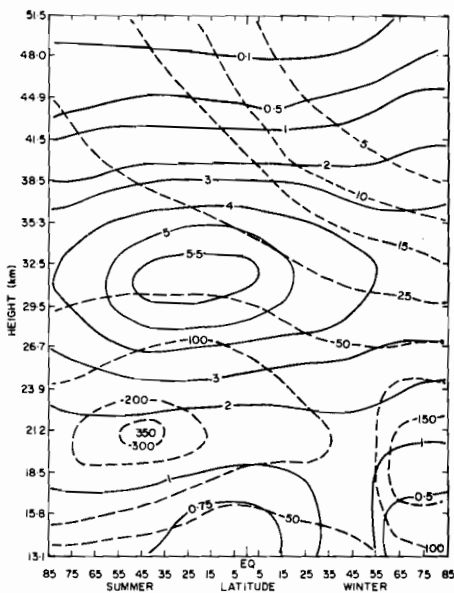


Fig. 6 Meridional cross-section representing the distribution of NO_2 (ppbv, solid lines) in the normal stratosphere and the percentage increase in the NO_2 mixing ratio (dashed lines) in the same experiments as in Fig. 1.

$O-H-N$ photochemical systems with transport processes playing an indirect role.

Fig. 3 presents an example of the variations of HO in the meridional plane for summer and winter seasons. It exhibits strong seasonal as well as height variations in the stratosphere. The radical shows maximum concentrations around 43 km in the summer hemisphere. The latitude-height variation of HO_2 is similar to that of HO except the height of maximum concentration is lower, roughly coinciding with the ozone maximum.

The time constant (time to achieve photochemical equilibrium) of the HO_x system is small compared to those of the ozone and NO_x systems in the stratosphere, and thus the transport processes do not appear to play a significant role in the distribution of HO and HO_2 . However, it should be remembered that the transport processes can have significant control over the distributions of ozone and NO_x which in turn control the concentration of HO_x .

There are no measurements of HO and HO_2 in the stratosphere to judge the accuracy of the model calculations. However, the computed distributions of HO and HO_2 should be considered valid in the sense that these radicals, together with the NO_x distribution, explain the ozone and temperature structure of the normal stratosphere in a self-consistent fashion. As one might expect in the case of HO_x , the computed profiles of HO and HO_2 at $30^\circ N$ in the summer hemisphere in this model are generally in good agreement with the

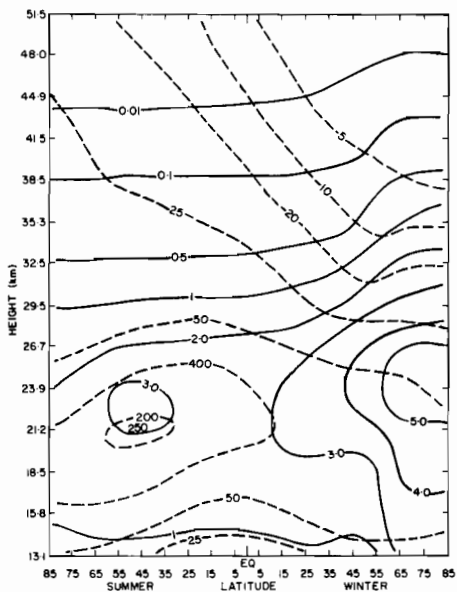


Fig. 7 Meridional cross-section representing the distribution of HNO_3 (ppbv, solid lines) in the normal stratosphere and the percentage increase in the HNO_3 mixing ratio (dashed lines) in the same experiments as in Fig. 1.

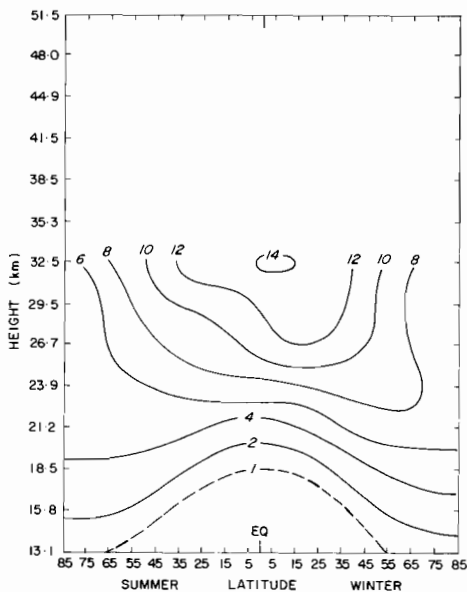


Fig. 8 Meridional cross-section of observed O_3 mixing ratio ($\mu g g^{-1}$) in summer and winter. The distribution is based on bi-monthly means of North American ozonesonde data compiled by Hering and Borden (1964).

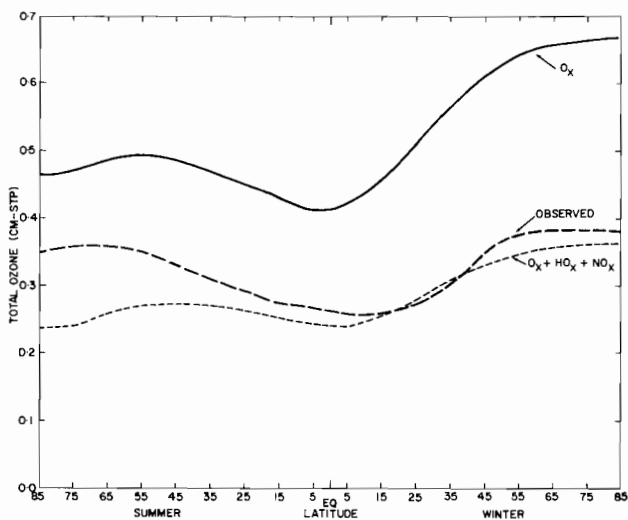


Fig. 9 Comparison of the latitudinal distribution of observed total ozone column (atm-cm) with the computed distributions in experiment 1 (using the reaction scheme of oxygen-hydrogen-nitrogen atmosphere). Also shown for comparison is the computation for the classical scheme of an oxygen-only atmosphere (top curve).

corresponding calculations in the one-dimensional model of McElroy *et al.* (1974).

N_2O is created at the earth's surface through biological activity, and it diffuses upward into the upper atmosphere (Bates and Hays, 1967). In the stratosphere, its destruction by photodissociation and oxidation with $O(^1D)$ provides the predominant source of NO_x . Additional contributions to NO_x may be produced by cosmic rays, mainly at high latitudes in the lower stratosphere (Nicolet, 1975). Since both N_2O and NO_x are influenced by ozone (through $O(^1D)$ and photodissociation rates) the concentration of which is, in turn, controlled by NO_x , the final distributions of N_2O and NO_x again result from the complex mutual interaction between the $O-H-N$ photochemical system and the transport processes.

The meridional distribution of N_2O is presented in Fig. 4 for summer and winter seasons while the distributions of NO , NO_2 , and HNO_3 resulting from the decomposition of NO_x are illustrated in Figs. 5, 6 and 7, respectively.

The distribution of N_2O shows that in the stratosphere mixing ratio decreases with height from the lower boundary (10 km) and becomes small above 45 km. In the meridional direction, the N_2O mixing ratio decreases from the tropics to high latitudes in both hemispheres. In the case of the NO_x ($NO + NO_2 + HNO_3$) mixing ratio, the distribution in the lower stratosphere resembles that of ozone, with mixing ratio increasing from tropics to high latitudes in both summer and winter hemispheres. In the upper stratosphere, however, the NO_x mixing ratio decreases from summer pole to winter pole. The height of the NO_x maximum and its variation above that height seem to be strongly influenced by the photochemical sink term associated with the reaction R17. As shown in Figs. 5, 6 and 7 the NO_x distribution consists predominantly of NO in the upper stratosphere, $NO + NO_2$ in the middle layer and HNO_3 in the lower stratosphere.

The present observational data on N_2O and NO_x (NO , NO_2 and HNO_3) are insufficient in terms of spatial and temporal variations to make detailed comparisons with the model results. However, the comparison of the model computations with the available observational data may provide an initial basis upon which the model results can be judged.

The comparison between the computed profile of N_2O at $45^\circ N$ in the summer hemisphere and the observations is given in Fig. 10. Also shown in Fig. 10 are the one-dimensional model calculations by Bates and Hays (1967), Crutzen (1974) and McElroy and McConnell (1971). It is particularly encouraging to see that the agreement between observations and model results is good.

In Fig. 11(a), the computed number densities of $NO + NO_2$ for summer at 45° latitude are compared with the simultaneous observations of Ackerman *et al.* (1975) for May 1974 at $43^\circ 35'$ latitude. Although the agreement between model results and observations appears to be good, it should be pointed out that both NO and NO_2 exhibit strong diurnal variations through reactions R8 and R10 which of course cannot be simulated in zonally and seasonally averaged models. Due to this limitation one should exercise caution in com-

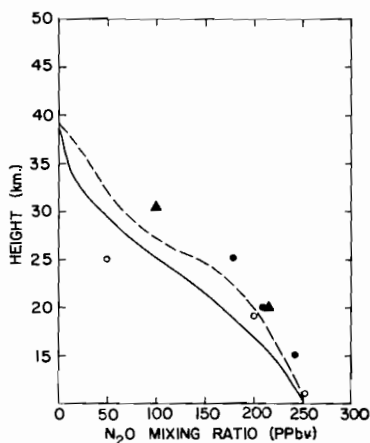


Fig. 10 Comparison of the computed altitudinal distributions of N_2O at $45^\circ N$ in the summer hemisphere with one-dimensional model results and measurements (units are parts per billion by volume). Solid lines, computed values (this study); dashed line, computed values (Crutzen, 1974); open circles, measured values (Schutz *et al.*, 1970); solid circles, computed values (Bates and Hays, 1967); solid triangles, computed values (McElroy and McConnell, 1971).

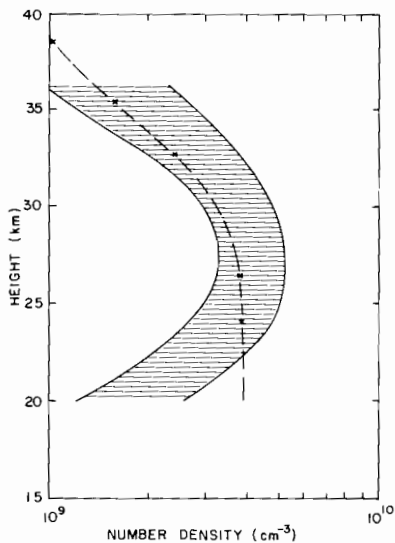


Fig. 11(a) Comparison of the computed distribution of NO plus NO_2 (left diagram) at $45^\circ N$ in the summer hemisphere with the simultaneous observations by Ackerman *et al.* (1975) for May at $43^\circ 35' N$ (the envelope of their measurements is represented by the shaded area); units are number densities.

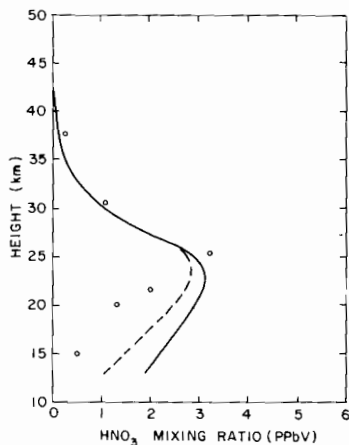


Fig. 11(b) Comparison of the computed distribution of HNO_3 with measurements (ppbv). Solid line, computed values (in this study); circles, measured values (Lazrus and Gandrud, 1974). The dashed curve represents the calculation with new lower boundary condition on NO_x .

paring the measurements of trace species which exhibit diurnal variations with the model calculations.

The computed distributions of both NO and NO_2 (see Figs. 5 and 6) exhibit strong seasonal variations which cannot be verified with the available observations. The variation of NO_2 in the lower stratosphere is of interest in that its mixing ratio has a maximum at $55^\circ N$ in the winter hemisphere and then suddenly drops to a low value at the winter pole. This may be attributed to a high value of HNO_3/NO_2 ratio in the winter polar stratosphere where there is no solar radiation.

The computed profile of HNO_3 at $45^\circ N$ in the summer hemisphere can be compared with direct sampling-filter measurements by Lazrus and Gandrud (1974) in Fig. 11(b). The agreement between observations and the model results is good above 20 km with the model calculating correctly the altitude and magnitude of the peak mixing ratio of HNO_3 . Below 20 km, however, the calculated values (solid line in Fig. 11(b)) are larger than the observations, which may be related to the incorrect specification (according to current measurements) of the lower boundary condition for NO_x . The seasonal and latitudinal variations of HNO_3 (Fig. 7) appear to be in qualitative agreement with the observed variations reported by Lazrus and Gandrud (1974) which exhibit an increase in HNO_3 from equator to high latitudes and higher mixing-ratio values in winter than in summer.

b Perturbed Stratosphere

The satisfactory agreement between the model results and the observations suggests that the model can be applied with reasonable confidence to assess the perturbation effects of HO_x and NO_x on ozone, the temperature and mean circulation.

The perturbation effect of HO_x has been tested by simply doubling the background water vapour concentration in the model. The results show that the total ozone decreased by about 1% on a globally averaged basis. This small percentage decrease suggests that ozone is relatively insensitive to the stratospheric water vapour content. This is due to the fact that the increased HO_x , resulting from the doubling of water vapour, acts to convert NO_2 molecules into nitric acid (reaction R29) which does not react with ozone, thereby reducing the catalytic destruction of ozone by NO_x . For example, a 30% increase of HO_x in the lower stratosphere (around 21 km) resulting from the water vapour perturbation has the effect of reducing the NO_2 by 10 to 15% converting it into HNO_3 . The net effect of the water vapour perturbation in the stratosphere is a slight decrease in the total ozone caused by the reduction in the ozone mixing ratio, mainly in the upper and lower stratosphere. In fact, the results show a slight increase in the ozone mixing ratio taking place in the middle layer coinciding with the level of ozone maximum.

It is clear from the above discussion that, although the direct effect of the water vapour perturbation on ozone is small, water vapour itself is important to the ozone balance because of the ability of its radicals to convert NO_2 into

HNO_3 . Indeed similar conclusions have been reached by Johnston (1974) and Crutzen (1974) based on one-dimensional model results, although the latter author has reported a slight increase in the total ozone due to doubling the water vapour in the stratosphere. Perhaps this discrepancy could be related to differences in the rate constants for the reactions R21 to R23. It should be pointed out that the rate constants for these reactions are temperature-dependent in our model while they remain as constants in Crutzen's calculations. The temperature changes due to water vapour perturbation are not significant except in the summer upper stratosphere where the reduction in the ozone mixing ratio produced cooling up to 4 K.

In order to determine the perturbation effects of NO_x on the structure of minor trace constituents and of temperature and ozone in the stratosphere, two sets of calculations were performed. In the first set, the artificial source of NO_x was injected at a rate of 1.8 megatons per year at 21 km and $45^\circ N$ in the summer hemisphere. This injection rate is considered to be representative of a fleet operation consisting of 500 Boeing-type SST's and, when distributed uniformly over a 10° latitude belt and a height spread of 3 km, it corresponds to an additional NO_x source of 10^5 molecules/cm³ sec. The second set of calculations is identical to the first set except the NO_x injection rate is 0.36 megatons per year and this may represent a fleet of 342 Concorde-type aircraft in the stratosphere. In addition, both sets of calculations have been repeated with the altitude of injection changed and also with the injection switched from summer to winter hemisphere at the same latitude.

The dashed lines superimposed on the natural distributions of ozone, temperature, HO , NO , NO_2 and HNO_3 represent the percentage changes resulting from the 1.8 megaton NO_x injection at 21 km and $45^\circ N$ in the summer hemisphere (Figs. 1 to 3 and 5 to 7). Evidently, the artificial NO_x injections of the magnitude discussed here could lead to a major perturbation in the natural level of NO_2 (Fig. 6) which in turn produces substantial changes in ozone and temperature structure in the lower and middle stratosphere (Figs. 1 and 2). Although the peak perturbation in NO_2 coincides with the location of the NO_x injection, the maximum changes in ozone and temperature shift towards the summer pole. This may be attributed partly to the transport effect and partly to the longer duration of sunlight and consequently more efficient photochemical processes near the summer pole. It is of considerable interest to note that the concentration of HO increases in the lower stratosphere (Fig. 3) as a result of the NO_x perturbation. As discussed earlier, the increased density of HO radical has a stabilizing influence on the ozone destruction through the conversion of NO_2 into HNO_3 . Without this effect, one would expect even greater reductions in ozone and temperature in the lower stratosphere.

The latitudinal variations of total ozone depletion resulting from the 1.8 megaton per year NO_x injection for the altitude bands centered at 21.2 and 18.5 km are shown in Fig. 12. Also shown in Fig. 12 is the latitudinal variation of total ozone depletion due to 0.35 megaton-per-year NO_x injection at 18.5

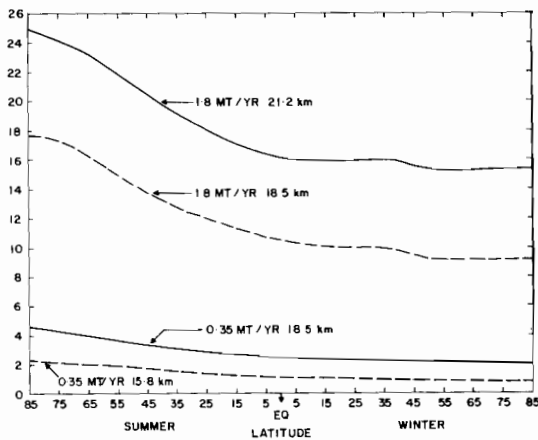


Fig. 12 Latitudinal variation of percentage total ozone depletion due to 1.8 megaton per year NO_x injection ($45^\circ N$, summer) for the altitude bands centered at 21.2 km (solid line), and 18.5 km (dashed line). The lower curves represent calculations with 0.35 megaton per year NO_x injection for the altitude bands centered at 18.5 and 15.8 km.

and 15.8 km. Evidently there is a marked variation (almost by a factor of 2) in the total ozone depletion from summer to winter latitudes. It is significant to note from Fig. 12 that ozone depletion is highly sensitive to the altitude of the NO_x injection. For instance, the 1.8 megaton per year injection at 21.2 km reduces the total ozone by 15 to 25% whereas 18.5-km injection leads to a reduction of no more than 9 to 18%. The results for a 0.35 megaton per year injection are quite similar to those for 1.8 megaton per year injection except the amplitude variations are much smaller.

Because of the sensitivity of total ozone depletion to the altitude of NO_x injection, the global average reduction of total ozone has been computed for the injection heights of 20 and 17 km, corresponding to projected flight levels for the Boeing-type supersonic transports (SST's) and Concorde/TU-114 SST's, respectively. Based on the first set of calculations, a fleet of 500 Boeing-type SST's flying at 20 km and injecting NO_x at a rate of 1.8 megatons per year in the summer hemisphere would have the effect of reducing the global average total ozone by 14.7%. Similar calculations in the second set show that a fleet of 342 Concorde/TU-114 SST's flying at 17 km and injecting NO_x at a rate of 0.35 megatons per year during the summer season would reduce the global average total ozone by 1.85%. These results are in general agreement with the DOT report of findings by Grobecker *et al.* (1974) which concludes that 375 Concorde/TU-114's and 500 Boeing type SST's would reduce the ozone by 1.5 and 12% respectively.

It has been calculated (Hesstvedt, 1973) that a 1% reduction in total ozone would result in a 2% increase in the erythemogenic ultraviolet radiation (0.29 to $0.32 \mu m$) reaching the earth's surface (which has been translated into 2% increase in skin cancer by one CIAP study). Based on this relationship the po-

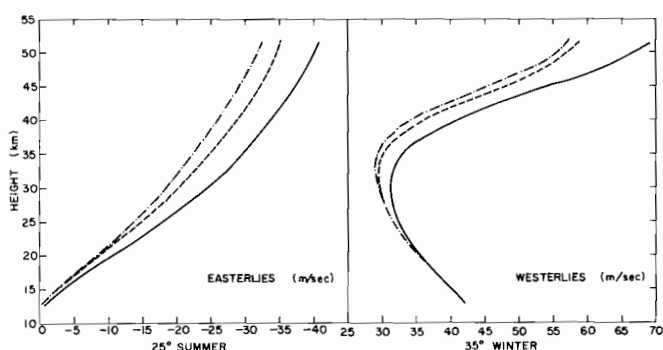


Fig. 13 Vertical profiles of zonal wind at selected latitudes representing the effects of water vapour and nitrogen oxides in the normal stratosphere (dashed lines) and in the stratosphere perturbed by 1.8 megaton per year NO_x injection at 21.2 km and $45^\circ N$ in the summer hemisphere (dash-dot lines). The solid lines correspond to the classical photochemical model.

tential biological effects resulting from the operation of a large SST fleet are of some significance.

Because of the coupling between radiative-photochemical and transport processes, the changes in ozone and temperature structure produced by the artificial injection of NO_x can also affect the zonal wind and mean meridional circulation in the stratosphere. Fig. 13 shows the influence of background water vapour and nitrogen oxides and the 1.8 megaton-per-year NO_x perturbation injected at 21 km and $45^\circ N$ (in the summer hemisphere) on the vertical profiles of the zonal wind. It may be seen from Fig. 13 that the NO_x perturbation has the effect of weakening both the easterlies at $25^\circ N$ in summer and the mid-latitude westerly jet at $35^\circ N$ in the winter hemisphere. However, the influence of background water vapour and nitrogen oxides is more significant than the effect of the 1.8-megaton-per-year NO_x perturbation. The NO_x perturbation considered here has no significant influence on the mean meridional motions although the background concentration has the effect of decreasing the subsidence motion at higher levels in the winter polar stratosphere.

c Sensitivity of the Model Results to an Alternate Choice of Input Parameters and Boundary Conditions

Although this model is completely interactive and one need not specify the temperature structure and mean meridional motions, the results still depend on the particular selection of input parameters (such as diffusion coefficients and solar spectral data) and boundary conditions. Since it is difficult to verify the accuracy of any particular choice of input parameters it may be useful to test the sensitivity of the model results to an alternate choice of these parameters preferably derived from more recent observational data. As mentioned earlier there are considerable differences in the solar fluxes and oxygen absorption cross-section data (Brewer and Wilson, 1965) used in this study and those compiled recently by Ackerman *et al.* (1970). Similarly there are differ-

ences between the values of diffusion parameters reported by Reed and German (1965) and those determined by Luther (1973). In order to test the sensitivity of the computed latitudinal distribution of total ozone, the experiment for the normal stratosphere has been repeated with recent solar spectral data given by Ackerman and diffusion coefficients reported by Luther. The results show that the new solar spectral data have the effect of producing significantly higher ozone mixing-ratio values in the middle and upper stratosphere and displacing the level of ozone maximum upward by about 5 km while the new set of diffusion coefficients contribute to lower values of ozone mixing ratio below the level of ozone maximum. The net effect is a small change in the total ozone distribution.

The second test experiment has been performed by introducing the latitude-height variation of NO production rates by cosmic rays, as given by Nicolet (1975), instead of the fixed value of $5 \text{ mol cm}^{-3} \text{ s}^{-1}$ which was used in the earlier run. The results indicate that there is no significant measurable difference in the meridional variation of the total ozone column between the two experiments although the ozone mixing-ratio values in the lower stratosphere, particularly in polar latitudes, are lower by about 1% in the later experiment. This is due to the localized nature of high NO production rates in the polar lower stratosphere (Nicolet, 1975).

As shown in Fig. 11 (b), there is considerable discrepancy between the computed results of HNO_3 and observations. To test the lower boundary influence, an experiment has been carried out with the lower boundary value of NO_x reduced to half its original value. As can be seen from the dashed curve in Fig. 11 (b), there is better HNO_3 agreement in the lower part of the lower stratosphere with this new boundary specification. The new lower boundary condition has also contributed to a better agreement with observations in the lower stratosphere in the case of NO and NO_2 . This suggests that the original NO_x lower boundary value of 3 ppbv was too high. In fact the current observations on NO_x appear to be supporting the later value (1.5 ppbv).

As a consequence of neglecting the hydrogen peroxide (H_2O_2) photochemistry in the chemical scheme adopted for this model, the reaction R27 appears as a sink for HO_x in equation (2). It is possible that the photodissociation of H_2O_2 could regenerate some of the HO_x lost in the reaction R27. To test this effect, the experiment for the normal stratosphere has been repeated by excluding reaction R27. The results show that the exclusion of the HO_x sink due to reaction R27 has the effect of overestimating the HO_x concentration by a factor 2 in the lower stratosphere and about 40% at higher levels in the upper stratosphere. However, it should be pointed out that there is a factor of 10 uncertainty in the rate coefficient for the reaction R28 and the value adopted for this study is its lower limit. The test results also show that by increasing the rate coefficient for reaction R28 by a factor of 10, the HO_x concentration decreases by a factor of 2 to 3 depending upon the latitude; height and season. Undoubtedly we need observations and better reaction rates to resolve the present uncertainties in the HO_x calculations.

It has been suggested that some of the excess NO produced at ionospheric levels under certain geophysical events (occurrences of auroras for example) can be transported downward in the stratosphere. Although it appears unlikely that this could take place (because of photodissociation of NO on its way downward) a purely hypothetical test experiment has been conducted by varying the prescribed downward flux of NO_x at the top boundary (55 km). The results indicate that downward fluxes of NO_x exceeding $10^6 \text{ mol cm}^{-2} \text{ s}^{-1}$ can produce significant effects on the ozone and temperature structure of the stratosphere.

Although the feedback effect of temperature variation of chemical reaction rates has always been included in the model, its stabilizing influence on ozone destruction has not been output explicitly. As pointed out by McElroy *et al.* (1974) a local increase of NO_x leads to a decrease in ozone which will be followed by the associated decrease in temperature. Because of the inverse relationship between ozone concentration and temperature (through temperature-dependent rate coefficients of reactions such as R1 and R3), particularly in the regions of the stratosphere where radiative-photochemical equilibrium conditions exist, the decrease in temperature leads to an increase in ozone mixing ratio. With a view to identifying the stabilizing influence of temperature-dependent rate coefficients on artificial NO_x perturbations, the 1.8-megaton-per-year NO_x injection (at 45°N and 21 km in the summer hemisphere) experiment has been repeated with a fixed temperature field. The results show that the global average reduction of total ozone with a fixed temperature field is 22% as compared to the value for the previous case. This suggests that the feedback of temperature variation on reaction-rate coefficients can have a significant influence on ozone destruction and the lack of this effect in a numerical model can lead to an inaccurate assessment of the effects of aircraft emissions in the stratosphere.

6 Summary and conclusions

A mean meridional circulation model of the stratosphere, incorporating radiative heating and photochemistry of the oxygen-hydrogen-nitrogen atmosphere, is used to compute simultaneously the meridional distributions of ozone, HO_x , N_2O , NO_x , temperature and the three components of mean motion under steady-state conditions, taking into account the principal interactions among them. The model results are shown to be in satisfactory agreement with the available observations in the normal stratosphere. This suggests that the natural variations of HO_x and NO_x , particularly the latter, interactively play a substantial role in the ozone and thermal balance of the stratosphere and significantly contribute to rectifying the initial discrepancies between earlier model results and observations.

The model has been applied to assess the perturbation effects of HO_x and NO_x resulting from the expected future aircraft emissions in the stratosphere. The results show that the increase of stratospheric NO_x resulting from a 1.8-megaton-per-year artificial NO_x injection at 21.2 km and 45°N in the summer

hemisphere would reduce the total ozone column by between 15 and 25% depending on the latitude and season, with a globally averaged value of 17.4%. It is also shown that, for the same NO_x injection rate, the ozone reduction is highly sensitive to the altitude of insertion (the higher the altitude the greater is the ozone reduction). Associated with the ozone reduction, significant changes take place in the temperature and chemical structure of the stratosphere. The behaviour of the stratosphere perturbed with a 0.35-megaton-per-year injection is quite similar to that described for the 1.8-megaton-per-year injection except the amplitude of variations in ozone, temperature and other minor constituents is much smaller. The effect of doubling the stratospheric water vapour content on total ozone reduction is shown to be much less (about 1%) than the effect of the 1.8-megaton-per-year NO_x perturbation on ozone. However, the water vapour perturbation has a significant stabilization effect on ozone reduction because of its ability to convert NO_2 into HNO_3 .

The results of the test experiments on the sensitivity of the model solutions to alternative choices of input parameters suggest that the incorporation of a new set of input parameters (diffusion coefficients and photodissociation data) based on more recent observations does not alter the main conclusion drawn in this study. The tests on the boundary conditions of NO_x indicate that the value (3 ppbv) specified at the lower boundary is excessive and one can improve the model results on odd nitrogen, particularly HNO_3 , in the lower stratosphere by reducing the NO_x lower boundary value by 50%.

Despite the limitations of the parameterized large-scale eddy mixing this interactive two-dimensional radiative-photochemical transport model is found to be extremely useful for the study of the meridional structure of temperature, ozone and the other minor trace constituents in the normal stratosphere and to determine the changes in that structure which might result from the introduction of artificial NO_x by a fleet of stratospheric aircraft. Further extensions to the model, involving the chlorine compounds, are now being undertaken in order to assess the impact of anthropogenic sources of freons (chlorofluoromethanes) on stratospheric structure and ozone distribution.

Acknowledgements

The author would like to thank Dr. B.W. Boville for his continued encouragement and advice; Dr. W.F.J. Evans for pointing out an error in the partitioning of HO_x in the earlier calculations and F. Szekely for help in the programming aspects of the problem. This work was supported by the Atmospheric Environment Service of Canada.

References

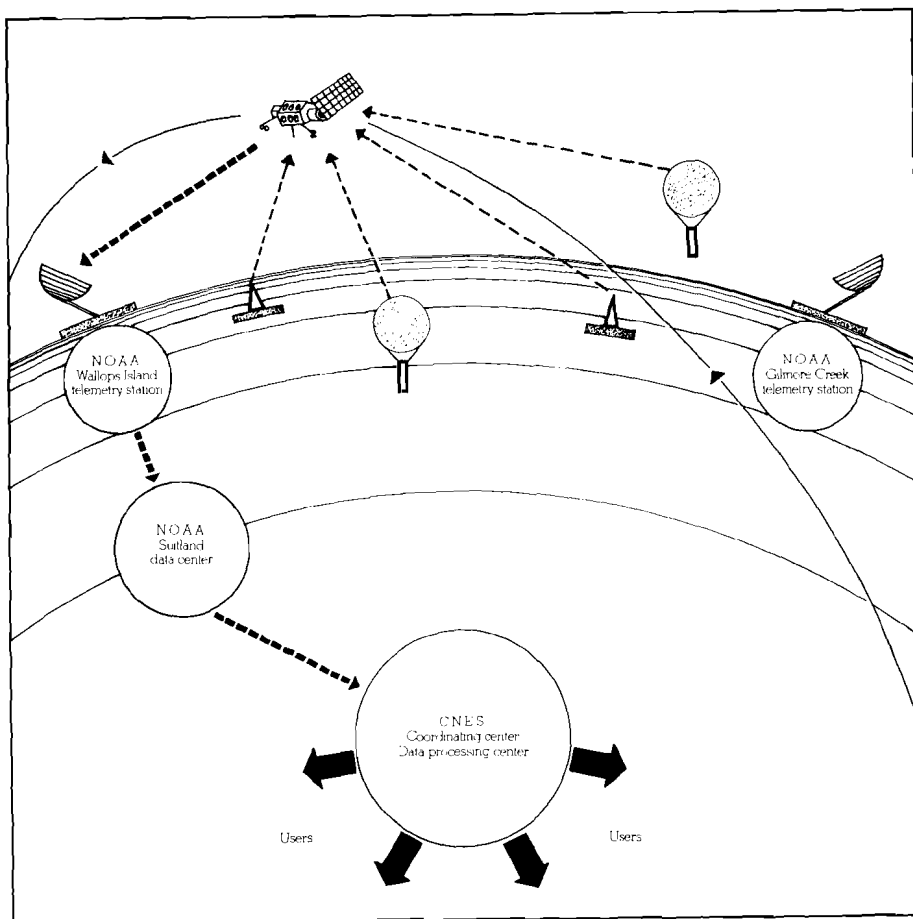
- ACKERMAN, M., F. BIAUMÉ and G. KOKARTS, 1970: Absorption cross sections of the Schumann-Runge bands of molecular oxygen. *Planet. Space Sci.*, **18**, 1639-1651.
- , J.C. FONTANELLA, D. FRIMOUT, A. GIRARD, N. LOUISNARD and C. MULLER, 1975: Simultaneous measurements of NO and NO_2 in the Stratosphere. *Planet. Space Sci.*, **23**, 651-660.
- , BATES, D.R. and P.B. HAYS, 1967: Atmo-

- spheric nitrogen oxide. *Planet. Space Sci.*, **15**, 189–197.
- BRASSEUR, G. and M. NICOLET, 1973: Chemospheric processes of nitrogen oxides in the stratosphere. *Planet. Space Sci.*, **21**, 939.
- BREWER, A.W. and A.W. WILSON, 1965: Measurement of solar ultra-violet radiation in the stratosphere. *Quart. J. Roy. Meteor. Soc.*, **91**, 452–461.
- BYRON-SCOTT, R., 1967: A stratospheric general circulation experiment incorporating diabatic heating and ozone photochemistry. Pub. in Meteor. No. 86, Arctic Met. Res. Group., Dept. of Meteor., McGill Univ., Montreal, Que., 201 pp., appendices.
- CHANG, J.S., 1974: Simulations, perturbations and interpretations. Proc. 3rd CIAP Conference, Cambridge, Mass., 26 Feb.–1 March.
- CHAPMAN, S., 1930: A theory of upper atmospheric ozone. *Mem. Roy. Meteor. Soc.*, **3**, 103–125.
- CIESLIK, S., and M. NICOLET, 1973: The aeronomic dissociation of nitric oxide. *Planet. Space Sci.*, **21**, 925–938.
- CRUTZEN, P.J., 1969: Determination of parameters appearing in the “dry” and the “wet” photochemical theories for ozone in the stratosphere. *Tellus* **21**, 368–388.
- 1971: Ozone production rates in an oxygen-hydrogen-nitrogen oxide atmosphere. *J. Geophys. Res.*, **76**, 7311–7327.
- 1972: SST's, a threat to the earth's ozone shield. *Ambio.*, **1**, 41–51.
- 1974: A review of upper atmospheric photochemistry. *Can. J. Chemistry*, **52**, 1569.
- CUNNOLD, D.M., F.N. ALYEA, N.A. PHILLIPS and R.G. PRINN, 1974: First results of the general circulation model applied to the SST, NO_x problem. Paper presented at the meeting of the AMS/AIAA 2nd Int. Conf. on the Environmental Impact of Aerospace Operations in the High Atmos., San Diego, Calif., 8–10 July.
- EHHALT, D.H., and L.E. HEIDT, 1973: The concentrations of molecular H_2 and CH_4 in the stratosphere. *Pure Appl. Geophys.*, **106–108**, 1352–1360.
- GARVIN, D., and R.F. HAMPSON, editors, 1974: Chemical kinetics data survey, VII tables of rate and photochemical data for modelling of the stratosphere (Revised), Nat. Bur of Stand., NBSIR 74–430.
- GROBECKER, A.J., S.C. CORONITI and R.H. CANNON, JR., 1974: Report of findings on the effects of stratospheric pollution by aircraft. U.S. Dept. of Transportation. Document is available to the public through the Nat. Tech. Info. Serv., Springfield, Virginia.
- HAMPSON, J., 1964: Photochemical behaviour of the ozone layer. Tech. Note 1627/64, CARDE, Val Cartier, Quebec, 20 pp.
- HERING, W.S. and T.R. BORDEN, 1964: Ozonesonde observations over North America, Vol. 2. Environ. Res. Papers No. 38, Proj. 8631, AFCRL, Bedford, Mass., 280 pp.
- HESSTVEDT, E., 1973: The effects of supersonic transport upon the ozone layer studied in a two-dimensional photochemical model with transport. AGARD Conference Proceedings No. 125, Item 6, London, England.
- HUNT, B.G., 1966: Photochemistry of ozone in a moist atmosphere. *J. Geophys. Res.*, **71**, 1385–1398.
- HUNTEN, D.M., 1974: Stratospheric Pollution and how it dissipates. Unpublished manuscript.
- JOHNSTON, H.S., 1971: Reduction of stratospheric ozone by nitrogen oxide catalysts from SST exhaust. *Science*, **173**, 517–522.
- 1973: Simplified sets of chemical reactions. Second Preliminary Draft, CIAP, **3**, Section 4.9.
- 1974: Annual report on Climatic Impact Assessment Program. Lawrence Berkeley Laboratory, University of California, Berkeley, California.
- , and R. GRAHAM, 1973: Gas-phase ultraviolet absorption spectrum of nitric acid vapour, *J. Phys. Chem.*, **77**, 62–63.
- JUNGE, C.E., 1963: *Air Chemistry and Radio-Activity*. Academic Press, New York and London, p. 37.
- KRUEGER, A.J., D.F. HEATH and C.L. MATEER, 1973: Variations in the stratospheric ozone field inferred from Nimbus satel-

- lite observations, *Pure Appl. Geophys.* **106-108**, 1254-1263.
- LAZRUS, A.L. and B.W. GANDRUD, 1974: Distribution of stratospheric nitric acid vapor. *J. Atmos. Sci.*, **31**, 1102-1108.
- LEOVY, C.B., 1969: Atmospheric ozone: An analytic model for photochemistry in the presence of water vapour. *J. Geophys. Res.*, **74**, 417-426.
- LUTHER, F.M., 1973: Monthly values of eddy diffusion coefficients in the lower stratosphere. AIAA Paper No. 73-498, AIAA/AMS International Conference on the Environmental Impact of Aerospace Operations in the Atmos., Denver, Colorado.
- MASTENBROOK, H.J., 1974: Stratospheric water vapour distribution and variability. Proceedings IAMAP/IAPSO First Special Assembly, Melbourne, Australia, 14-25 January.
- MCELROY, M.B., S.C. WOFRY, J.E. PENNER and J.C. MCCONNELL, 1974: Atmospheric ozone: possible impact of stratospheric aviation. *J. Atmos. Sci.*, **31**, 287-300.
- and J.C. MCCONNELL, 1971: Nitrous oxide: a natural source of stratospheric NO. *J. Atmos. Sci.*, **28**, 1095-1098.
- MURGATROYD, R.J. and F. SINGLETON, 1961: Possible meridional circulations in the stratosphere and mesosphere. *Quart. J. Roy. Meteor. Soc.*, **87**, 125-135.
- NICOLET, M., 1975: On the production of nitric oxide by cosmic rays in the mesosphere and stratosphere. Paper presented at the 4th CIAP Conference, Cambridge, Mass., 4-7 Feb.
- OORT, A.H., and E.M. RASMUSSEN, 1971: Atmospheric circulation statistics, NOAA Professional Paper No. 5.
- PRINN, R.G., F.N. ALYEA and D.M. CUNNOLD, 1975: Stratospheric distributions of odd nitrogen and odd hydrogen in a two-dimensional model. *J. Geophys. Res.*, **80**, 4997-5004.
- RAO, V.R.K., 1973: Numerical experiments on the steady state meridional structure and ozone distribution in the stratosphere. *Mon. Wea. Rev.*, **101**, 510-527.
- and A.D. CHRISTIE, 1973: The effects of water vapour and oxides of nitrogen on ozone and temperature structure of the stratosphere. *J. Atmos. Sci.*, **30**, 667-676.
- RAO-VUPPUTURI, R.K., 1974a: The role of stratospheric pollutant gases (H_2O , NO_x) in the ozone balance and its implication for the seasonal climate of the stratosphere. Proc. IAMAP/IAPSO First Special Assembly, Melbourne, Australia, 14-25 January.
- 1974b: A zonally averaged circulation model of the stratosphere incorporating radiative heating and ozone photochemistry in an oxygen-hydrogen-nitrogen atmosphere. Proc. 3rd CIAP Conference, Cambridge, Mass., 26 Feb.-1 March.
- 1975: Seasonal and latitudinal variations of N_2O and NO_x in the stratosphere. *J. Geophys. Res.*, **80**, 1125-1132.
- REED, R. and K.E. GERMAN, 1965: A contribution to the problem of stratospheric diffusion by large scale mixing. *Mon. Wea. Rev.*, **93**, 313-321.
- SCHUTZ, K., C. JUNGE, R. BECK and B. ALBRECHT, 1970: Studies of atmospheric N_2O . *J. Geophys. Res.*, **75**, 2230-2246.
- SHIMAZAKI, T. and T. OGAWA, 1974: Theoretical model of minor constituents' distribution in the stratosphere and the impact of SST exhaust gases. Proc. IAMAP/IAPSO First Special Assembly, Melbourne, Australia, 14-25 Jan.
- STEWART, T.W., 1973: Response of stratospheric ozone to the simulated injection of nitric oxide. Paper presented at the Fall American Geophysical Union Meeting, San Francisco, California.
- WHITTEN, R.C. and R.P. TURCO, 1974: The effect of SST emission on the earth's ozone layer. Proc. IAMAP/IAPSO First Special Assembly, Melbourne, Australia, 14-25 January.
- WIDHOPF, G.F., 1974: Meridional distributions of trace species in the stratosphere and the effects of SST pollutants. Paper presented at the Amer. Geophys. Union Fall Annual Meeting, San Francisco, California, 12-17 December.
- WILLIAMS, G.P. and D.R. DAVIES, 1965: A mean motion model of the general circulation. *Quart. J. Roy. Meteor. Soc.*, **91**, 471-489.

NOTES AND CORRESPONDENCE

THE "ARGOS" SPACE-BASED PLATFORM LOCATION AND DATA COLLECTION SYSTEM



From mid-1978 until 1986, specialists in the Earth sciences, the ocean sciences and the sciences of the atmosphere will be able to make use of the ARGOS operational platform location and data collection system.

The ARGOS system is intended to gather information concerning the environment from small automatic stations distributed all over the globe, and to locate mobile platforms such as balloons, drifting buoys, etc.

General description

The ARGOS system consists of various fixed stations and mobile platforms on Earth, reception and data collection facilities on board TIROS-N series satellites,

and the ground-based data collection, processing and redistribution facilities.

ARGOS system platforms can be fitted with between 4 and 32 sensors each; they automatically transmit coded messages at regular intervals without having to be interrogated.

The system's reception and data collection facilities are located on board operational meteorological satellites of the TIROS-N series. Since two of these satellites will be in polar orbits at any one time, the system guarantees continuous worldwide coverage. Each satellite picks up a mixture of messages transmitted by the platforms within its reception area; it performs signal acquisition (on a random access basis), data decommutation, and frequency measurements, and then generates a message to be fed to the satellite's central telemetry memory.

After interrogation by one of the NOAA telemetry network stations, the satellite transmits its stored telemetry messages. The in-coming messages are re-transmitted to the NESS station at Suitland, Maryland. Complete blocks of ARGOS data are then relayed to the CNES Space Center at Toulouse where platform location calculations and data decommutation operations are performed. The processed results are communicated to users less than 6 hours after the measurements are made. Arrangements can also be envisaged for the real-time processing of data on a regional basis. In this case, the satellite would transmit in real time, but at a reduced bit rate, over a VHF channel. However, this will only be possible with data-collection-only platforms.

User platforms

Each message transmitted by a platform comprises 80 to 304 bits, or 32 to 256 useful bits, i.e., 4 to 32 8-bit words. Since each transmitted word can correspond to the output of one sensor, each platform may be fitted with from 4 to 32 sensors.

For mobile or moving platforms that must be located, the optimal repetition period is 40 seconds; for data-collection-only platforms the optimal repetition period is 200 seconds.

All ARGOS platforms contain a common transmitter package consisting of a stable oscillator and a signal processor. The balance of a given platform's equipment consists of the user's sensors and an interface – interface specifications are determined by the number and types of sensors. The transmitter sensor inputs are of the analog (variable voltage or frequency) and serial digital types. The transmitter power rating is about 3 Watts and the transmission frequency is 400 MHz. The mass (approximately 2 kg), dimensions, and power consumption (about 200 mW on average) of the standard transmitter package have been optimized to meet the expected operational requirements.

A company in the PROSPACE group, E.M.D. (ELECTRONIQUE MARCEL DASSAULT), has been awarded a CNES contract to study, develop and manufacture ARGOS platforms for trials and orbit determination. E.M.D. is also producing the ARGOS equipment to be placed on board the TIROS-N satellites. This company previously supplied platforms for the EOLE program and has acquired consider-

able experience and know-how in the field of satellite platform location and data collection. It is this experience, and the company's manufacturing resources, that will enable E.M.D. to supply platforms of all types (for buoys, ships, and land applications) that are both CNES certificated and of the highest quality.

It should be noted, however, that users are free to supply their own platforms, provided they meet certain criteria regarding interference with the rest of the system. Further details can be obtained on request.

If operated solely with data-collection-only type platforms distributed evenly over the entire Earth, the system's total capacity would be 16,000.

If operated only with location and data collection type platforms equipped with 4 sensors each, the total capacity would be between 3000 and 4000.

Some 200 platforms can be accessed simultaneously by one satellite.

The probability of successful reception of messages transmitted by a platform is a function of latitude; outside the zone between 40°N and 40°S the probability is virtually 100%. Where platform location is performed, the accuracy is between 3 and 5 km and is determined, in part, by the type of platform (balloon, buoy, etc.), the quality of its sub-assemblies, and, in particular, the stability of the oscillator.

A detailed brochure describing the ARGOS system, the conditions for becoming a user, and the various data processing arrangements offered will soon be published. To obtain a copy write to: CNES/DGP/PRO, 129, rue de l'Université, 75007 PARIS, France.

The ARGOS system is being developed as a joint Franco-American project; the participating agencies are:

- CNES (Centre National d'Etudes Spatiales) - France.
- NASA (National Aeronautics and Space Administration) - U.S.A.
- NOAA (National Oceanic and Atmospheric Administration) - U.S.A.

ENVIRONMENTAL FACTORS IN THE HEATING OF BUILDINGS. L.E. Anapol'skaya and L.S. Gandin. Translated from Russian by H. Olaru; translation edited by P. Greenberg. John Wiley & Sons, 1975, 238 pp.

Until recently, the required capacity of heating systems for buildings in Canada and the amount of insulation in exterior walls has been determined mainly on the basis of January design-temperatures. These temperatures have been selected so that, in an average year, only 1 or 2½ per cent of the hours in January will be colder than these temperatures. The economical operation of the heating system is also taken into consideration. The annual fuel requirements are estimated using the normal annual number of degree-days below 65°F (or, starting this year, below 18°C).

These two climatic parameters, design-temperatures and degree-days, are based on temperature alone. It is well-known that other factors, particularly wind speed and solar radiation, have a significant influence on the heat requirements of buildings, and that conclusions based on temperature alone are seldom accurate.

The heating requirements of a building change from hour to hour in response to changes in the various weather elements and also to changes in internal heat sources including the number of occupants and the varying uses of electric energy. High-speed electronic computers have made it possible to study these changes hour by hour and thus obtain more accurate estimates of both the required capacity of the heating system and the fuel requirements. Such computations, however, are very complex and require a lot of expensive computer time.

There is a need for some method to compute heating capacity and fuel requirements that is more accurate than the traditional design-temperature and degree-day approach but not as complex and expensive as the hour-by-hour method using electronic computers.

L.E. Anapol'skaya and L.S. Gandin in their book *Environmental Factors in the Heating of Buildings* have provided a possible answer to this need. Their book, translated from Russian into English by H. Olaru and edited by P. Greenberg, has been issued by the Israel Program for Scientific Translations.

The first chapter deals with the meteorological factors of maximum heat loss taking temperature and wind into account. The conductive heat loss through walls depends only slightly on wind speed but the infiltrative heat loss through cracks around windows and doors greatly depends on wind speed and, of course, on the number and tightness of the windows. Using typical values for the various building parameters they define an effective temperature, T_e . Their equation for T_e in terms of building parameters permits them to discuss in quantitative terms the relative importance of conductive and infiltrative heat losses. (Qualitatively, of course, we know that in a windy area heat losses can best be reduced by making windows tighter, but in a very cold area with light winds it is more important to increase wall insulation.)

In this book, the effective temperature for a typical building has been used in much the same way as we have used temperature alone to provide a design-temperature. T_e values of 0.1 per cent probability (i.e., when only 0.1 per cent of the time in an average year is colder than T_e) and of 0.4 per cent probability have been used to divide the USSR into eleven zones, each with a range of 5°C down to -50°C and a range of 10°C below -50°C.

Chapter II deals with radiative heat exchanges at walls and windows. The equations become very complex, involving the absorption of solar radiation by walls of various orientations and the long-wave radiation between outside walls and the surroundings. For windows the transmitted solar radiation is an additional, but very important, complicating factor. These equations are finally reduced to a manageable form and combined with

equations from Chapter I to provide a new effective temperature taking into account the conductive and infiltrative heat losses and the radiative gains as well as internal heat sources.

The third and final chapter deals with fuel requirements. The heat deficit is defined as the temperature difference between the desired inside temperature and the effective temperature (developed in Chapter 2). Heat deficits are calculated for each month of the heating season (based on monthly normals) and then summed to give an index of the winter's severity in degree-months. Variability from year to year and the great differences in the duration and the severity of the heating season in different areas of the USSR are discussed in some detail. The two maps included in this Chapter show the distribution of the heat deficit in degree-months for the eastern or western wall of a typical building, and the duration of the heating season.

The authors seem to be very much aware of the complexities of the thermal regime of buildings. They have explained and justified the necessary simplifying assumptions and pointed out the limitations of the equations they use. Most of the book (including the maps) is based on the assumption of steady-state conditions, but there is an appendix dealing briefly with the non-steady-state thermal regime.

Probability theory originally dealt with discrete events so that on applying it to a continuous variable, such as air temperature, it is important to indicate clearly the duration that is being treated as a discrete event. For example, the authors state: " $T_e = -40^\circ\text{C}$ occurs 230 times a year in Yakutsk." What they really mean is that $T_e = -40$ (or lower) occurs at 230 of the 6-hourly synoptic observations in a year, which represent about 1380 hours.

There are a few typographical errors and incorrect statements that could be confusing but in general the book is clearly written.

This book is recommended as an excellent example of the application of climatology to a complex problem. The design of buildings and their heating systems which are economical in both initial cost and operating costs is becoming increasingly important. The methods described by Anapol'skaya and Gandin deserve serious consideration.

Donald W. Boyd
Division of Building Research
National Research Council of Canada
Ottawa

METEOROLOGY AND CLIMATOLOGY, VOLUME 1, ITOGI Summaries of Scientific Progress, Geophysics Series, I.P. Danilina, A.P. Kapitsa, Eds., G.K. Hall, Boston, 224 pp., \$29.

This book is the first in the ITOGI series on meteorology and climatology, part of the Geophysics series issued by VINITI, the All-Union Institute for Scientific and Technical Information of the USSR. It reviews the most significant research done in the two or three years prior to original publication in Russian (1971 in this case). Apparently the following subjects will be covered by biennial volumes of this type: Oceanology, Meteorology and Climatology, Physics of the Earth, Glaciology and Geomagnetism and the Upper Atmosphere.

The contents of the present volume contain the following reviews: physical meteorology by A.Kh. Khrigian, satellite meteorology by K.Ya. Kondrat'yev, climatology by B.L. Dzerdzheyewskiy, agricultural meteorology by Yu.I. Chirkov and V.A. Shablevskaya, photochemistry of the ozonosphere by I.M. Kravenko, and glacial climatology by A.N. Krenke.

Authors have followed the series theme closely although some reviews tend towards listing of abstracts, while in others the author's interest shows through. References were somewhat oriented towards Russian sources. As the previous paragraph suggests topics

such as dynamical meteorology, synoptic meteorology and so on were not covered. Production is good. The book contains no illustrations.

These are useful quick reviews. They are perhaps for the library rather than the individual, especially if they appear at the rate promised.

E.R. Walker
Frozen Sea Research Group
Victoria, B.C.

PHYSICAL AND DYNAMIC CLIMATOLOGY, Proceedings of the Symposium on Physical and Dynamic Climatology, Leningrad, August 1971, WMO (GIDROMETEOROLOGIZDAT) Leningrad, 1974, 400 pp., Sw. fr. 30.

This publication of proceedings of the WMO/IAMAP conference on Physical and Dynamic Climatology, held in Leningrad in August 1971, is, as is usual with Proceedings publications, a mixture. The topics in the book are: energy balance of the earth, physics of local and microclimate, numerical models of climate, general circulation of the atmosphere, climatic fluctuations and modifications.

Most space is given to climatic fluctuations but these climatic fluctuation papers are perhaps overshadowed by the recent spate of reports, on conferences on climatic change, at Norwich, at Stockholm, and from various U.S.A. sources. The rest of the present book deals fleetingly with topics from Obukhov's note on 'Global Invariants of Atmospheric Motions' to a report on radar observation of local shower climatology.

The book is cheaply but quite adequately produced, as more texts might well be. To sum up, a book perhaps more for a reference library than for the individual. But glance through it!

E.R. Walker
Frozen Sea Research Group
Victoria, B.C.

CALL FOR PAPERS — ELEVENTH ANNUAL CONGRESS

The Eleventh Annual Congress and Annual General Meeting of the Canadian Meteorological Society will be held at the Winnipeg Convention Centre, Winnipeg, Manitoba, 1-3 June 1977. The theme session in meteorology will be entitled "Great Plains Meteorology" and will consist of invited and some contributed papers. There will be the usual sessions devoted to other topics, according to the papers submitted. As at the last two congresses, the Oceanography Division will be arranging sessions on oceanography as well.

Titles and definitive abstracts (less than 300 words) should reach the program committee by 1 February 1977. Papers on meteorology should be sent to Mr. H.M. Fraser, Atmospheric Environment Service, 600-185 Carlton St., Winnipeg, Manitoba, R3C 3J1. Papers on oceanography should be sent to Dr. N. Boston, c/o Beak Consultants, 1550 Alberni St., Vancouver, B.C., V6G 1A5.

Meteorology Under Public Discussion in Australia

The Australian Minister for Science has issued a discussion paper or green paper entitled "Towards New Perspectives for Australian Meteorological Services." This paper invites comments from interested groups and individuals on possible changes in the provision or organization of meteorological services. Major issues to be opened up for discussion and comment include such questions as:

- (a) are the services provided by the Australian Bureau of Meteorology well suited to general national requirements and specific customer needs?
- (b) would it be more efficient or more economical for some of the present activities of the Bureau to be placed elsewhere?
- (c) with regard to what might be feasible with existing scientific knowledge and with realisable technology, should additional or expanded services be provided?
- (d) are present arrangements for research in meteorology satisfactory?
- (e) should the tertiary institutions assume greater responsibility for technical and professional training in meteorology?
- (f) are our international commitments in meteorology in balance with national operations and needs?

The Australian Bureau of Meteorology last year spent over A\$31 million and employed approximately 2,000 full-time staff. Part-time (800) and unpaid observers (7,300) were also engaged in observational work. Cost-benefit studies show that Bureau's services provide annual savings to Australia between A\$250-550 million.

Thirty-fifth Eastern Snow Conference

The thirty-fifth meeting of the Eastern Snow Conference will be held at Belleville, Ontario, Canada, 3 and 4 February 1977.

APPEL DE TEXTES — ONZIEME CONGRES ANNUEL

La Société Météorologique du Canada tiendra son congrès annuel et sa réunion générale au Winnipeg Convention Centre, Winnipeg, Manitoba, du 1er au 3 juin 1977. La session-thème sera intitulée "La météorologie des Prairies". Les autres sessions seront consacrées, suivant la coutume, à divers domaines de la météorologie déterminés en fonction des articles soumis pour présentation. Pour la troisième année, la Division d'océanographie organisera des sessions traitant de sujets dans ce domaine.

Les titres ainsi que les sommaires définitifs (maximum 300 mots) devront parvenir au comité du programme d'ici le *1er février 1977*. Les textes scientifiques en météorologie devront être envoyés à M.H.M. Fraser, Service de l'environnement atmosphérique, 600-185 Carlton, Winnipeg, Manitoba, R3C 3J1, tandis que ceux traitant d'océanographie devront être expédiés au Dr. N. Boston, a/s Beak Consultants, 1500 Alberni, Vancouver, B.C., V6G 1A5.

INFORMATION FOR AUTHORS

Editorial policy. *Atmosphere* is a medium for the publication of the results of original research, survey articles, essays and book reviews in all fields of atmospheric science. It is published quarterly by the CMS with the aid of a grant from the Canadian Government. Articles may be in either English or French. Contributors need not be members of the CMS nor need they be Canadian; foreign contributions are welcomed. All contributions will be subject to a critical review before acceptance. Because of space limitations articles should not exceed 16 printed pages and preferably should be shorter.

Manuscripts should be submitted to: *Atmosphere*, Dept. of Meteorology, McGill University, P.O. Box 6070, Montreal, Quebec H3C 3G1. Three copies should be submitted, typewritten with double spacing and wide margins. Heading and sub-headings should be clearly designated. A concise, relevant and substantial abstract is required.

Tables should be prepared on separate sheets, each with concise headings.

Figures should be provided in the form of three copies of an original which should be retained by the author for later revision if required. A list of legends should be typed separately. Labelling should be made in generous size so that characters after reduction are easy to read. Line drawings should be drafted with India ink at least twice the final size on white paper or tracing cloth. Photographs (halftones) should be glossy prints at least twice the final size.

Units. The International System (SI) of metric units is preferred. Units should be abbreviated only if accompanied by numerals, e.g., '10 m', but 'several metres.'

Footnotes to the text should be avoided.

Literature citations should be indicated in the text by author and date. The list of references should be arranged alphabetically by author, and chronologically for each author, if necessary.

RENSEIGNEMENTS POUR LES AUTEURS

Politique éditoriale. *Atmosphère* est un organe de publication de résultats de recherche originale d'articles sommaires, d'essais et de critiques dans n'importe quel domaine des sciences de l'atmosphère. Il est publié par la SMC à l'aide d'une subvention accordée par le gouvernement canadien. Les articles peuvent être en anglais ou en français. Il n'est pas nécessaire que les auteurs soient membre de la SMC; les contributions étrangères sont bien-venues. A cause des limitations d'espace les articles ne doivent pas dépasser 16 pages dans le format final. Tout article sera soumis à un critique indépendant avant d'être accepté.

Les manuscrits doivent être envoyés à: *Atmosphère*, Dépt. de Météorologie, L'Université McGill, C.P. 6070, Montréal, Québec H3C 3G1. Ils doivent être soumis en trois exemplaires dactylographiés à double interlignes avec de larges marges. Les titres et sous-titres doivent être clairement indiqués. Chaque article doit comporter un résumé qui soit concis, pertinent et substantiel.

Les tableaux doivent être préparés et présentés séparément accompagnés d'un titre et d'un numéro explicatifs concis.

Les graphiques doivent être présentés en trois copies dont les originaux devraient être conservés par l'auteur au cas où ils seraient nécessaire de les reviser. Une liste des légendes des graphiques doit être dactylographiée séparément. L'étiquetage doit être de grand format de façon à ce qu'il soit facilement lisible après réduction du format. Le traçage des lignes doit s'effectuer au moyen d'encre de chine en doublant, au moins, le format final, le tout sur papier blanc ou sur papier à calquer et identifié adéquatement. Les photographies (demi-teintes) devraient être présentées sur épreuves glacées au double du format final.

Les unités. Le Système International (SI) d'unités métriques est préférable. Les unités devraient être abrégées seulement lorsqu'elles sont accompagnées de nombres, ex: "10m", mais "plusieurs mètres".

Les notes de renvoi au texte doivent être évitées.

Les citations littéraires doivent être indiquées dans le texte selon l'auteur et la date. La liste des références doit être présentée dans l'ordre alphabétique, par auteur et, si nécessaire, dans l'ordre chronologique pour chaque auteur.

The Canadian Meteorological Society came into being on January 1, 1967, replacing the Canadian Branch of the Royal Meteorological Society, which had been established in 1940. The Society exists for the advancement of Meteorology, and membership is open to persons and organizations having an interest in Meteorology. At nine local centres of the Society, meetings are held on subjects of meteorological interest. *Atmosphere* as the scientific journal of the CMS is distributed free to all members. Each spring an annual congress is convened to serve as the National Meteorological Congress.

Correspondence regarding Society affairs should be directed to the Corresponding Secretary, Canadian Meteorological Society, c/o Dept. of Geography, Simon Fraser University, Burnaby, B.C., V5A 1S6.

There are three types of membership – Member, Student Member and Sustaining Member. For 1976 the dues are \$20.00, \$5.00 and \$60.00 (min.), respectively. The annual Institutional subscription rate for *Atmosphere* is \$15.00.

Correspondence relating to CMS membership or to institutional subscriptions should be directed to the University of Toronto Press, Journals Department, 5201 Dufferin St., Downsview, Ontario, Canada, M3H 5T8. Cheques should be made payable to the University of Toronto Press.

La Société météorologique du Canada a été fondée le 1^{er} janvier 1967, en remplacement de la Division canadienne de la Société royale de météorologie, établie en 1940. Cette société existe pour le progrès de la météorologie et toute personne ou organisation qui s'intéresse à la météorologie peut en faire partie. Aux neuf centres locaux de la Société, on peut y faire des conférences sur divers sujets d'intérêt météorologique. *Atmosphere*, la revue scientifique de la SMC, est distribuée gratuitement à tous les membres. À chaque printemps, la Société organise un congrès qui sert de Congrès national de météorologie.

Toute correspondance concernant les activités de la Société devrait être adressée au Secrétaire-correspondant, Société météorologique du Canada, Département de Géographie, L'Université Simon Fraser, Burnaby, B.C., V5A 1S6.

Il y a trois types de membres: Membre, Membre-étudiant, et Membre de soutien. La cotisation est, pour 1976, de \$20.00, \$5.00 et \$60.00 (min.) respectivement. Les Institutions peuvent souscrire à *Atmosphère* au coût de \$15.00 par année.

La correspondance concernant les souscriptions au SMC ou les souscriptions des institutions doit être envoyée aux Presses de l'Université de Toronto, Département des périodiques, 5201 Dufferin St., Downsview, Ontario, Canada, M3H 5T8. Les chèques doivent être payables aux Presses de l'Université de Toronto.

Council / Conseil d'Administration 1976-77

President/Président – J.E. Hay
Vice President/Vice-Président – K.F. Harry
Past President/Président sortant –
P.E. Merilees

Corresponding
Secretary/Secrétaire-correspondant –
R.B. Sagar

Treasurer/Trésorier – D.G. Schaefer
Recording Secretary/
Secrétaire d'assemblée – L.E. Parent

Councillors-at-large/Conseillers
–M.G. Ferland, D.B. Fraser,
A.D.J. O'Neill

Chairmen of Local Centres/Présidents des centres

Oceanography Division/Division
d'océanographie:

Chairman/Président – D.M. Farmer
Secretary/Secrétaire – P.H. LeBlond
Councillors/Conseillers – E.P. Jones,
B. Sundby

ATMOSPHERE

Editor/Rédacteur – I.D. Rutherford

Associate Editors/Rédacteurs associés – J. Derome, C. East, J.B. Gregory, W. Gutzman, P.H. LeBlond, R. List, C.L. Mateer, G.A. McBean, D.N. McMullen, P.E. Merilees, R.R. Rogers, V.R. Turner, R.E. Thomson, E.J. Truhlar, E. Vowinckel

Sustaining Members/Membres de soutien – Air Canada. – MacLaren Atlantic Ltd.